

UNIVERSIDADE ESTADUAL DE CAMPINAS

INSTITUTO DE BIOLOGIA



LISANDRA MARQUES GAVA

**“CARACTERIZAÇÃO E INTERAÇÃO DO DOMÍNIO
C-TERMINAL DA CHAPERONA HSP90 HUMANA E DAS
CO-CHAPERONAS TOM70 E HOP”**

Este exemplar corresponde à redação final
da tese defendida pelo(a) candidato (a)
LISANDRA MARQUES GAVA
e aprovada pela Comissão Julgadora.
Carlos Ramos

Tese apresentada ao Instituto de
Biologia para obtenção do Título de
Doutor em Biologia Funcional e
Molecular, na área de Bioquímica.

Orientador: Prof. Dr. Carlos Henrique Inácio Ramos

Campinas, 2011

FICHA CATALOGRÁFICA ELABORADA POR
SÍLVIA CELESTE SÁLVIO – CRB8/7039
BIBLIOTECA DO INSTITUTO DE BIOLOGIA - UNICAMP

G24c	<p>Gava, Lisandra Marques, 1982- Caracterização e interação do domínio C-terminal da chaperona Hsp90 humana e das co-chaperonas Tom70 e Hop / Lisandra Marques Gava. – Campinas, SP: [s.n.], 2011.</p> <p>Orientador: Carlos Henrique Inácio Ramos. Tese (doutorado) – Universidade Estadual de Campinas, Instituto de Biologia.</p> <p>1. Chaperonas moleculares. 2. Co-chaperonas. 3. Ultracentrifugação analítica. 4. Interações proteína-proteína. 5. Calorimetria de titulação isotérmica. I. Ramos, Carlos Henrique Inácio. II. Universidade Estadual de Campinas. Instituto de Biologia. III. Título.</p>
------	--

Informações para Biblioteca Digital

Título em Inglês: Characterization and interaction of the C-terminal domain of the human chaperone Hsp90 and co-chaperones Tom70 and Hop

Palavras-chave em Inglês:

Molecular chaperones
Co-chaperones
Analytical ultracentrifugation
Protein-protein interactions
Isothermal titration calorimetry

Área de concentração: Bioquímica

Titulação: Doutor em Biologia Funcional e Molecular

Banca examinadora:

Carlos Henrique Inácio Ramos [Orientador]
Sérgio Marangoni
Carlos Alberto Montanari
Yraima Moura Lopes Cordeiro
Marcelo Matos Santoro

Data da defesa: 15-08-2011

Programa de Pós Graduação: Biologia Funcional e Molecular

Campinas, 15 de agosto de 2011.

BANCA EXAMINADORA

Prof. Dr. Carlos Henrique Inácio Ramos (orientador)



Assinatura

Prof. Dr. Sérgio Marangoni



Assinatura

Prof. Dr. Carlos Alberto Montanari



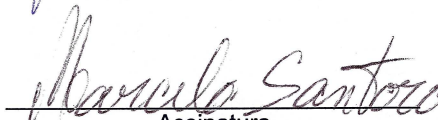
Assinatura

Profa. Dra. Yraima Moura Lopes Cordeiro



Assinatura

Prof. Dr. Marcelo Matos Santoro



Assinatura

Prof. Dr. Carlos Francisco Sampaio Bonafé

Assinatura

Prof. Dr. Fábio Cesar Gozzo

Assinatura

Prof. Dr. Hiroshi Aoyama

Assinatura



Solicitação/Procolo: CHIR 2007-2

Nome do aluno: Lisandra Marques Gava.

Nível: doutorado

Período: 03/2007 – 02/2012

Nome do orientador: Carlos H. I. Ramos

Resumo:

A função biológica das proteínas está diretamente ligada à sua estrutura tridimensional obtida através do processo de enovelamento protéico. Neste contexto, proteínas denominadas genericamente de chaperones moleculares exercem papel fundamental atuando tanto no auxílio ao enovelamento correto de algumas proteínas, como no reenovelamento sob condições de estresse e dissociação de agregados protéicos. Hsc70 e Hsp90 colaboram formando uma maquinaria chaperone que é multifuncional, possui vários componentes, parece não ter correspondente em procariotos, e que desempenha um importante papel na proteção contra estresse ambiental e genético. Pelo menos 100 proteínas diferentes são clientes (substratos) deste sistema, sendo que diversas proteínas de sinalização celular como quinases e receptores esteróides requerem a Hsp90 para atingir seu estado nativo na célula. Apesar de se conhecer alguns dos substratos de Hsp90, as características estruturais das interações ainda permanecem desconhecidas. O objetivo desse trabalho é mapear e caracterizar interações da Hsp90 humana com co-chaperones, cujos complexos exercem importante papel funcionalidade do sistema e, portanto, na viabilidade do organismo. Além de estudar e caracterizar a Hsp90 e algumas co-chaperonas do sistema humano.

O projeto de pesquisa acima descrito, a ser conduzido pela aluna de doutorado Lisandra Marques Gava, recebeu autorização desta Comissão Interna de Biossegurança.

Presidente em exercício da CIBio-IQ: Carlos H. I. Ramos

SUMÁRIO

AGRADECIMENTOS	vi
RESUMO.....	viii
ABSTRACT	x
LISTA DE FIGURAS	xii
LISTA DE ABREVIATURAS E SIGLAS.....	xiii
1. CAPÍTULO 1	
1. Introdução	1
1.1 Enovelamento de proteínas.....	1
1.2 Chaperonas moleculares.....	3
1.3 Hsp90	7
1.4 Co-chaperonas	12
1.5 Hop.....	14
1.6 Tom70	16
1.7 A Hsp90 como um alvo para a terapia do câncer – Artigo de revisão....	21
1.8 Objetivos	33
1.8.1 Objetivo geral	33
1.8.2 Objetivos específicos.....	33
2. CAPÍTULO 2	
Artigo científico: Human Hsp70/Hsp90 organizing protein (Hop) D456G is a mixture of monomeric and dimeric species	35
3. CAPÍTULO 3	
Artigo científico: Human mitochondrial receptor Tom70 functions as a monomer	44
4. CAPÍTULO 4	
Artigo científico: Stoichiometry and thermodynamics of the interaction between the C-terminus of human 90 kDa heat shock protein Hsp90 and the mitochondrial translocase of outer membrane	57
5. CAPÍTULO 5	
5. Discussão geral	65
5.1 Hop.....	65
5.2 Tom70	67
5.3 C-Hsp90	68
5.4 Interação entre C-Hsp90 e Tom70.....	70
5. CAPÍTULO 6	
6. Conclusões.....	74
5. CAPÍTULO 7	
7. Referências bibliográficas.....	76

AGRADECIMENTOS

Agradeço inicialmente ao Prof. Dr. Carlos Henrique Inácio Ramos, pela oportunidade e orientação. Pelas discussões científicas, supervisão dos experimentos, relatórios e demais trabalhos científicos. Pela ótima convivência durante esses anos, pelo apoio e incentivo à construção da minha carreira científica.

À FAPESP, que financiou diretamente a realização desse projeto com a concessão da bolsa de doutorado; e as demais agências de fomento e outros financiamentos: CNPq, CAPES, FUNCAMP, FIRCA-NIH, INCT-INBEB, SBBq.

Aos membros da Pós-graduação em Biologia Funcional e Molecular do Departamento de Bioquímica do Instituto de Biologia da UNICAMP, agradeço aos professores do curso e ao pessoal de apoio em especial à secretária Andréia A. Vigilato pela paciência e auxílio na preparação dos documentos necessários para o exame de qualificação e defesa.

Ao Instituto de Química da Unicamp, pelas instalações do Laboratório de Bioquímica de Proteínas, Laboratório Institucional de Manipulação de OGMs (LimOGem) ambos sob coordenação do Prof. Dr. Carlos H.I.Ramos e demais laboratórios de calorimetria, espectroscopia e dicroísmo circular.

Ao Laboratório Nacional de Biociências, pela ótima infra-estrutura disponível, onde realizei integralmente o primeiro ano de doutorado e ao pessoal técnico que auxiliou a realização de tantos experimentos; agradeço em especial ao Laboratório de Espectroscopia e Calorimetria, instalação onde grande parte dos experimentos foi realizada.

Agradeço a todos os técnicos, alunos de iniciação científica e pós-graduação do grupo de pesquisa do Prof. Dr. Carlos H. I. Ramos. Em especial à Veruska Mazon Soares, grande amiga e minha madrinha, que me recebeu tão bem no laboratório, sempre zelou com muito cuidado e dedicação do laboratório, que se disponibilizou a ajudar em todos os momentos que precisei. Agradeço pela amizade construída durante esses anos e pelo carinho inestimável. Agradeço em especial aos amigos e companheiros de laboratório: Ana Olímpia, Ana Paula Rossi, Yuri Mendonça, Thiago Seraphim, Thiago Cagliari, Daniel Corrêa, Tininha Lira, Karina Gui, Danieli Gonçalves que fizeram parte da minha vida pessoal e profissional nesses últimos anos, que diretamente influenciaram e auxiliaram a realização do doutorado. À Fernanda Alves e Letícia Zanphorlin, pela convivência amistosa e risadas no dia a dia. Aos demais membros do grupo, aos alunos do LNBio, da BFM e do IQ que também contribuíram para a realização e construção desse trabalho, discutindo, corrigindo e ensinando.

Agradeço à minha família, meus pais Brás e Isabel, que me incentivaram incondicionalmente desde o primeiro dia na universidade. Pelo apoio, incentivo, estímulo. Eu os admiro mais que tudo e todos. Aos meus irmãos Armando e João Carlos, cujo carinho e incentivo me ajudaram a permanecer firme e continuar, vocês fazem a minha vida mais feliz. Ao meu amigo-irmão Tadaiti Ozato Jr., padrinho companheiro e incentivador de tantos anos. Amo muito todos vocês!

Agradeço, especialmente, ao meu marido Júlio César Borges. Meu amor, meu amigo, meu orientador particular. Agradeço por todos esses anos de apoio, incentivo, críticas, correções, amor, dedicação e companheirismo. Amo você. *“I carry your heart with me (I carry it in my heart)”*.

Resumo

A função biológica das proteínas está relacionada à sua estrutura tridimensional adquirida pelo processo de enovelamento proteico. Neste contexto, proteínas denominadas, genericamente, de chaperonas moleculares exercem papel fundamental atuando no auxílio do enovelamento correto, no reenovelamento e na dissociação de agregados proteicos. A Hsp90 é uma das chaperonas moleculares mais importantes, é essencial para a viabilidade celular em eucariotos e está normalmente associada a proteínas atuantes no ciclo e sinalização celular, o que torna essa chaperona um alvo bastante interessante para abordagens terapêuticas de diversas doenças. A Hsp90 pode ser modulada por co-chaperonas diversas. Nesse trabalho foram caracterizadas as proteínas C-Hsp90 (domínio C-terminal da Hsp90 humana), e as co-chaperonas Hop e Tom70, além da interação entre C-Hsp90 e Tom70. Foram aplicadas técnicas de dicroísmo circular e emissão de fluorescência do triptofano; seguidas pela caracterização por ultracentrifugação analítica, gel filtração analítica, espalhamento dinâmico de luz, cromatografia de gel filtração acoplada a espalhamento de luz em multi-ângulos (SEC-MALS) e gel nativo. Para os ensaios de interação foram aplicadas técnicas de *pull-down*, SEC-MALS e calorimetria de titulação isotérmica. As proteínas foram produzidas puras e enoveladas, com estado oligomérico determinado como dímero para C-Hsp90 e monômero para Hop e Tom70, sendo que essas também foram encontradas como espécies diméricas. A estequiometria de interação entre a C-Hsp90 e Tom70 foi determinada em 1 monômero da Tom70 para 1 dímero da C-Hsp90, com K_D de 360 ± 30 nM, $\Delta H_{app} = -2,6 \pm 0,1$ kcal/mol e $\Delta S = 21 \pm 1$ cal/mol.K, sugerindo que a

interação é dirigida por entalpia e entropia. Os resultados obtidos nesse trabalho contribuem para uma melhor compreensão do sistema Hsp90, que está envolvido em diversos processos celulares essenciais e patológicos, como doenças neurodegenerativas, processos inflamatórios, infecções e câncer.

Abstract

The biological function of proteins is related to its three dimensional structure acquired via protein folding process. In this context, the molecular chaperones play a key role acting as auxiliary protein on protein folding, refolding and dissociation of protein aggregates. Hsp90 is one of the most important molecular chaperones, is essential for cell viability in eukaryotes and is usually associated with proteins involved in cell cycling and cell signaling, which makes these chaperone a very interesting targeting for therapeutic approaches for several diseases. The chaperone activity of Hsp90 can be modulated by other proteins, called co-chaperones. In this work, we characterized the protein C-Hsp90 (C-terminal domain of human Hsp90) and the co-chaperones Hop and Tom70, and also the interaction between C-Hsp90 and Tom70. Circular dichroism and fluorescence emission of tryptophan was first applied for initial characterization of the proteins, followed by analytical ultracentrifugation, analytical gel filtration, dynamic light scattering, size exclusion chromatography – multi angle light scattering (SEC-MALS) and native gel. The interaction between C-Hsp90 and Tom70 were measured by techniques like pull-down, SEC-MALS and isothermal titration calorimetry. The proteins were produced pure and soluble and their oligomeric state were determined as dimer for C-Hsp90, and monomer for Hop and Tom70, these two co-chaperones were also found as dimeric species. The stoichiometry of interaction between C-Hsp90 and Tom70 was determined by SEC-MALS and ITC as been 1 dimer of C-Hsp90 to 1 monomer of Tom70, with a K_D of 360 ± 30 nM, $\Delta H_{app} = -2.6 \pm 0.1$ kcal/mol and $\Delta S = 21 \pm 1$ cal/mol.K,

suggesting that these interaction is driven by both, enthalpy and entropy. The results contribute to a better understanding of the important Hsp90 machinery, which is involved in many essential cellular and pathological processes, such as neurodegenerative diseases, inflammation, infection and cancer.

LISTA DE FIGURAS

Figura 1: Papel das chaperonas moleculares na célula.	7
Figura 2: Dinâmica conformacional da Hsp90 no ciclo da atividade chaperona.	9
Figura 3: Estrutura terciária da Hsp90	10
Figura 4: TPR2A da Hop em complexo com o MEEVD da Hsp90.	15
Figura 5: Papel das chaperonas e co-chaperonas na translocação de proteínas para a mitocôndria.	18
Figura 6: Estrutura do domínio TPR da Tom71 em complexo com o MEEVD	19
Figura 7: Sequência de aminoácidos da proteína Tom70 humana.....	19

LISTA DE ABREVIATURAS E SIGLAS

17-AAG: 17-N-alilamino-17-demetoxigeldanamicina

Å: Angstrom (1×10^{-10} metros)

ADP: adenosina 5' Di-fosfato

Aha1: proteína ativadora da Hsp90 1 (Activator of Hsp90 ATPase 1)

ATP: adenosina 5' tri-fosfato

BNPAGE: gel nativo azul (Blue Native Poliacrilamide Gel Electrophoresis)

CD: dicroísmo circular

Cdc37: proteína ortóloga da p50 em levedura (Cell Division Cycle 37 homologue)

CHIP: proteína interatora do C-terminal da Hsp70 (C-terminal Hsp70-interacting protein)

C-Hsp90: domínio C-terminal da Hsp90

Cyp40: ciclofilina 40

D: coeficiente de difusão

$D_{20,w}$: coeficiente de difusão em água e na temperatura de 20 °C

$D^0_{20,w}$: coeficiente de difusão em água, na temperatura de 20 °C e concentração zero de proteína

Da: Dalton

Deg: grau (degree)

DLS: Espalhamento dinâmico de luz (Dynamic Light Scattering)

DNA: Ácido desoxirribonucléico (DeoxyriboNucleic Acid)

DnaJA1: co-chaperona da classe das Hsp40

DnaJA2: co-chaperona da classe das Hsp40

DP: motivo proteico rico em resíduos de ácido aspártico e prolina

f : coeficiente friccional

f_0/f : razão friccional ou fator de Perrin

- GIP:** Poro de importação da mitocôndria (General Import Pore)
- Grp94:** Hsp90 homóloga do retículo endoplasmático
- Hop:** proteína organizadora das Hsp70-Hsp90 (Hsp70-Hsp90 organizing protein)
- Hsp:** proteína de choque-térmico (Heat Shock Protein)
- Hsp40:** proteína de choque térmico de 40 kDa
- Hsp70:** proteína de choque térmico de 70 kDa
- Hsp75/Trap1:** Hsp90 homóloga mitocondrial
- Hsp90:** proteína de choque térmico de 90 kDa
- Hsp90 α :** Hsp90 homóloga citosólica induzida por estresse
- Hsp90 β :** Hsp90 homóloga citosólica constitutiva
- HtpG:** Hsp90 ortóloga de bactéria
- ITC:** Calorimetria de titulação isotérmica (Isothermal Titration Calorimetry)
- IUP:** proteína intrinsecamente desenovelada (Intrinsically Unfolded Proteins)
- K:** unidade de temperatura – Kelvin
- K_D :** constante de dissociação
- kDa:** kilodalton ($1,66 \times 10^{-21}$ g)
- MAPK:** proteína cinase ativadora da mitose (Mitogen Activated Protein Kinase)
- MM:** massa molecular
- n :** estequiometria da ligação
- nm:** nanômetro (10^{-9} metros)
- NOS:** óxido nítrico sintetase (Nitric Oxide Synthase)
- N-WASP:** proteína organizador da actina (Neural Wiskott–Aldrich syndrome protein)
- °C:** unidade de temperatura – graus Celsius
- p23/ PTGES3:** proteína co-chaperona da Hsp90 de 23 kDa (Prostaglandin E Synthase 3)
- PDB:** banco de dados de proteínas (Protein Data Bank)
- PP5:** co-chaperona da Hsp90 envolvida no ciclo celular

Raf1: serina/treonina cinase

R_s: raio de Stokes

s: segundos

S: Svedberg (10^{-13} segundos)

SE: Sedimentação em equilíbrio

SEC-MALS: gel filtração acoplada a espalhamento de luz em multi-ângulos (Size Exclusion Chromatography – Multi Angle Light Scattering)

Sti1 ou p60: proteína ortóloga da Hop em levedura

TEV: proteína do vírus do tabaco (Tobacco Etch Virus)

Tim22 : Proteína translocadora da membrana mitocondrial interna de 22 kDa

Tim23: Proteína translocadora da membrana mitocondrial interna de 23 kDa

T_m: temperatura média de transição

TOM: Translocase da membrana mitocondrial externa (Translocase of Outer Mitochondrial Membrane)

Tom22: Proteína translocadora da membrana mitocondrial externa de 22 kDa

Tom40: Proteína translocadora da membrana mitocondrial externa de 40 kDa

Tom70: Proteína translocadora da membrana mitocondrial externa de 70 kDa

Tom71: Proteína translocadora da membrana mitocondrial externa de 71 kDa de levedura

TPR: motivo de repetição de 34 resíduos de aminoácidos ou tetratricopeptídeo

Trp: triptofano

UCA: ultracentrifugação analítica

VS: Velocidade de sedimentação

ΔH_{app} : variação de entalpia aparente

ΔS : variação de entropia

CAPÍTULO 1

1. Introdução

1.1 Enovelamento de proteínas

Proteínas são as macromoléculas biológicas mais complexas e versáteis quando analisadas sob um ponto de vista estrutural. São funcionalmente sofisticadas e estão envolvidas na grande maioria das funções celulares (Vabulas et al., 2010). São biopolímeros lineares que adotam uma estrutura tridimensional característica, também denominada de estrutura nativa. A princípio uma proteína deve estar enovelada no estado nativo para ser funcional. Embora a classe das IUPs (*Intrinsically Unfolded Proteins*) – proteínas intrinsecamente desenoveladas – seja uma classe de proteínas funcionalmente ativas, que atuam em diversos processos regulatórios na célula (Tompa, 2002; Tompa, 2005; Dyson & Wright, 2005). A estrutura tridimensional de uma proteína é mantida, sobretudo, por interações não covalentes entre cadeias laterais de aminoácidos, o processo de aquisição dessa estrutura é chamado enovelamento proteico (Wegele et al., 2004; Ramos & Ferreira, 2005).

As teorias a respeito do enovelamento de proteínas foram inicialmente baseadas nos experimentos realizados na década de 60 por Anfinsen e seus colaboradores (Anfinsen et al., 1961; Anfinsen, 1973). Em 1972, Christian Anfinsen recebeu o Prêmio Nobel de Química por mostrar que o processo de enovelamento de uma proteína é autônomo e espontâneo. Fundamentada em experimentos *in vitro* com a ribonuclease A, a teoria de Anfinsen sugere que a estrutura tridimensional correta de uma proteína é atingida espontaneamente *in vivo* assim que a proteína deixa o ribossomo e que a sequência de aminoácidos

de uma proteína contém todas as informações necessárias para que o enovelamento ocorra (Anfinsen, 1973).

Ainda sobre o enovelamento proteico, ao questionar como as proteínas atingem sua estrutura tridimensional dentre todas as conformações possíveis, Cyrus Levinthal, com base em estudos de dinâmica, mostrou que o enovelamento proteico não pode ocorrer por uma exploração estocástica de todas as conformações nativas possíveis, pois mesmo a busca para uma pequena proteína exigiria um tempo infinitamente longo, essa definição ficou conhecida como o “paradoxo de Levinthal”, (Levinthal, 1969).

A investigação sobre enovelamento proteico tem sido intensa nos últimos quarenta anos, pois se trata de um alvo de estudo de grande valor médico e biotecnológico, visto que o processo de enovelamento, assim como a manutenção e perda da estrutura nativa estão relacionados à ocorrência de diversas doenças (Tiroli-Cepeda & Ramos, 2011). Estudos subsequentes às teorias de Anfinsen mostraram que a definição de enovelamento proteico, tido como um processo espontâneo sem a necessidade de fatores adicionais e com toda a informação necessária contida na sequência de aminoácidos não pode ser aplicado a qualquer proteína. Na verdade, se aplica apenas a uma minoria de proteínas, muitas delas pequenas e relativamente estáveis.

Trabalhos posteriores demonstraram que algumas proteínas necessitam do auxílio de outras proteínas para seu enovelamento correto e/ou associação com outras macromoléculas biológicas. O termo “chaperona molecular” foi proposto para descrever essas proteínas auxiliares (Laskey et al., 1978; Ellis, 1987), um termo bastante apropriado considerando que a palavra *chaperone* (do inglês: dama de companhia) sugere que tais proteínas atuem evitando interações

indesejáveis. Assim, o conceito original de que as proteínas enovelam e se associam via um processo espontâneo foi complementado pelo conceito de enovelamento/associação assistido, que envolve as funções de evitar o enovelamento incorreto, o desenovelamento e a agregação de proteínas dentro da célula (Lund & Ellis, 2008).

1.2 Chaperonas moleculares

O termo chaperona molecular apareceu pela primeira vez em 1978 para descrever as propriedades da nucleoplasmina, uma proteína ácida nuclear, necessária para a formação de nucleossomos. A nucleoplasmina atua na associação entre histonas e DNA, interagindo diretamente com histonas, neutralizando sua carga positiva e prevenindo interações indesejáveis (Laskey et al., 1978). Na década seguinte, alguns trabalhos demonstraram que cadeias polipeptídicas recém sintetizadas ligam a outras proteínas pré-existentes – as chaperonas moleculares – antes de se associarem a complexos funcionais (Barraclough & Ellis, 1980) e que algumas famílias dessas chaperonas requerem a hidrólise de ATP para atuarem no enovelamento de outras proteínas (Ostermann et al., 1989).

Ellis, em 1987, designou o termo chaperona, genericamente, para uma variedade de proteínas celulares, cujo papel principal é a associação a outras proteínas desenoveladas ou parcialmente enoveladas (Ellis, 1987). Chaperonas moleculares são atualmente definidas como um grupo amplo e diverso de proteínas que compartilham propriedades funcionais de auxiliar o enovelamento correto *in vivo*, prevenindo interações improdutivas que poderiam levar à agregação de proteínas ou desagregando-as posteriormente; de auxiliar a associação/dissociação de proteínas e outras macromoléculas biológicas; de

auxiliar no transporte de proteínas para compartimentos sub-celulares específicos e no controle de conformações ativas/inativas (Lund & Ellis, 2008).

As chaperonas moleculares também foram descritas como proteínas de choque-térmico ou *heat-shock proteins* (Hsp), por apresentarem indução de sua síntese em células submetidas a condições de estresse térmico. A importância das proteínas de choque térmico foi inicialmente notada devido ao aumento drástico na transcrição de genes em *Drosophila* após a exposição dessas a condição de choque térmico. Um aumento accidental na temperatura da incubadora permitiu que Ritossa, em 1962, pudesse observar (usando microscópio de luz) o aparecimento de padrões de “puffs” (ou anéis de Balbiani) distintos nos cromossomos politênicos das glândulas salivares de *Drosophila* em comparação à ausência de choque térmico, indicando que a transcrição de genes localizados nessas regiões é diferenciada sob essa condição de estresse térmico (Ritossa, 1962; Ritossa, 1996).

Entretanto, o termo *Heat Shock Protein* foi cunhado apenas doze anos depois, quando as proteínas específicas codificadas por esses genes localizados nos “puffs” foram identificadas como as proteínas de choque térmico (Tissiere et al., 1974). Assim, chaperonas moleculares e proteínas de choque térmico, são classes de proteínas sobrepostas funcionalmente, mas não idênticas (Lund & Ellis, 2008). Fenômenos similares também foram observados em procariontos e outros eucariotos (Kelley & Schlesinger, 1978; Lemaux et al., 1978; Mcalister & Finkelstein, 1980) sugerindo que a resposta ao choque térmico é um mecanismo universal e evolutivamente bastante antigo.

No enovelamento proteico, assim que uma cadeia polipeptídica deixa o ribossomo, ela deve se enovelar de maneira eficiente garantindo sua

funcionalidade no ambiente celular. No caso de proteínas não-enoveladas ou parcialmente enoveladas, os resíduos de aminoácidos hidrofóbicos que deveriam ter sido internalizados na matriz proteica, permanecem acessíveis ao solvente, tornando a proteína suscetível à agregação (Ramos & Ferreira, 2005). As chaperonas são capazes de reconhecer essa superfície hidrofóbica exposta e interagirem com essa região, evitando, de modo eficiente, a agregação. As chaperonas atuam não somente impedindo a agregação intermolecular, mas também são capazes de prevenir ou reverter o enovelamento incorreto, todavia sem modificar a estrutura nativa final (Hendrick & Hartl, 1993; Fink, 1999; Ramos & Ferreira, 2005; Borges & Ramos, 2005).

Além da participação no processo de enovelamento, as chaperonas moleculares atuam como um sistema de controle de qualidade, reconhecendo, mantendo e marcando/enviando proteínas desenoveladas ou incorretamente enoveladas para degradação (Welch & Brown, 1996). O funcionamento normal do sistema de controle de qualidade proteica é crucial para a viabilidade celular, sobretudo quando consideramos a alta concentração de macromoléculas no ambiente intracelular (Ellis, 2001; Tiroli-Cepeda & Ramos, 2011). O funcionamento adequado mantém o balanço de proteínas não-nativas alvos para o reenovelamento ou degradação, uma mudança nesse equilíbrio pode ser prejudicial para célula, podendo levar à morte celular (Wolfe & Cyr, 2011).

As chaperonas moleculares também atuam na transdução de sinal, essas proteínas agem como componentes integrais de redes de sinalização celular, nas quais podem atuar na maturação, assim como na regulação da transição entre estados ativos e inativos de moléculas de sinalização, como receptores, reguladores transcricionais e proteínas cinases (Soti et al., 2005; Gaestel, 2006).

Várias doenças associadas com o sistema nervoso central e periférico resultam do acúmulo de proteínas desenoveladas ou anormais nas células, algumas chaperonas moleculares estão envolvidas nos processos dessas doenças, chamadas de neurodegenerativas. A regulação da expressão das chaperonas não apenas previne a agregação proteica, mas também pode reenovelar proteínas desnaturadas e ressolubilizar agregados proteicos (Ansar et al., 2007; Lu et al., 2009). Portanto, as chaperonas moleculares são alvos promissores para o tratamento de doenças como a da doença de Alzheimer, doença de Parkinson, esclerose múltipla, esclerose amiotrófica lateral, desordens causadas por expansões de poliglutaminas e doença de Huntington (Peterson & Blagg, 2009).

A ação das chaperonas moleculares inclui também a translocação de proteínas para organelas celulares. Após a síntese no citosol, a maioria das proteínas mitocondriais, por exemplo, deve atravessar as membranas da mitocôndria para atingir sua localização funcional. Durante esse processo, as proteínas são desenoveladas e depois reenoveladas até atingirem suas conformações nativas. As chaperonas moleculares mitocondriais exercem funções importantes em diversos passos desse mecanismo de translocação. Atuam no reconhecimento e marcação das proteínas mitocondriais precursoras, no desenovelamento dos domínios citosólicos das mesmas, na sua translocação pelas membranas e, finalmente, no enovelamento da proteína importada na matriz mitocondrial (Stuart et al., 1994; Ryan et al., 1997; Voos & Rottgers, 2002; van der Laan et al., 2010).

No esquema apresentado na figura 1, estão exemplificados alguns dos processos celulares nos quais há participação das chaperonas moleculares.

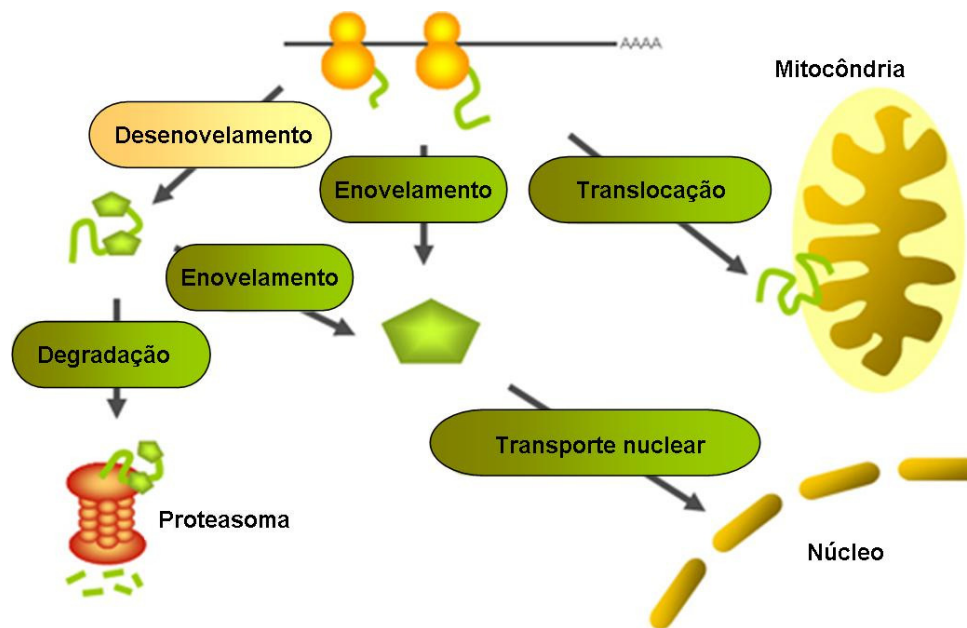


Figura 1: Papel das chaperonas moleculares na célula. As ações celulares das chaperonas, como por exemplo, a atuação no enovelamento proteico, no controle de qualidade de proteínas e na translocação para subcompartimentos celulares são destacadas no esquema (Adaptada de Ji-Sook Hahn, 2007, <http://biomolecule.snu.ac.kr/research.html>).

1.3 Hsp90

A Hsp90 – *Heat Shock Protein 90* – é uma chaperona altamente conservada (Borkovich et al., 1989; Csermely et al., 1998; Young et al., 2001; Taipale et al., 2010), amplamente distribuída, encontrada em bactéria e em todos os eucariotos, mas, aparentemente, ausente em archaea (Wegele et al., 2004). A Hsp90 é uma chaperona abundante, representa 1 a 2% do total de proteínas citosólicas na ausência de estresse (Welch & Feramisco, 1982). Ainda que seja essencial para a viabilidade de eucariotos, em quaisquer condições, a proteína bacteriana ortóloga HtpG é dispensável quando o organismo não está sob condições de estresse (Borkovich et al., 1989; Versteeg et al., 1999). A Hsp90 participa da estabilização e ativação de mais de duzentas proteínas, denominadas

proteínas clientes (ou substrato), que dependem dela para atingir e/ou manter sua conformação funcional, muitas dessas clientes são essenciais para sinalização celular constitutiva e respostas adaptativas a situações de estresse (Mayer & Bukau, 1999; Young et al., 2001; McClellan et al., 2007; Li et al., 2011).

Sua ampla clientela inclui proteínas estruturalmente e funcionalmente distintas como, por exemplo, a telomerase (Holt et al., 1999; Keppler et al., 2006), a proteína organizadora de actina: N-WASP (Park et al., 2005), a óxido nítrico sintetase – NOS (Garcia-Cardena et al., 1998), assim como uma série de receptores de hormônios nucleares (Pratt & Toft, 2003) e uma seleção de proteínas cinases (Pearl, 2005). Mesmo entre as proteínas clientes que são funcionalmente relacionadas, pode haver um elevado grau de especificidade, com homólogos próximos apresentando dependência radicalmente diferente da Hsp90 para sua ativação (Pearl & Prodromou, 2006).

Em contraste com outras chaperonas moleculares, a Hsp90 parece ser específica em relação à interação com suas clientes, contudo, as bases moleculares de tal especificidade ainda não são bem compreendidas. Para receptores de hormônios esteróides, que são provavelmente os clientes mais bem estudados, em termos de associação com a Hsp90, está claro que para o funcionamento do sistema da Hsp90 é necessária uma interação anterior com o sistema Hsp70/Hsp40, que por sua vez, é acoplado ao sistema Hsp90 via co-chaperonas: imunofilinas, Hop e p23 (Kimmins & Macrae, 2000; Pratt & Toft, 2003; Felts et al., 2007).

A Hsp90 é alvo de várias modificações pós-traducionais que afetam sua atividade chaperona (Scroggins & Neckers, 2007). Estudos recentes indicam que tais modificações regulam especificamente a interação entre a Hsp90 e algumas

proteínas clientes. Várias modificações covalentes reversíveis têm sido identificadas, incluindo S-nitrosilação, fosforilação, ubiquitinação e acetilação (Wandinger et al., 2008; Trepel et al., 2010).

Enfim, a Hsp90 é tida como um mediador chave da homeostase celular, função que realiza sendo um facilitador de diversas interações proteína-proteína do tipo transiente e de baixa afinidade (Pratt et al., 2008; DeZwaan & Freeman, 2008). Nos últimos anos a complexa regulação da Hsp90 pela qual participa da fisiologia celular tem sido esclarecida. Houve uma evolução considerável no que diz respeito ao entendimento da dinâmica conformacional da Hsp90 (Krukenberg et al., 2011). Essa dinâmica pode ser observada na figura a seguir (figura 2), onde é apresentada de maneira simplificada no ciclo de atividade chaperona da Hsp90.

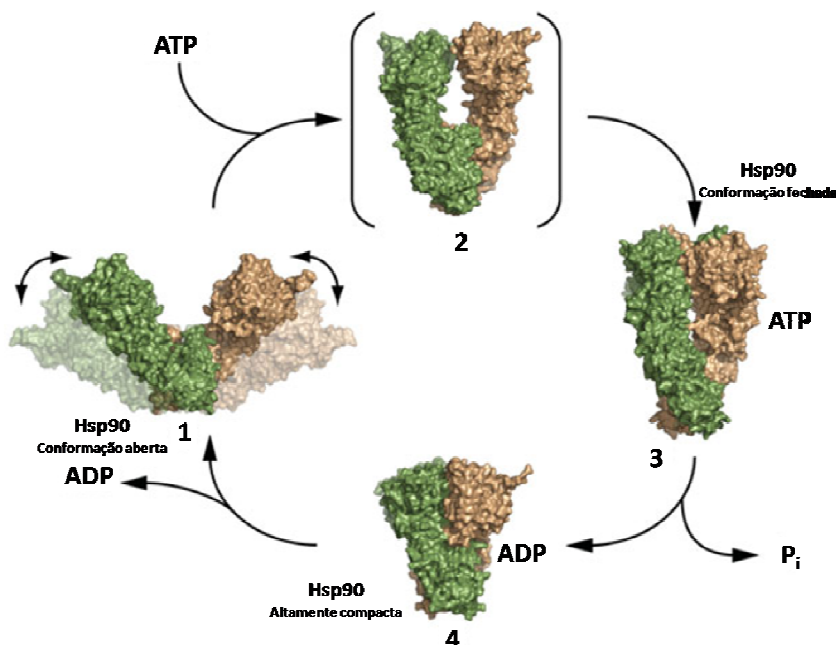


Figura 2: Dinâmica conformacional da Hsp90 no ciclo da atividade chaperona. As estruturas conhecidas da Hsp90 sugerem que o seu ciclo conformacional seja regulado por nucleotídeos. Nesse ciclo, a ligação de ATP leva a proteína de uma estrutura aberta (1 – quando recebe a proteína cliente) para uma estrutura fechada, com o N-terminal dimerizado (3). A estrutura na conformação (2) representa um possível intermediário desse ciclo. A ligação do ADP, após a hidrólise do ATP, causa uma maior compactação

da proteína (4) e a liberação do nucleotídeo reinicia o ciclo conformacional, também liberando a proteína cliente. (Figura retirada e adaptada de (Krukenberg et al., 2011)).

A respeito da arquitetura da Hsp90, em humanos há quatro isoformas: duas citosólicas (Hsp90 α e Hsp90 β); uma mitocondrial (Trap1); e uma específica do retículo endoplasmático (Grp94). Todas as isoformas atuam obrigatoriamente como dímeros, que consistem em três domínios por monômero (Figura 3).

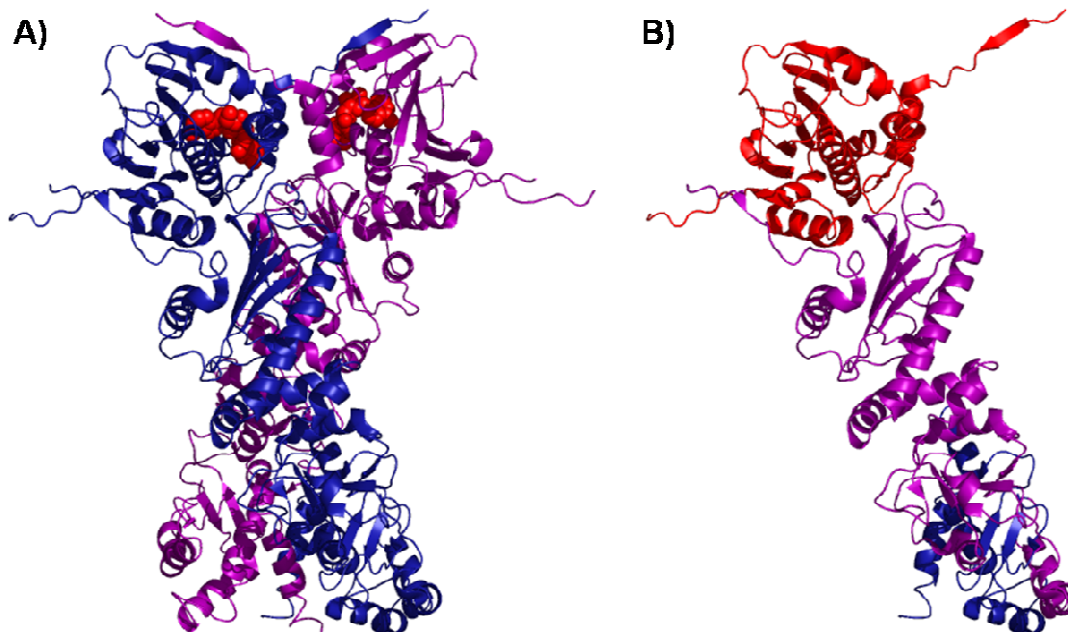


Figura 3: Estrutura terciária da Hsp90. Estrutura terciária da Hsp90 de *Saccharomyces cerevisiae* que apresenta 82% de similaridade com a Hsp90 α humana. (A) Um monômero está representado em azul e o outro em roxo, em vermelho está representada a molécula de ATP, ligada em cada N-terminal. (B) Em vermelho (topo) está representado domínio N-terminal, dos resíduos 2-216; o domínio central está em roxo, representando os resíduos 262-560 e em azul (abaixo) o C-terminal, resíduos 561-677. (Número de acesso ao PDB: 2CG9). Figura gerada usando o programa Pymol (DeLano, 2004).

O domínio N-terminal possui um sítio de ligação a nucleotídeo altamente conservado, possui aproximadamente 30 kDa e está conectado à um domínio central (de aproximadamente 35 kDa) por uma região desestruturada, altamente carregada, com a incidência repetitiva de resíduos de aspartato, glutamato e lisina (Stebbins et al., 1997; Pearl & Prodromou, 2006). Essa região é variável, em

tamanho e composição, entre as espécies e isoformas, é ausente na Hsp75/Trap1 (homóloga mitocondrial) e na HtpG bacteriana e em outros procariotos (Bardwell & Craig, 1987; Song et al., 1995; Chen & Smith, 1998). A função dessa região ainda não está bem estabelecida, em termos gerais parece contribuir para a flexibilidade da proteína e pode estar envolvida na modulação da atividade chaperona da Hsp90 (Scheibel et al., 1999; Hainzl et al., 2009). O domínio C-terminal tem aproximadamente 20 kDa é responsável pela dimerização da Hsp90 (Minami et al., 1994).

O domínio N-terminal apresenta um sítio regulatório que liga e hidrolisa ATP mediando uma série de ciclos de associação-dissociação entre a Hsp90 e as proteínas clientes envolvendo amplas mudanças conformacionais na Hsp90, que sofre rearranjo de seus domínios, como visto na figura 2 (Cunningham et al., 2008). Alguns trabalhos recentes propuseram a existência de um segundo sítio de ligação de nucleotídeo no domínio C-terminal da Hsp90 (Marcu et al., 2000; Soti et al., 2002; Garnier et al., 2002), sendo que este segundo sítio só deve ser ocupado após a ligação de ATP no sítio do N-terminal (Soti et al., 2003). O domínio C-terminal também está envolvido na interação com várias co-chaperonas e proteínas clientes. O pentapeptídeo MEEVD no C-terminal da Hsp90 citoplasmática é o sítio de interação característico com os domínios TPR (tetratricopeptídeo) de co-chaperonas e algumas clientes (Prodromou et al., 1999; Wegele et al., 2004). O sub-item 1.7 desse capítulo apresenta uma revisão detalhada da Hsp90 e sua implicação na terapia do câncer.

1.4 Co-chaperonas

As co-chaperonas são proteínas capazes de modular a atividade das chaperonas. Algumas co-chaperonas como as Hsp40 são, individualmente, chaperonas moleculares, devido à sua habilidade de prevenir a agregação de polipeptídeos (Caplan, 2003). Sob uma perspectiva funcional, as co-chaperonas são proteínas capazes de mediar a interação das chaperonas com uma determinada proteína cliente, apresentando-a para Hsp90 e/ou Hsp70, e então coordenando o ciclo de ligação e liberação pelas chaperonas de maneira a facilitar o enovelamento/manutenção ou a desagregação proteicas.

Em eucariotos, a Hsp90 é, frequentemente, encontrada em grandes complexos com co-chaperonas, que por sua vez, exercem efeitos diversos nas funções da Hsp90. As co-chaperonas atuam recrutando diferentes proteínas clientes para a Hsp90, regulando seu ciclo conformacional e de hidrólise de ATP, e subsequentemente controlando o enovelamento de proteínas clientes (Krukenberg et al., 2011). Fazendo-se uma comparação genômica das co-chaperonas da Hsp90, é possível detectar que os organismos possuem uma compilação singular de co-chaperonas, sugerindo que essas combinações específicas de co-chaperonas são capazes de adequar a atividade da Hsp90 para melhor se adaptar às condições de cada organismo em particular (Johnson & Brown, 2009).

Algumas co-chaperonas como a Aha1 (*activator of Hsp90 ATPase 1*), a p23 – também conhecida como PTGES3 (*prostaglandin E synthase 3*), a Hop (*Hsp70/Hsp90 organizing protein*, também chamada Sti1 ou p60) e a p50 ou Cdc 37 (*cell division cycle 37 homologue*), modulam o ciclo da Hsp90 afetando a dinâmica conformacional da proteína (Panaretou et al., 2002; Ali et al., 2006;

Onuoha et al., 2008; Forafonov et al., 2008; Mickler et al., 2009). Esse tipo de modulação é bastante importante, pois regula o tempo de permanência das proteínas clientes no complexo chaperona.

Algumas co-chaperonas são adaptadores que entregam clientes específicas à Hsp90. Por exemplo, a p50/Cdc37 entrega proteínas cinases; a Hop, por sua vez, participa da entrega de receptores de hormônios esteróides à Hsp90 (Smith & Workman, 2009; Trepel et al., 2010). Outras co-chaperonas afetam a Hsp90 pois catalisam reações como a ligação de ubiquitina (a ubiquitina ligase E3 ou CHIP) e desfosforilação (a fosfatase PP5). A ubiquitinação de proteínas clientes da Hsp90, dependente da CHIP (*C-terminal Hsp70-interacting protein*), as direciona para o complexo proteassoma, encurtando ciclos adicionais de renovelamento mediado por chaperonas (Trepel et al., 2010). Em células, a desfosforilação da Cdc37 mediada pela PP5 regula a habilidade da Hsp90 interagir com a proteína cinase Raf1, inibe a ativação MAPK dependente da Raf1 e sensibiliza as células para inibição da Hsp90 (Vaughan et al., 2008).

A expressão de co-chaperonas também está envolvida com a sensibilização de células cancerígenas a inibidores da Hsp90. A deleção da p23 em levedura, causa hipersensibilidade aos inibidores geldanamicina e radicicol (McDowell et al., 2009), e a super-expressão da co-chaperona, como visto no câncer, protege a célula da ação desses compostos (Forafonov et al., 2008). De modo similar, o silenciamento gênico da Aha1 e Cdc37, que também são super-expressas em câncer (Smith & Workman, 2009), sensibiliza as células para geldanamicina e 17-AAG (derivado da geldanamicina) (Gray et al., 2007; Holmes et al., 2008). Assim, co-chaperonas e/ou sua interação com a Hsp90 podem ser

eleitas como excelente alvo para terapias anti-câncer, especialmente quando combinada com inibidores da Hsp90 (Holmes et al., 2008).

Quanto à sua classificação, embora haja mais de 100 co-chaperonas diferentes em mamíferos, a maioria delas pode ser classificada em duas classes principais, baseada na estrutura de seus domínios. São as “Domínio-J” encontradas nas Hsp40, co-chaperonas da Hsp70 e as que apresentam unidades repetitivas de tetratricopeptídeos (TPR), co-chaperonas que interagem com a Hsp70 (no motivo C-terminal IEEVD) e com a Hsp90, no motivo C-terminal: MEEVD, como a Hop, Tom70 e CHIP, por exemplo (Caplan, 2003).

1.5 Hop

A Hop (*Hsp70/Hsp90-organizing protein*) a princípio identificada em levedura como Sti1 – *stress inducible protein 1* (Nicolet & Craig, 1989), é capaz de se associar diretamente à ambas chaperonas, Hsp70 e Hsp90 e também medeia a associação entre elas, que é dependente da hidrólise de ATP e troca ADP/ATP (Chen & Smith, 1998; Hernandez et al., 2002; Carrigan et al., 2006; Gonçalves et al., 2010).

A ligação da Hop às chaperonas moleculares Hsp70 e Hsp90 ocorre por meio de múltiplos domínios TPR, cada um é formado por motivos TPR, com estrutura hélice-volta-hélice com 34 resíduos aminoácidos (Blatch & Lassel, 1999; Smith, 2004). A Hop possui três domínios TPR: TPR1, TPR2A e TPR2B, intercalados com repetições de resíduos de ácido aspártico e prolina (DP) no seguinte arranjo: TRP1-DP1-TPR2A-TPR2B-DP2. A interação entre o motivo MEEVD da Hsp90 ocorre com o TPR2A (Figura 4).

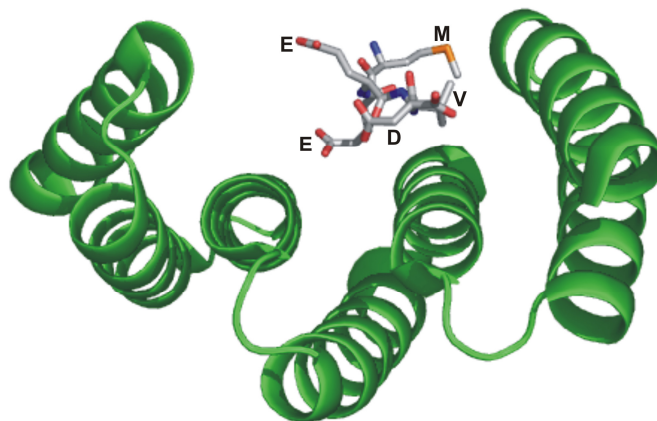


Figura 4: TPR2A da Hop em complexo com o MEEVD da Hsp90. Estrutura cristalográfica do domínio TPR2A da Hop humana em complexo com o pentapeptídeo MEEVD da Hsp90. Número de acesso ao PDB: 1ELR. (Figura retirada de Gava et al., 2011).

A Hop otimiza a interação entre Hsp70 e Hsp90 que requer interações altamente coordenadas para o enovelamento e regulação conformacional de uma variedade de proteínas. O complexo Hop-Hsp70-Hsp90 está envolvido no enovelamento e maturação de proteínas regulatórias essenciais para a viabilidade celular (Wegele et al., 2004), como hormônios esteróides, fatores de transcrição e cinases, algumas dessas estão envolvidas na progressão do câncer (Kubota et al., 2010); a Hop também está envolvida na estabilização de proteínas do prion (Zanata et al., 2002).

Os domínios TPR ligam chaperonas e outras proteínas do sistema em redes cooperativas e podem participar da ação da Hsp90 como um estabilizador do fenótipo cancerígeno, nesse sentido, complexos TPR-Hsp90 são potenciais alvos para drogas. Adicionalmente, a presença de múltiplos domínios TPR permite que a Hop possa ligar, simultaneamente, os sítios EEVD da Hsp70 e Hsp90

O papel da Hop em progressão tumoral ainda não está completamente esclarecido, mas existem relatos de super-expressão da Hop em alguns tipos de carcinoma (Sun et al., 2007; Kubota et al., 2010). Recentemente, Walsh e colaboradores, por meio de experimentos de *knockdown* reportaram a Hop como um potencial alvo terapêutico para o tratamento de câncer pancreático (Walsh et al., 2011). Nesse sentido, o rompimento ou impedimento do complexo Hop-Hsp90 pode ser um novo alvo para anular as vias de estabilização de proteínas do câncer dependentes da Hsp90.

1.6 Tom70

A mitocôndria é crucial para a bioenergética de células eucarióticas, também está envolvida em diversos processos celulares importantes, incluindo a síntese de metabólitos, o metabolismo de lipídeos, produção de radicais livres e homeostase de íons metálicos (Pfanner et al., 2004; Wu & Sha, 2006). Em humanos, há cerca de 1500 proteínas diferentes na mitocôndria que embora contenha um sistema gênico completo na matriz mitocondrial, tem apenas ~1% de suas proteínas codificadas pelo seu genoma e sintetizada em sua matriz. A grande maioria das proteínas mitocondriais é codificada por genes nucleares e sintetizada como proteínas precursoras nos ribossomos no citosol (Endo et al., 2003; van der Laan et al., 2010).

As proteínas precursoras possuem regiões ou sequências sinalizadoras que são reconhecidas por receptores ou translocases da membrana mitocondrial externa, designados Tom (do inglês, *Translocase of the mitochondrial outer membrane*), que formam o complexo TOM. O complexo TOM tem dois receptores integrais de membrana, Tom20 e Tom70. A Tom20 reconhece a sequência sinalizadora anfipática do N-terminal de proteínas precursoras via interações

hidrofóbicas (Brix et al., 1997; Abe et al., 2000; Chacinska et al., 2009); enquanto a Tom70 liga sequências sinalizadoras hidrofóbicas no interior dessas proteínas, muitas dessas são carreadores de metabólitos da membrana interna (Brix et al., 1997; Ryan et al., 1999; Chacinska et al., 2009). Após a interação com esses receptores, as proteínas são encaminhadas para o poro de translocação Tom22-Tom40, também chamado de complexo GIP (do inglês *general import pore*); e então são classificadas e destinadas ao sub-compartimento apropriado; há ainda duas translocases na membrana interna, a Tim22 e Tim23 (Chacinska et al., 2009).

A via de importação mediada pela Tom70 é dependente de chaperonas (Figura 5). Antes da importação, as proteínas precursoras dependentes da Tom70 interagem com as chaperonas citosólicas Hsp70 e Hsp90, e com as co-chaperonas DnaJA1 e DnaJA2 (Young et al., 2003; Fan et al., 2006; Bhangoo et al., 2007; Fan et al., 2010). Hsp70 e Hsp90 executam um papel importante ao endereçar essas precursoras ao complexo TOM (Young et al., 2003), também protegem as proteínas precursoras da agregação e/ou desenovelamento, enquanto permanecem no citosol (Beddoe & Lithgow, 2002).

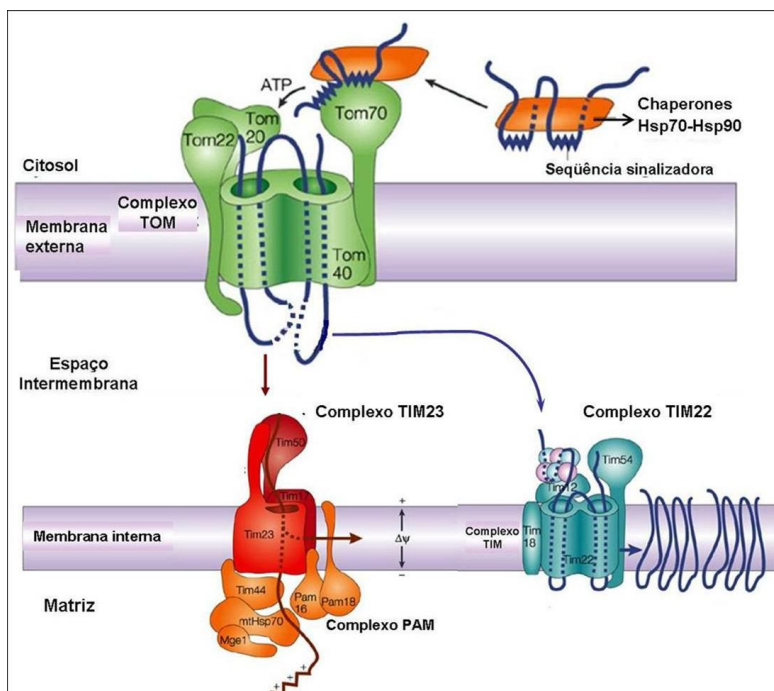


Figura 5: Papel das chaperonas e co-chaperonas na translocação de proteínas para a mitocôndria. No esquema estão mostrados os complexos TOM e TIM. Nesse esquema (no citosol) está em foco o reconhecimento de proteínas precursoras pela Tom70, essas proteínas são mantidas estáveis no citosol e apresentadas à Tom70 pelas chaperonas citosólicas Hsp70 e Hsp90 (Figura retirada e adaptada de Rehling et al., 2004).

A Tom70 contém um domínio N-terminal transmembrana seguido por um domínio TPR citosólico (também chamado de grampo TPR ou *TPR clamp*), que foi caracterizado estruturalmente pela primeira vez para a co-chaperona Hop (Scheufler et al., 2000). Esse domínio TPR serve como um sítio de interação para a Hsp70 e Hsp90 e, portanto para complexos multi-chaperona contendo a proteína precursora. A Tom70 contém onze motivos TPR que estão agrupados em dois domínios. A Tom70 humana contém 608 resíduos de aminoácidos, sendo que a região citosólica da proteína engloba os resíduos 111 a 608. Na região N-terminal da porção citosólica estão três motivos TPR que formam um encaixe para a interação com o peptídeo EEVD das chaperonas Hsp70/Hsp90 (Figura 6),

já o domínio C-terminal da Tom70 contém um bolsão de ligação à proteína precursora (Wu & Sha, 2006; Li et al., 2009; Fan & Young, 2011).

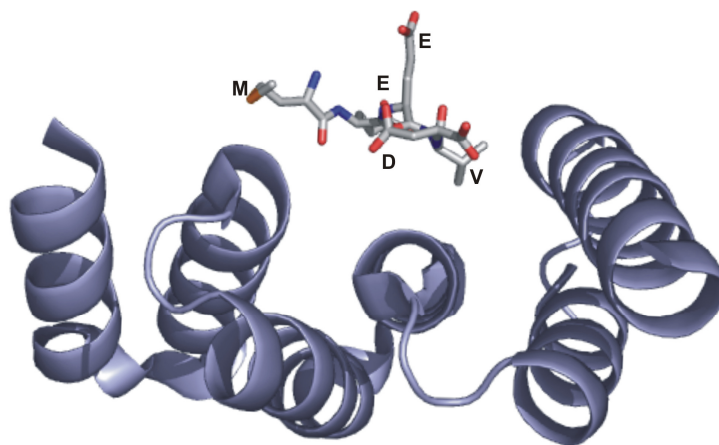


Figura 6: Estrutura do domínio TPR da Tom71 em complexo com o MEEVD. Estrutura cristalográfica da Tom71 de levedura. Representação do domínio TPR que interagem com o pentapeptídeo MEEVD da Hsp90. Número de acesso ao PDB: 3FP2. (Figura retirada de Gava et al., 2011).

Nesse trabalho foi utilizada apenas a porção citosólica da proteína Tom70 humana recombinante, cuja sequência está apresentada na figura 7 a seguir.

- A)** MAASKPVEAAVVAAPVPS SSGSGVGGGTTAGPPTGGLEPRWQLALAVGAPLLL GAGAIYLWSRQQRRREA
RGRGDASGLKRN SERKTPEGRAS PAPGSGHPEGPGAHLDMNS LDRAQAANKNGNKYFKAGKYEQAIQC
YTEAISLCPTKNDLSTFYQNRAAAFEQLQKWKEVAQDCTKAVELNPKYVKALFRRAKAHEKLDNKK
ECLEDVTAVCILEGFQNQQSMLLADKVLKLLGKEKAKEKYKNREPLMSPQFIKSYFSSFTDDII SQP
MLKGEKSDKDEKKEGEALEVKENSGYLKAKQYMEENYDKI I SECSKEIDAEGKYMAEALLLRATFYLL
LIGNANAAPDLKVI SLKEANVKLRANALIKRGS MYMQQQPLLSTQDFNMAADIDPQNADVYHHRG
QLKILLDQVEEAVADFD ECI RLRPE SALAQAKCFALYRQAYTGNNSSQIQAAAMKGFEEVIKFFPRCA
EGYALYAQALTDQQQFGKADEMYDKCIDLEPDNATYVHKGLLQLQWKQDLDRGLELISKAI EIDNKC
DFAYETMGTIEVQRGNMEKAIDMFNKAINLAKSEMMAHLYSLCDAAHAQTEVAKKYGLKPPTL
- B)** MSYYHHHHHDYDIPTTENLYFQGALDRAQAANKNGNKYFKAGKYEQAIQCYTEAISLCPTKNDLST
TFYQNRAAAFEQLQKWKEVAQDCTKAVELNPKYVKALFRRAKAHEKLDNKKKECLEDVTAVCILEGFQ
NQQSMLLADKVLKLLGKEKAKEKYKNREPLMSPQFIKSYFSSFTDDII SQPMLKGEKSDKDEKKEGEA
LEVKENSGYLKAKQYMEENYDKI I SECSKEIDAEGKYMAEALLLRATFYLLIGNANAAPDLKVI S
LKEANVKLRANALIKRGS MYMQQQPLLSTQDFNMAADIDPQNADVYHHRGQLKILLDQVEEAVADFD
ECI RLRPE SALAQAKCFALYRQAYTGNNSSQIQAAAMKGFEEVIKFFPRCAEGYALYAQALTDQQQFG
KADEMYDKCIDLEPDNATYVHKGLLQLQWKQDLDRGLELISKAI EIDNKCDFAYETMGTIEVQRGNM
EKAIDMFNKAINLAKSEMMAHLYSLCDAAHAQTEVAKKYGLKPPTL

Figura 7: Sequência de aminoácidos da proteína Tom70 humana. A) Sequência de aminoácidos da proteína Tom70 humana completa. Em cinza estão representados os resíduos de aminoácidos da região transmembrana da proteína; B) Sequência de

aminoácidos da proteína Tom70 humana recombinante, porção citosólica. Em vermelho estão representados os resíduos de aminoácidos da cauda de poli-histidina presente da proteína recombinante utilizada nesse trabalho.

Como discutido anteriormente, a elucidação da estrutura e modo de ação dessas co-chaperonas assim como o entendimento da interação dessas com a chaperona Hsp90, é um alvo de estudo bastante interessante. E o posicionamento desse sistema como um alvo para terapias de doenças, como o câncer, torna tal investigação ainda mais relevante para compreender como interferir nessas interações TPR-Hsp90, usando tal interferência como uma estratégia para impedir a entrega e repasse de proteínas clientes da Hsp90.

Na seção a seguir está apresentado o artigo de revisão “A Hsp90 como um alvo para a terapia do câncer” (*Human 90 kDa Heat Shock Protein Hsp90 as a Target for Cancer Therapeutics*), parte integrante da introdução da tese. Essa revisão aborda as chaperonas moleculares sob um ponto de vista geral e seu envolvimento em doenças. Nesta revisão existe uma abordagem detalhada sobre a Hsp90 no que diz respeito à sua estrutura, função e interação. A implicação da Hsp90 no câncer também é discutida, abordando os inibidores conhecidos e testados para a Hsp90 no tratamento do câncer.

Human 90 kDa Heat Shock Protein Hsp90 as a Target for Cancer Therapeutics

Lisandra M. Gava^{1,2} and Carlos H.I. Ramos^{*,2}

¹Institute of Biology and ²Institute of Chemistry, University of Campinas-UNICAMP, P.O. Box 6154, 13083-970, Campinas, SP, Brazil

Abstract: Protein misfolding causes a phenotype of disorders that is modulated by the action of multi-complexes formed by molecular chaperones and the proteasome machine. Hsp90 is a molecular chaperone involved in maintaining folding, stability and function of many proteins involved in apoptosis, signal-transduction pathways and cell-cycle regulation. Many of these proteins are usually deregulated in cancers and by keeping them active Hsp90 helps the stabilization of tumorigenic cells. Therefore, inhibition of Hsp90 will result in degradation of its client proteins *via* the proteasome followed by a down regulation of several properties of the malignant phenotype. As a consequence, Hsp90 has been considered to be an appealing target for cancer therapeutics because its inhibition can affect multiple oncogenic pathways simultaneously. Major efforts have generated Hsp90 inhibitors that passed Phase I clinical trials and have entered Phase II trials. Furthermore, other compounds are in development to improve efficacy as antitumor agents. In conclusion, the development of Hsp90 inhibitors is considered to be a good example of medicinal chemistry. Specific important aspects of Hsp90 structure and function, the role of the chaperone in cancer and the development of Hsp90 inhibitors that causes growth arrest and apoptosis in cancer cells are discussed.

Keywords: Hsp90 inhibitors, molecular chaperone, cancer therapeutics, geldanamycin, antitumor drugs, medicinal chemistry.

1. CHAPERONES AND PATHOLOGY

The necessary information for a protein to fold to its native conformation lies in the amino-acid sequence (for a specific review see [1]). However, efficient reversible folding and unfolding has been usually observed only for small proteins whereas for many others, refolding experiments result in partially unfolded, or even completely misfolded molecules, and in aggregation. Aggregation is unproductive since the function of most proteins is ordinarily related to its native conformation, although Intrinsically Unfolded Proteins, or IUP, seem to have cellular functions [2]. Protein aggregation has become a general problem because any protein sequence has the potential to form amyloid fibrils given the appropriate conditions [3,4]. In agreement with the aforementioned, the deleterious effect of aggregates has been connected to major pathological effects and tissue deposition of protein aggregates *in vivo* causes degenerative diseases and organ damage [5]. There are two aspects of protein folding in the cellular context that further aggravate the pathological effects of protein misfolding. Protein aggregation is enhanced by crowding effects inside the cell [6] and aggregates may become infectious by promoting aggregation of native conformers as is the case with prions [7].

Inside the cell the folding of many proteins is assisted by molecular chaperones that are also referred to as heat-shock proteins (Hsp) for being first described as proteins induced during thermal stress [8-10]. In a general way, molecular chaperones help other proteins to fold and are considered cellular housekeepers due to their capability of activating

cellular processes by regulating the folding/function of key proteins. For instance, when cells are submitted to an increase in temperature, a heat-shock response (HSR) is activated and mRNAs related to Hsps are detected subsequently. The importance of molecular chaperones for the organism can also be evaluated by the high number of genes belonging to molecular chaperones present in the genome and the high expression of these genes. Take plants for instance, their cells trigger the expression of molecular chaperones to increase their chance of survival in the extreme environmental stress to which they are usually exposed. The genome of the model plant *Arabidopsis thaliana* has been sequenced and the gene expression profile, measured by RNA expression, of many plants, among them sugarcane and eucalyptus, have been investigated. The data provided by these works can be mined specifically for molecular chaperones and used to generate new information about them (The TIGR *Arabidopsis thaliana* Database: <http://www.tigr.org/tdb/e2k1/ath1/>; [11, 12, 13]). The general picture from the mined data is that about 20% of the expressed molecular chaperones belong to the Hsp70 family, about 20% to Hsp70 co-chaperones and about 10% to the Hsp90 family. This result emphasizes the importance of Hsp70 and Hsp90 as regulators of many cellular processes.

Molecular chaperones also have a prophylactic action because they prevent proteins with aggregative potential to form amyloid fibrils. In addition to that, some specialized molecular chaperones have the ability to dissolubilize aggregates, a powerful characteristic that opens the possibility to use them as therapeutics against diseases caused by misfolded proteins. It is conceivable that an accumulation of misfolded proteins with time would overload the chaperone system accounting for the increase in the number of diseases verified in the elderly [14]. Consequently, some researchers

*Address correspondence to this author at the Institute of Chemistry, University of Campinas-UNICAMP. P.O. Box 6154, 13083-970, Campinas, SP, Brazil; Tel: 55-19-3521-3144; Fax: 55-19-3521-3023; E-mail: cramos@iqm.unicamp.br

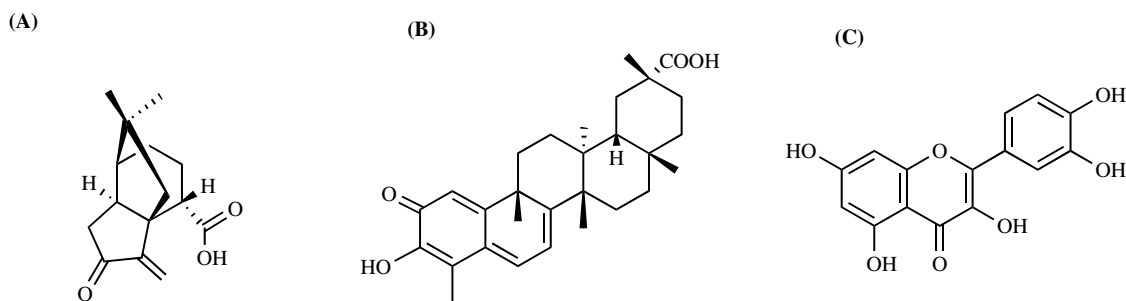


Fig. (1). (A) Terrecyclic acid A, (B) celastrol and (C) quercetin.

have pointed out that misfolded proteins would play a role in the manifestation of as much as half of the human diseases (see Reference [15] and references therein). We may conclude that a complex formed by molecular chaperones and the proteasome (responsible for protein degradation) constitute the quality control system that deals with proper protein folding and degradation. This complex system would then modulate the phenotype of disorders caused by protein misfolding.

Protein misfolding causes both the loss of function, as in the case of some cancer diseases, and again of damaging function, as in the case of Alzheimer and Parkinson diseases. These deleterious actions motivate developing small molecules capable of manipulating chaperones and protein homeostasis. As an example, compounds that could induce a high expression of molecular chaperones would be important as therapeutic agents to increase the yield of correctly folded proteins and to decrease the number of aggregates in pathological conditions.

The heat shock response (HSR) is transcriptionally regulated by heat shock factors (HSFs) that triggers the expression of molecular chaperones. There are three HSFs in humans: HSF1, HSF2 and HSF4. Several chaperones, most importantly Hsp70 and Hsp90, were shown to bind to HSF1 and keep it in an inactive form. In a situation of stress mis-

folded proteins compete with HSF for the binding site consequently releasing HSF that migrates to the cell nucleus [16]. HSF1 is activated by proteasome inhibitors, by molecules that regulate inflammation and by Hsp90 inhibitors (see below). Some compounds that increase the action of HSF are in clinical trials and had positive impact on oxidative stress and on some cancers [17,18]: terrecyclic acid A [19], celastrol [20], and quercetin [21,22] (Fig. 1). The aforementioned compounds have also critical importance when considering targeting Hsp90 for chemotherapy [18].

2. STRUCTURE, INTERACTION AND FUNCTION OF HUMAN HSP90

Hsp90 is a specialized ATP-dependent protein folding tool, which is essential for the growth of eukaryotic cells [23]. This chaperone is a homodimer and each monomer consists of a highly conserved N-terminal domain (~30 kDa) that contains an ATP-binding site followed by a charged region of unknown function, a flexible domain located in the middle (~35 kDa) and a C-terminal domain (~20 kDa) that is responsible for dimerization (Fig. 2). The N-terminal ATPase domain has a regulatory pocket that binds and hydrolyzes ATP to mediate a series of association-dissociation cycles between Hsp90 and client proteins. This domain contains the Bergerat-fold, in which the nucleotide adopts a bent shape, and was previously found in bacterial gyrases and

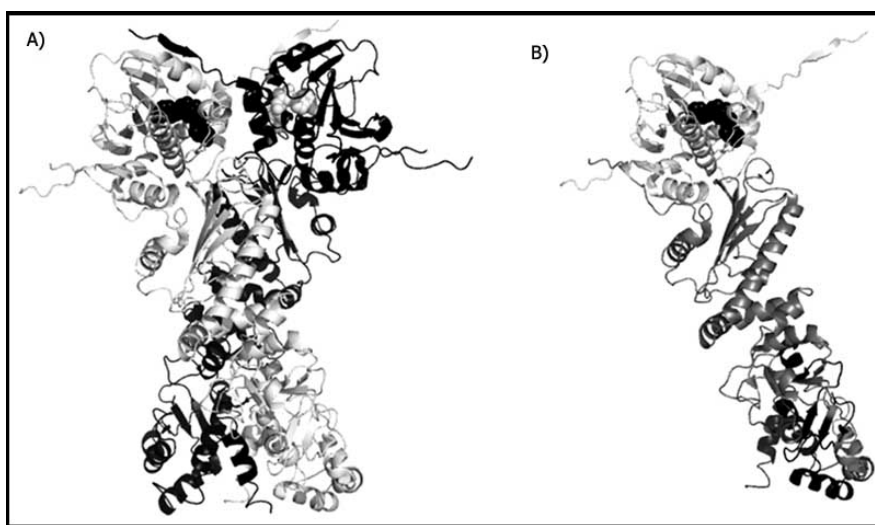


Fig. (2). Tertiary structure of Hsp90 from *Saccharomyces cerevisiae* which is 82% similar to human Hsp90 α . A) One monomer is in black and the other in white. B) Top white: N-terminal domain residues (2-216), middle gray: central domain residues (262-560) and bottom black: C-terminal domain residues (561-677). AMP-PNP is represented by spheres. PDB accession number 2CG9. All molecular graphics were produced with PyMOL (<http://pymol.sourceforge.net/>).

topoisomerases [24,25]. A second nucleotide-binding site is also present at the C-terminal of Hsp90 [26-28] (see below).

Fig. (3) shows the crystal structure of the N-terminal of Hsp90 both in the apo form and bound to ADP. The N-terminal domain of Hsp90 is composed of nine helices and eight strands of antiparallel β sheets that together fold into an $\alpha+\beta$ sandwich, in which a deep pocket is formed by the residues involved with ATP/ADP binding (Fig. 3). This pocket has diverse hydrophobic and polar character and the residues involved in binding either directly or throughout water-mediated hydrogen bonds are Leu48, Asn51, Asp54, Ala55, Lys58, Ile91, Asp93, Ile96, Gly97, Met98, Asn106, Leu107, Lys112, Gly135, Phe138, Val150, Thr184 and Val186 [25,29,30].

Despite being an heat-shock protein, Hsp90 is ubiquitously expressed under normal conditions and corresponds to about 1-2% of total cellular protein content making them one of the most abundantly expressed cytoplasmic proteins in several organisms [31]. As a matter of fact, the Hsp90 family is highly expressed in plant cells, 10-20% of all 5'EST annotated to molecular chaperone category in eucalyptus and sugarcane belonging to Hsp90 [11]. The Hsp90 homolog in bacteria (HtpG) is non-essential whereas eukaryotic cytosolic Hsp90 is essential and accomplishes numerous roles. In addition to that, there are different isoforms of Hsp90 in the human cell [32]. Most relevant for this review are the cytosolic isoforms Hsp90 α (gene HSP90AA1), which is heat-inducible and Hsp90 β (gene HSP90AB1), which is constitutive (Fig. 4). They have different roles, e.g. Hsp90 α is involved in cancer cell invasiveness [33] but there is still much to be known about the biological functions of the different isoforms of Hsp90.

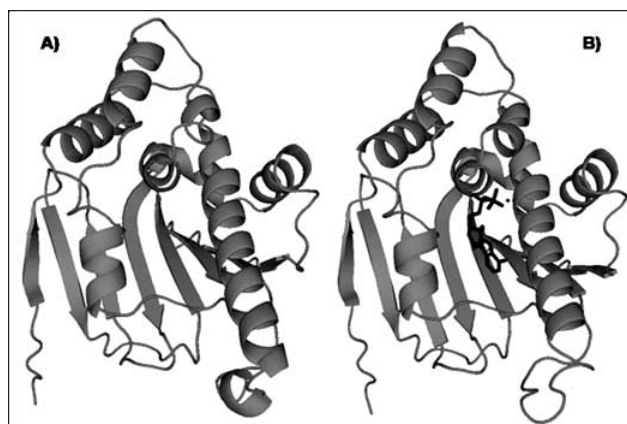


Fig. (3). Crystal structure of the N-termini of Hsp90 in the apo form (PDB accession number 1YES) and bound to ADP (PDB accession number 1BYQ). The N-terminal domain of Hsp90 is composed of nine helices and eight strands of antiparallel β sheets that together fold into an $\alpha+\beta$ sandwich. Residues involved either directly or throughout water-mediated hydrogen bonds are Leu48, Asn51, Asp54, Ala55, Lys58, Ile91, Asp93, Ile96, Gly97, Met98, Asn106, Leu107, Lys112, Gly135, Phe138, Val150, Thr184 and Val186 [25]. Not all residues are shown.

One basic property of chaperones is their ability to specifically target and form complexes with other chaperones. Hsp90 collaborates with Hsp70 to form a multi-chaperone machinery, which is a dynamic, multifunctional and multicomponent system that plays a pivotal role in protecting biological organisms from environmental and genetic stresses [34]. Although Hsp70 and Hsp90 are sufficient for folding their functions are amplified by the help provided by

	10	20	30	40	50	60	70	80	90	100	110	120																																																																																																					
Hsp90 α	MPEETQ	ODOPNE	EEVEVTF	AFQAEIA	QLSLII	INTFY	SNKEIF	LRELIS	NSDALD	KIRYES	SLTDP	SKLDSG	KELHIN	LPNKQ	RTLT	IVDTG	IGHTK	ADL	INN	LGTIA	KSGTK	AFNE																																																																																											
Hsp90 β	MPEEVH	-----	HGEEVE	VTFAFQ	AEIAQL	LSLII	INTFY	SNKEIF	LRELIS	NSDALD	KIRYES	SLTDP	SKLDSG	KELKID	IIPN	QERTL	TIVDT	GIGHT	KADL	INN	LGTIA	KSGTK	AFNE																																																																																										
	10	20	30	40	50	60	70	80	90	100	110	120																																																																																																					
	130	140	150	160	170	180	190	200	210	220	230	240																																																																																																					
Hsp90 α	ALQAGAD	ISHIGQ	FVGFYS	AYLVAE	KVIVIT	KHNDDE	QYANESS	AGGSF	TVRDT	GEP	MGRG	TKVIL	HLKED	QTEYLE	ERRIKE	IVKKS	QF	I	GYP	ITL	FV	KERD	KEVSD	DEAE	EKEED																																																																																								
Hsp90 β	ALQAGAD	ISHIGQ	FVGFYS	AYLVAE	KVVVIT	KHNDDE	QYANESS	AGGSF	TVRADH	GEP	IGRGT	KVIL	HLKED	QTEYLE	ERRR	KEVVK	KSQF	I	GYP	ITL	YLE	KERE	KE	IS	DEAE	EEEEK																																																																																							
	120	130	140	150	160	170	180	190	200	210	220	230																																																																																																					
	250	260	270	280	290	300	310	320	330	340	350	360																																																																																																					
Hsp90 α	KEEEEK	KEEKE	SEDKPE	IEDV	GSDEE	EEKKG	DKKKKK	KIKKEY	IDQEEL	NKTKP	I	WTRN	PDD	ITNEE	YGEF	YKSL	TND	WED	HL	AV	KHF	SVE	GQLE	F	RALL	FV	PR	AP	FDL	FEN	RKK	KNN																																																																																	
Hsp90 β	---EKEE	KDD	EEKPK	IEDV	GSDEE	DDSG	RDKKK	TKIKKEY	IDQEEL	NKTKP	I	WTRN	PDD	ITQEE	YGEF	YKSL	TND	WED	HL	AV	KHF	SVE	GQLE	F	RALL	F	IP	RA	FDL	FEN	RKK	KNN																																																																																	
	240	250	260	270	280	290	300	310	320	330	340	350																																																																																																					
	370	380	390	400	410	420	430	440	450	460	470	480																																																																																																					
Hsp90 α	IKLV	YRVF	INDN	CEEL	IPEY	LNF	IRGV	VDS	EDL	PLNIS	REHL	QSKIL	KVIR	KNL	VKRC	LEL	F	TEL	AED	KEN	YK	F	YQ	F	SKNI	I	KL	G	H	E	D	S	Q	N	R	K	L	S	E	L	L	R	Y	T	S	A	G	D	E	N	V	S	L	K	D	Y																																																									
Hsp90 β	IKLV	YRVF	INDS	CELI	IPEY	LNF	IRGV	VDS	EDL	PLNIS	REHL	QSKIL	KVIR	KNV	VKRC	LEL	F	SEL	AED	KEN	YK	F	Y	A	F	S	KNL	I	KL	G	H	E	D	S	T	N	R	R	L	S	E	L	L	R	Y	T	S	Q	S	G	D	E	N	T	S	L	S	E	Y																																																						
	360	370	380	390	400	410	420	430	440	450	460	470																																																																																																					
	490	500	510	520	530	540	550	560	570	580	590	600																																																																																																					
Hsp90 α	CTR	KENQ	KHII	YIT	GET	KDQ	VANS	AF	VER	L	R	K	H	G	L	E	V	I	H	I	E	P	I	D	E	Y	C	V	Q	L	K	E	F	E	G	K	T	L	V	S	V	T	K	E	L	E	L	P	E	D	E	E	E	K	K	K	E	K	T	F	E	N	L	C	K	I	N	K	D	I	L	E	K	K	V	E	K	V	V	S	N	R	L	V	T	S	P	C	C	I	V																						
Hsp90 β	VSR	KET	Q	K	S	I	Y	I	T	G	E	S	K	E	Q	V	A	N	S	A	F	V	E	R	V	R	K	R	G	F	E	V	V	Y	H	T	E	P	I	D	E	Y	C	V	Q	L	K	E	F	D	G	K	L	E	V	S	V	T	K	E	L	P	E	D	E	E	E	K	K	K	E	S	K	A	F	E	N	L	C	K	L	H	K	E	I	L	D	K	K	V	K	V	T	S	N	R	L	V	S	P	C	C	I	V									
	480	490	500	510	520	530	540	550	560	570	580	590																																																																																																					
	610	620	630	640	650	660	670	680	690	700	710	720																																																																																																					
Hsp90 α	T	S	T	Y	G	T	A	N	H	E	R	I	N	K	A	Q	A	L	R	D	N	S	T	H	G	Y	H	A	K	H	L	E	I	N	P	D	H	S	I	I	E	T	L	R	Q	K	A	E	A	D	K	N	D	K	S	V	K	D	L	V	L	L	F	E	T	A	L	L	S	S	G	F	S	L	E	D	P	Q	T	H	A	N	R	I	Y	R	H	I	K	L	G	L	G	I	D	E	D	D	T	A	D	T	S	A	A	V	T	E	N	P	P	L	E
Hsp90 β	T	S	T	Y	G	T	A	N	H	E	R	I	N	K	A	Q	A	L	R	D	N	S	T	H	G	Y	H	A	K	H	L	E	I	N	P	D	H	P	I	V	E	T	L	R	Q	K	A	E	A	D	K	N	D	K	V	K	D	L	V	L	L	F	E	T	A	L	L	S	S	G	F	S	L	E	D	P	Q	T	H	S	N	R	I	Y	R	H	I	K	L	G	L	G	I	D	E	V	A	A	E	P	N	A	V	P	D	E	I	P	P	L	E		
	600	610	620	630	640	650	660	670	680	690	700	710																																																																																																					
	730																																																																																																																
Hsp90 α	G	D	D	T	S	R	M	E	E	V	D																																																																																																						
Hsp90 β	G	D	E	A	S	R	M	E	E	V	D																																																																																																						

Fig. (4). Sequence alignment of human cytosolic Hsp90 isoforms, α and β , which are 86.8% identical. Multiple sequence alignment was performed by Clustal W (<http://align.genome.jp/>).

co-chaperones in modulation, acceleration, potentiation, and stabilization of folding (see Table 1 for a list of important co-chaperones involved with Hsp90). A list of K_D values for binding for selected Hsp90 factors can be found in Reference [35]. Hsp90 co-chaperones promote the interconversion of the ATP- and ADP-bound states and modulate the formation of client specific complexes [36].

In eukaryotes, the Hsp70-Hsp90 machinery is formed by Hsp70, Hsp90, and co-chaperones HOP, Hsp40 and p23. As a direct support to this hypothesis functional Hsp90-heterocomplex can be assembled *in vitro* by mixing the purified chaperones and co-chaperones listed above. The function of Hsp90 is driven by a dynamic association with its client proteins and their co-chaperones to form protein complexes. The tetratricopeptide repeat (TPR) is a degenerate 34-residue motif present in a subset of co-chaperones that binds Hsp90. TPR is formed by a compact helical domain of six consecutive α -helices arranged in a regular right-handed superhelix, generating an amphipathic groove that is capable of interacting with 7-12 residues of the polypeptide. The binding site for TPR is in the C-terminus where a domain formed by a MEEVD motif is present [37].

The Hsp90 chaperone is highly regulated. For instance, its ATPase activity regulates the substrate binding cycle and HOP inhibits this activity by preventing nucleotide binding. The high affinity state of Hsp90 for client proteins is switched to the lower affinity state by ATP binding, which hydrolyze the affinity back to high. The p23 co-chaperone recognizes Hsp90 bound to ATP and stimulates dissociation of the complex. In addition, Aha1 stimulates the ATPase activity of Hsp90 by about tenfold [38] and CHIP (C-terminus of Hsp70-interacting protein) connects Hsp90 to the ubiquitin complex, helping to control the degradation of proteins by the proteasome. As a matter of fact, there is evidence that in several tumor cell lines, Hsp90 might be exclusively bound to co-chaperones in a state of high affinity for nucleotide [39] (see below).

3. HSP90 AND CANCER

A recent and large-scale study using yeast as model [40] showed that at least 200 client proteins make physical interactions with Hsp90. One of the most important conclusions of this work is that Hsp90 is connected with a wide range of cellular functions. As examples of its diversity Hsp90 is involved in epigenetic gene regulation by interacting with proteins that are chromatin remodeling factors and Hsp90 participates in inherent genetic variation [41].

New client proteins for Hsp90 seem to be discovered continuously and an up to date list of Hsp90 'interactors' can be found at <http://www.picard.ch/DP/downloads/Hsp90interactors.pdf>. Important to the cancer therapeutics field is that signal transduction proteins including many kinases and steroid hormones are also clients of Hsp90, which maintains their conformation, stability and function [41-43]. These structurally labile signal transducers have a crucial role in cell cycle, growth control, apoptosis and developmental processes. In fact, the largest single group of Hsp90 client proteins are protein kinases such as oncogenic kinases c-Src, b-Raf, PKB/Akt1, ErbB2 and Cdk4 [44,45]. Many of them, like ErbB2, Src, Raf, and cyclin-dependent serine kinases are key players in malignant transformation [46,47]. Hsp90 is also necessary for the maturation of the nuclear hormone receptors and the hypoxia-inducible factor-1, and is associated with nitric oxide synthases and the antiapoptotic protein. The chaperone acts in regulating proteins involved in both the intrinsic and extrinsic apoptotic pathways [36] and the accumulation of mutant forms of the tumor suppressor transcription factor p53 [46,47].

Increased chaperone expression favors oncogenesis because they increase the chance that cancer cells survive in extreme environmental stress. For instance, free radicals generated by hypoxia and acidosis can cause significant physical damage to cellular proteins, which will be protected by the expression of molecular chaperones. Therefore, the fact that Hsp90 maintain its client proteins in an activated

Table 1. Important Hsp90 Co-Chaperones

Co-Chaperone	Class	Main Function	Ref.
p23	<i>Other</i>	Essential for assembly of stable steroid receptor heterocomplexes; coupling factor (ATPase inhibitor)	[118]
Cdc37	<i>Other</i>	Kinase-specific and co-chaperone	[119]
Aha1	<i>Other</i>	ATPase activator	[120]
HOP	<i>TPR</i>	Essential for assembly of stable steroid receptor heterocomplexes; Hsp70/Hsp90 adaptor protein	[121,122]
Tom70	<i>TPR</i>	Mitochondrial protein import	[123]
Sgt1	<i>TPR</i>	Binding partner (nucleotide-dependent)	[124]
Unc45	<i>TPR</i>	Myosin folding and assembly	[125]
FKBP51 FKBP52	<i>PP1ases</i>	Essential for assembly of stable steroid receptor heterocomplexes	[126]
Cyp40	<i>PP1ases</i>	Essential for assembly of stable steroid receptor heterocomplexes	[126,127]
PP5	<i>Hsp90 phosphatase</i>	Modulation of Hsp90 substrate maturation	[128]
CHIP	<i>Ubiquitin ligase</i>	Protein quality control system – protein labeling for degradation	[129,130]

state combined with the protective role of molecular chaperones toward damaged proteins help to stabilize tumorigenic cells. For that, Hsp90 has to have highly ATPase activity, which is usually potentiated by co-chaperones, thus it is worth noting that Hsp90 complexes from tumor cells are almost entirely bound to HOP and p23 [39].

Hanahan and Weinberg [48] proposed six essential alterations in cell physiology that are characteristic of most if not all cancers: self-sufficiency in growth signals, insensitivity to growth-inhibitory (antigrowth) signals, evasion of programmed cell death (apoptosis), limitless replicative potential, sustained angiogenesis, and tissue invasion and metastasis. Hsp90 is essential for the stability and function of many oncogenic client proteins which are usually deregulated in cancers and contribute to the hallmark traits of malignance aforementioned [49-51] (a small list of Hsp90 client proteins involved with malignance are summarized in Table 2). Oncogenic mutations increase the instability of the client proteins therefore requiring increased amounts of Hsp90. Thus, the Hsp90 action stabilizes mutated oncogenic proteins required for the transformed phenotype that would otherwise be lethal [41]. In conclusion, Hsp90 has the ability to maintain the functional conformations of mutant and aberrant oncoproteins and grants survival advantage to tumor cells.

Another important finding is that survivin, an apoptosis inhibitor and essential regulator of mitosis, is maintained by Hsp90. Disruption of the survivin-Hsp90 complex results in proteasomal degradation of survivin, mitochondrial-dependent apoptosis, and cell cycle arrest [52]. Therefore, the association between survivin and Hsp90 reduces the chance of apoptosis and promotes the proliferation of tumor cells. Hsp90 is also an important determinant of tumor cell invasion and metastasis because it is expressed in the surface of melanoma metastases and cell surface Hsp90 seems to be crucial for the invasiveness of sarcoma cells *in vitro* [33,53,54].

The information discussed above forms the basis for using Hsp90 as a target for cancer therapeutics because inhibition of Hsp90 will significantly weaken a cancer cell and will cause regression of tumor growth. Client proteins are degraded in the absence of the chaperoning activity of Hsp90 and consequently inhibition of the chaperone results in degradation of its client proteins *via* the ubiquitin-proteasome

Table 2. Important Hsp90 Client-Proteins Involved with Cancer

Client Protein	Function
ErbB2	Proliferation, differentiation, and oncogenesis
Bcr-Abl	Pathogenesis of chronic myelogenous leukemia
Akt/PKB	Anti-apoptosis
C-RAF	Growth factor independence
CDK4	Resistance to anti-growth signals
PLK-1	Mitotic regulator kinase
Mutant p53	Tumor suppressor
HIF-1 α	Angiogenesis stability
hTERT	Unlimited replicative potential

pathway. As a consequence, the down-regulation of signal being propagated via numerous signaling pathways and modulation of all aspects of the malignant phenotype will follow [50]. Therefore, Hsp90 provides a broader target for anticancer therapies than single, oncogenically activated signaling pathways. As a matter of fact, Hsp90 inhibition *in vitro* leads to growth arrest and apoptosis in cancer cells [51,55] and causes a defect in a number of proliferative signals, including the Akt-dependent survival pathway [56-58]. Hsp90 inhibition may also sensitize tumor cells against various attacks by helping their lysis under hypoxia and complement attack [59,60].

Hsp90 inhibitors, by interacting specifically with a single molecular target, the Hsp90 chaperone, causes the inactivation, destabilization, and eventual degradation of Hsp90 client proteins. As mentioned below, inhibitors of Hsp90 have shown promising antitumor activity in preclinical model systems [41,51]. The genetic knockout of Hsp90 in eukaryotes is lethal and therefore it was not obvious that the chaperone may be a target in disease. Nonetheless, compounds that target Hsp90 have the potential to treat cancers (see below).

4. THERAPY: INHIBITORS AND CLINICAL TRIALS

The Hsp90 inhibitors currently in clinical trial share the property of displacing nucleotide from their binding pocket located at the N-terminus of Hsp90. Therefore, these inhibitors promote a significant decrease in the activity of oncogenic kinases and disrupt the activity of numerous receptors and transcription factors that are known to be involved in oncogenesis. For such reasons, compounds that target Hsp90 have been identified as potential anticancer agents. In contrast to most direct inhibitors, which are often fairly specific for a given protein, Hsp90 inhibitors can affect multiple oncogenic pathways simultaneously. The ability to diminish the level of many protein targets in parallel is therapeutically attractive because they behave as typical multi-target drugs, a feature potentially more efficient than highly selective single-target drugs [61,62].

Important classes of compounds found to be inhibitors against Hsp90 mediated oncogenic in the last decade are summarized in Table 3. They are geldanamycin, its less toxic analogs, 17AAG and 17DMAG, radicicol and its more stable oxime derivatives, purine-scaffold inhibitors and novobiocin [41,49-51]. These compounds target the ATP-binding pocket and since ATP binds to the Bergerat fold in Hsp90, its inhibitors are likely to adopt a bent conformation as well to achieve high affinity binding. Fig. (5) shows the pocket that forms the ADP/ATP-binding site located at the N-terminus of Hsp90 in the apo form, in complex with ADP, with geldanamycin and with its analog 17-DMAG.

Now that the proof-of-principle regarding Hsp90 inhibitors has been established by several phase I trials, there are several efforts are underway to synthesize drug candidates with higher affinity for Hsp90 and in developing clinical assays to test these inhibitors. There is also an increase in the study of the crystal structure of Hsp90 with inhibitors to understand their mode of action and to screen potential ligands. For all these reasons and others mentioned elsewhere, the development of Hsp90 inhibitors is considered to be a good example of medicinal chemistry [50,51,63]. For a recent list

Table 3. Important Hsp90 Inhibitors

Inhibitor	Class	Binding
Geldanamycin	<i>ansamycin</i>	N-terminus
17-AAG	<i>ansamycin</i>	N-terminus
17-DMAG	<i>ansamycin</i>	N-terminus
Radicicol	<i>Macrocyclic antibiotic</i>	N-terminus
KF58333	<i>Oxime derivatives</i>	N-terminus
PU3 and analogs	<i>Purine scaffold</i>	N-terminus
Novobiocin	<i>Coumarins</i>	N- and C-termini
Cisplatin	<i>Platinum complex</i>	C-terminus

of Hsp90 drugs which are on clinical trials and their present status see Reference [64].

4.1. Geldanamycin

Geldanamycin (Fig. 6) is a benzoquinone microbial product classified as ansamycin antibiotic that competes with ATP for the N-terminal binding site of Hsp90 [65,66]. Although the antitumor property of this molecule has been known for a long time [67], its association with Hsp90 was discovered several years later [68]. Geldanamycin was shown to activate HSF [69] and consequently the expression of Hsp40, Hsp70 and Hsp90 [70].

Geldanamycin interferes with the Hsp90 function and generates proteosomal degradation of several key regulatory proteins, including tyrosine kinases and steroid receptors, many of which are involved in promoting malignancy [45,71]. This natural ligand also causes differentiation and

apoptosis in a cell-line-dependent manner [56] and its affinity for Hsp90 complexes from tumor cells is 100-fold higher than for Hsp90 from non-tumor cells. However, geldanamycin does not have acceptable pharmacological properties for clinical application because its solubility is low and it appears broadly cytotoxic. Geldanamycin causes acute hepatic necrosis and nephrotoxicity in dogs [72] and is also toxic for rats [73,74]. These results precluded testing in humans.

4.2. Geldanamycin Analogs

Stimulated by the low solubility and high cytotoxicity of geldanamycin additional natural products and natural product derivatives have been identified and developed to inhibit the Hsp90 protein folding machinery. An important review published in 2005 [63] informed that more than 500 compounds related to geldanamycin were reported at that time, some of them able to inhibit Hsp90 at femtomol levels [75].

One of the first Hsp90 inhibitors developed with lower toxicity was the geldanamycin analog 17-allylamino, 17-demethoxygeldanamycin (17-AAG) (Fig. 6). This analog has all the Hsp90-related characteristics of geldanamycin but shows lower toxicity [76-79]. 17AAG also activates HSF [69] and the expression of Hsp40, Hsp70 and Hsp90 [70] and downregulates several client proteins including Raf-1, cdk4 and Akt [80]. The National Cancer Institute initiated Phase I clinical trials with 17-AAG in 1999 that are now complete and several Phase II trials are in progress [62,71,79]. Also, the latest results with 17-AAG in breast cancer and melanoma are especially encouraging [81-83]. These trials demonstrate that 17-AAG inhibits the biological function of Hsp90 in patients with breast cancer, multiple myeloma and other cancers. Several preclinical studies have shown that 17-AAG may enhance the efficacy of a variety of chemotherapeutic agents. 17-AAG was combined with taxol to enhance cytotoxic effects on taxol-resistant ErbB2-

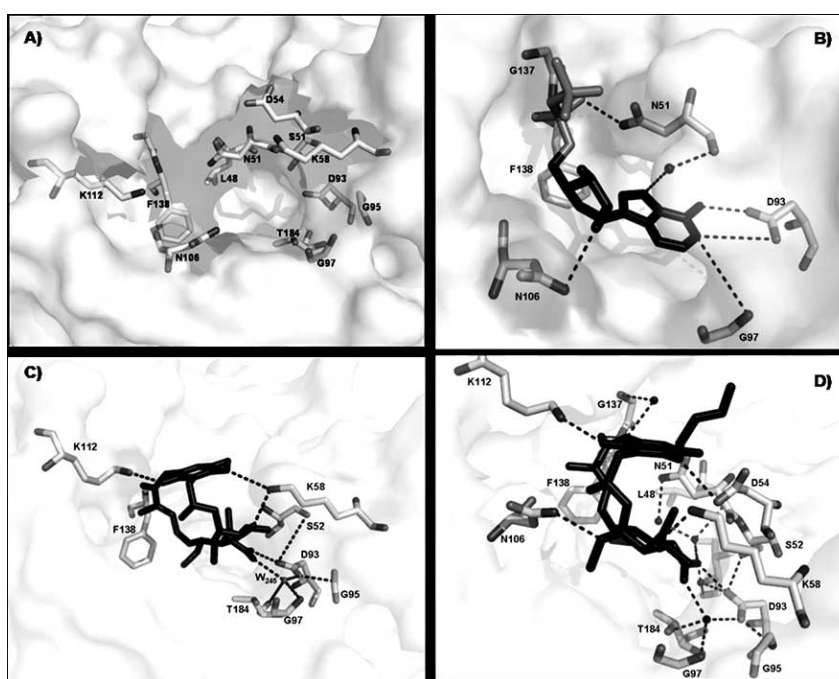


Fig. (5). Figure shows the pocket that forms the ADP/ATP-binding site located at the N-terminus of Hsp90 in the apo form (A), in complex with ADP (B), with geldanamycin (C) and with its analog 17-DMAG (D). PDB accession numbers: 1YES, 1BYQ, 1YET and 1OSF, respectively.

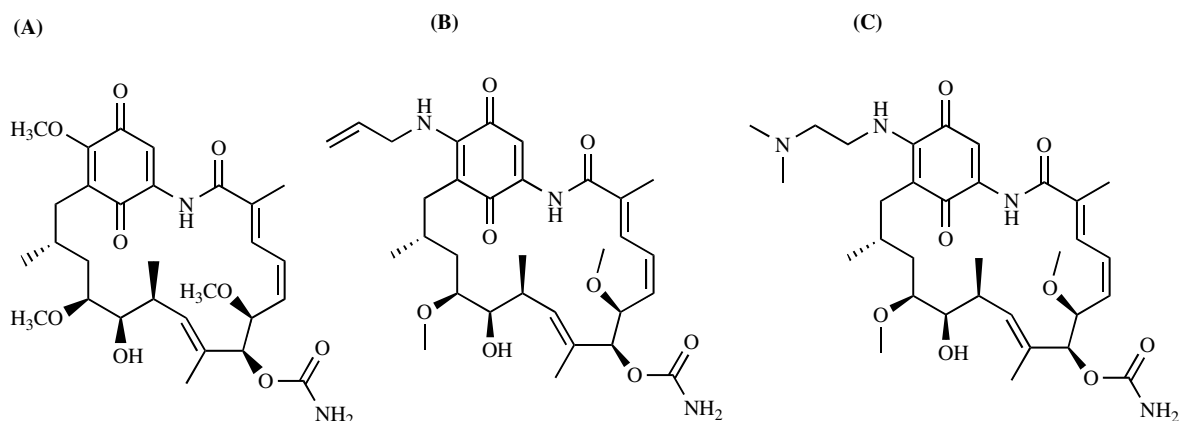


Fig. (6). (A) Geldanamycin and its analogs (B) 17-AAG and (C) 17-DMAG.

overexpressing breast cancer cells [56] and with angiogenesis inhibitors in breast tumors with encouraging results [84]. 17-AAG is also capable to potentiate both the *in vitro* and *in vivo* radiation response of cervical carcinoma cells [85]. However, there are several limitations with 17-AAG such as restricted solubility, hepatotoxicity, and its formulation, which is difficult to handle [50]. However, the positive clinical results with 17-AAG show that the Hsp90 target can be inhibited without causing unacceptable toxicity.

The development of another geldanamycin analog, 17-dimethylaminoethylamino-17-demethoxy-geldanamycin (17-DMAG) (Fig. 6) was made in an effort to improve the solubility and bioavailability of 17-AAG [51,63,82,86]. The depletion of Hsp90 was more pronounced in cells exposed to 17-DMAG than treated with 17-AAG, 17-DMAG is easier to formulate and since it is water soluble it has the potential to be orally bioavailable [86,87]. 17-DMAG has entered clinical trials.

The binding of 17-DMAG with human Hsp90 β has been studied in solution by a combination of Hydrogen/Deuterium techniques analyzed by mass spectrometry [88]. The results showed that peptide comprising residues 123-133, 201-208 and 620-635 of Hsp90 (Fig. 4) are protected in the presence of 17-DMAG. The results point to conformational changes in all three domains of Hsp90 caused by binding of 17-DMAG demonstrating that long-range effects are present. To sum up, the binding of the inhibitor induces a change both in the interaction between the C-terminal and middle domains and in the interface between the N-terminal and middle domains [88].

4.3. Radicicol, Purine Scaffold Inhibitors and Novobiocin

Radicicol (Fig. 7) is a 14-membered macrocyclic antibiotic isolated as an antibiotic of fungal origin [89] that has effects on tumor cells similar to those of ansamycins [90]. However, radicicol, as geldanamycin, is inactive *in vivo* due to its instability in serum and does not have acceptable pharmacological properties for clinical application. On the other hand, oxime derivatives of radicicol have potent anti-tumor activity *in vivo* via destabilization of the binding of Hsp90 with specific client proteins [91,92]. Oxime derivatives are more stable than radicicol, do not cause serious liver toxicity and work both *in vivo* and *in vitro* [93].

The binding of radicicol with human Hsp90 β has also been studied in solution by a combination of Hydrogen/Deuterium techniques analyzed by mass spectrometry [88]. The results showed that peptides comprising residues 123-133, 584-589, and 620-635 of Hsp90 (Fig. 4) are protected in the presence of radicicol and the Phenyl ring of Phe133 makes hydrophobic contact with the coplanar aromatic ring of radicicol. Also, the results for radicicol are in good agreement with those for 17-DMAG (see above) indicating that the different classes of inhibitors induce equivalent changes in the conformation of Hsp90.

The discovery of the antibacteriotoxic novobiocin (Fig. 7) as an Hsp90 inhibitor involved two important findings. One was the screening of a structurally distinct small molecule with affinity for Hsp90 and the second was the identification of an uncharacterized ATP binding site at the C-terminal domain of Hsp90. Novobiocin binds both to the N- and to

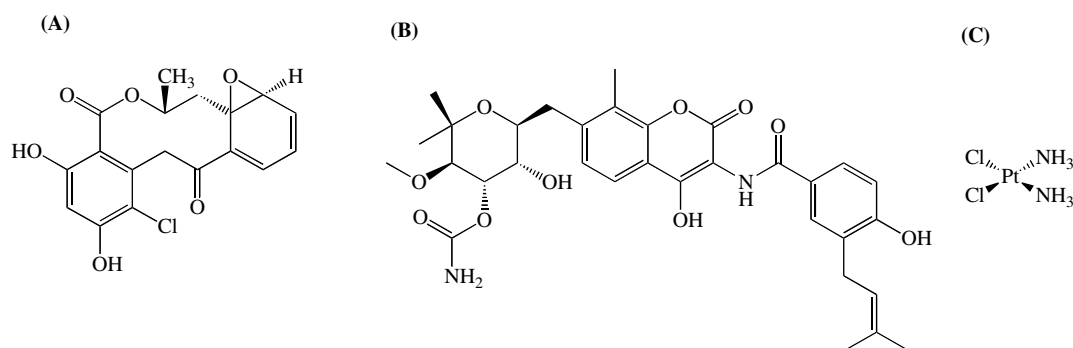


Fig. (7). (A) Radicicol, (B) novobiocin and (C) cisplatin.

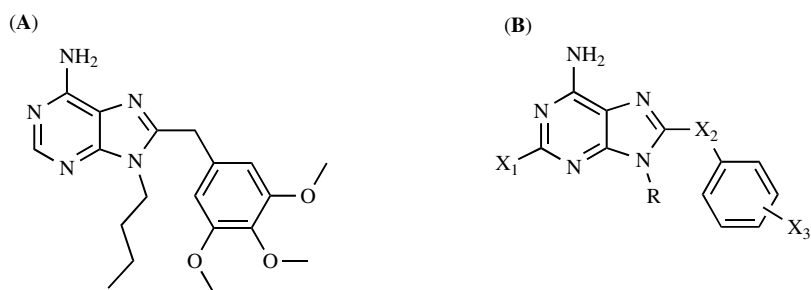


Fig. (8). Purine scaffold molecules. **(A)** PU3 and **(B)** analogs.

the C-termini of Hsp90 [26,28,94]. These findings were obtained using both competitive assays with geldanamycin and radicicol and deletion mutants consisting of either the N-terminal domain or the C-terminal domain. Novobiocin reduces the cellular level of several oncogenic protein kinases, including HER-2 and Raf-1, and inhibited the association of Hsp70 and p23 with Hsp90 [26,94]. Although the inhibitory action of novobiocin has been identified as very low, the development of novobiocin analogs for Hsp90 inhibition allowed the identification of compounds with higher potency that caused the degradation of several Hsp90 client proteins in both breast and prostate cancer cell lines [95]. Another compound, cisplatin (Fig. 7), is a selective C-terminal nucleotide competitor that strengthens the Hsp90-Hsp70 complex and has potential to be used as a model target to the development of new drugs against cancer using Hsp90 as target [28].

Chiosis and colleagues have designed small molecules that bind to Hsp90 by making use of existent crystallographic data [36,96,97]. These small-molecules use purine as scaffold and are highly potent Hsp90 inhibitors with improved drug-like properties (Fig. 8).

5. FUTURE DIRECTIONS

There are several new strategies and recently discovered compounds that have inhibitory action against Hsp90 and

potential to enter preclinical trials for antitumor characterization. A structure-based design approach has been used to generate potent resorcinolic pyrazole/isoxazole amide analogs as Hsp90 inhibitors with therapeutic potential that have entered Phase I clinical trials. These molecules have antiproliferative effects and cause induction of Hsp70 and Hsp27, depletion of client proteins, statistically significant growth inhibition and regressions in human tumor xenografts [98,99]. A new compound, macbecin (Fig. 9), compares favorably to geldanamycin, being more soluble, stable, and more potent. This quinone-containing Hsp90 inhibitor induces both tumor cell growth inhibition and the degradation of Hsp90 client proteins [100]. Tanespimycin, a 17-AAG derivative, in combination with trastuzumab [101] and IPI-504 [102] (Fig. 9) are improved formulations which are being used as Hsp90 inhibitors with relative success in clinical trials.

Although many new screening have been used to select new compounds with inhibitory action against Hsp90, the improvement of pharmacological properties and potency of the natural pharmacophores remains important. It is worth mentioning the use of phenolic derivatives of geldanamycin isolated from *Streptomyces sp* [103], the combination of 17AAG with carboplatin [104] (Fig. 9), and SNX-2112, which was selected by a purine-based affinity resin [105].

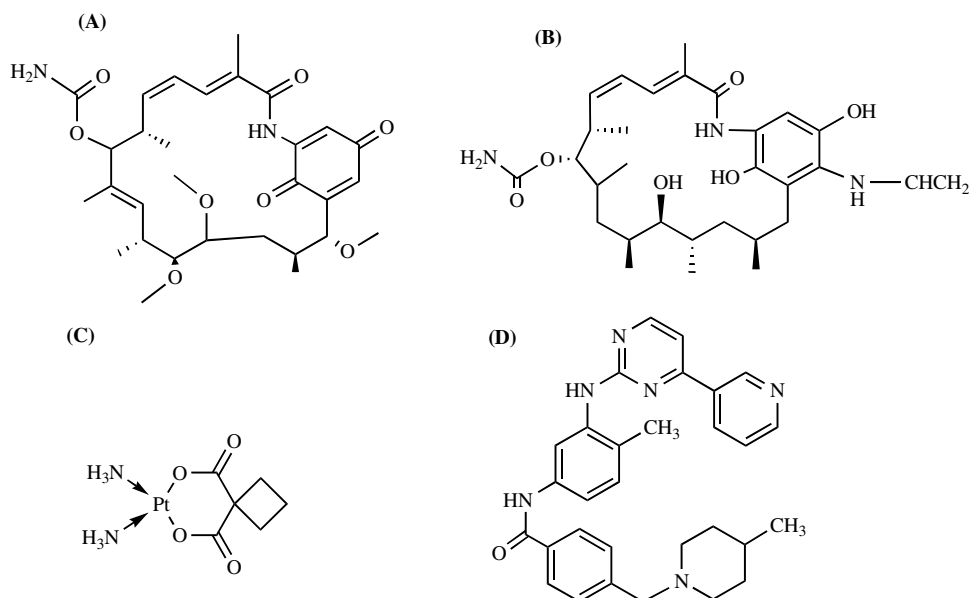


Fig. (9). **(A)** Macbecin, **(B)** IPI-504, **(C)** carboplatin and **(D)** imatinib.

Furthermore, the importance of posttranslational modifications in regulating Hsp90 function has not been entirely elucidated yet. Hsp90 is regulated by co-chaperones and by post-translational modification, such as phosphorylation, acetylation, and ubiquitinylation. Hyperacetylation of Hsp90 disrupts assembly with co-chaperones, in particular, the affinity of co-chaperone p23 for Hsp90 was dramatically reduced. Since the association with p23 requires ATP binding activity it is likely that hyperacetylation of Hsp90 lowers this activity. In fact, hyperacetylation of Hsp90 seems to inhibit its ATP-binding and decreases association of Hsp90 with its client proteins [106]. Inhibitors of acetylation have effects similar to those caused by compounds targeting the ATP-pocket at the N-terminus of Hsp90 that decrease the ATPase activity. These effects induce growth arrest and apoptosis in a variety of human cancer cells, reduced expression of mutant, but not wild-type, p53, depletion of Her1, Her2, and Raf-1 proteins, lower ERK1/2 activity, and Hsp70 induction in both Her2 overexpressing breast cancer cells and lymphocytes. These potential epigenetic regulatory signals have consequences for various biological processes and potentially important implications for the development of cancer therapeutics [107].

S-nitrosylation is also another important regulator of Hsp90 activity. The nitrosylating agent NO modifies and inhibits both human Hsp90 ATPase activity and its positive effect on the substrate eNOS [108]. Heat shock increases the turnover of Hsp90 phosphate groups [109] and apparently phosphorylation decreases the ATPase activity of Hsp90. A previous work [110] has found that Hsp90 phosphorylation leads to the release of the chaperone from the target protein and can be inhibited by geldanamycin. Another importance of post-translational modifications for the function of Hsp90 in cancer is that of the action of phosphorylation on the interaction of Hsp90 and apoptosome [111]. Hsp90 inhibits the apoptosome [112] and failure of apoptosis contributes to oncogenesis [48]. Kurokawa *et al.* [111] showed that hypophosphorylation of Hsp90 β at Ser 226 and Ser 255 promotes apoptosome inhibition suggesting that kinases and phosphatases regulating Hsp90 β phosphorylation are potential therapeutic targets and that tyrosine kinase inhibitors such as imatinib [113] (Fig. 9) could be used in combination with specific inhibitors of Hsp90.

Curiously, Hsp90 inhibitors have little effect on normal cells but have high affinity for recombinant Hsp90 proteins produced by bacteria, likely because they target Hsp90 that do not have post-translation modifications [50,51]. These observations are likely to be the focus of future studies with significant biological and clinical ramifications.

Another very promising area of research in this field is the association of Hsp90 with peptides which are specific in cancers [114]. Ishii *et al.* [115] showed that a restricted cytotoxic T lymphocyte epitope of a mouse leukemia was associated with Hsp90 in the cytosol. Recently, Callahan and co-authors [116] have shown that Hsp90 plays a global role in direct antigen presentation to MHC I molecules which are responsible for presenting antigens of cancers and viruses to CD8+ T cells. Therefore, the association of cancer specific antigenic peptides to HSP90 may serve as an indication to the immune system. To sum up, post-translation modifica-

tions that affect properly Hsp90 function (see above) would also affect the presentation of cancer specific antigens.

Since general increasing in chaperone expression favors oncogenesis, the early promise of Hsp90 inhibitors is stimulating interest in additional chaperone targets. For instance, Hsp70 has been considered a promising target because it limits response to Hsp90 inhibition [117]. One way or the other, it has been exciting to the study cancer therapeutics using Hsp90 as a target. Important research has yet to be done such as having high resolution structure of the entire human Hsp90 in complex with many ligands and co-chaperones, defining the exactly function of each Hsp90 isoform and screening compounds with better solubility and less toxic effects. However, an important part of the effort has already been accomplished and encouraging recent results with compounds already in clinical trial are raising positive hope.

ACKNOWLEDGEMENTS

Research in the laboratory of CHIR is supported by grants from Fundação de Amparo a Pesquisa do Estado de São Paulo (FAPESP), Ministério da Ciência e Tecnologia/Conselho Nacional de Pesquisa e Desenvolvimento (MCT/CNPq), and NIH-R03TW007437 funded by the Fogarty International Center. LMG has a doctoral fellowship from FAPESP.

ABBREVIATIONS

17-AAG	=	17-(allylamino)-17-demethoxygeldanamycin
17-DMAG	=	17-dimethylaminoethylamino-17-demethoxygeldanamycin
CHIP	=	C-terminus of Hsp70 interacting protein
EST	=	Expression sequence tag
HOP	=	Hsp70-Hsp90 organizing protein
HSF	=	Heat-shock factor
HSR	=	Heat-shock response
Hsp70	=	70 kDa heat-shock protein
Hsp90	=	90 kDa heat-shock protein
TPR	=	Tetratricopeptide repeat

REFERENCES

- [1] Ramos CHI, Ferreira ST. Protein folding, misfolding and aggregation: evolving concepts and conformational diseases. *Protein Pept Lett* 2005; 12: 213-22.
- [2] Dyson HJ, Wright PE. Intrinsically unstructured proteins and their functions. *Nat Rev Mol Cell Biol* 2005; 6:197-208.
- [3] Fandrich M, Fletcher MA, Dobson CM. Amyloid fibrils from muscle myoglobin. *Nature* 2001; 410: 165-66.
- [4] Fandrich M, Dobson CM. The behaviour of polyamino acids reveals an inverse side chain effect in amyloid structure formation. *EMBO J* 2002; 21: 5682-90.
- [5] Dobson CM. Experimental investigation of protein folding and misfolding. *Methods* 2004; 34: 4-14.
- [6] Minton AP. Implications of macromolecular crowding for protein assembly. *Curr Op Struct Biol* 2000; 10:34-9.
- [7] Prusiner SB. Shattuck lecture--neurodegenerative diseases and prions. *N Engl J Med* 2001; 344:1516-26.
- [8] Beissinger M, Buchner J. How chaperones fold proteins. *Biol Chem* 1998; 379: 245-59.

- [9] Hartl FU, Hayer-Hartl M. Molecular chaperones in the cytosol, from nascent chain to folded protein. *Science* 2002; 295: 1852-8.
- [10] Borges JC, Ramos CHI. Protein folding assisted by chaperones. *Protein Pept Lett* 2008; 12: 256-61.
- [11] Borges JC, Peroto MC, Ramos CHI. Molecular Chaperone Genes in the SugarCane Expressed Sequence Database (SUCEST). *Gen Mol Biol* 2001; 24: 85-92.
- [12] Borges JC, Cagliari TC, Ramos CHI. Expression and variability of molecular chaperones in the sugarcane expressome. *J Plant Physiol* 2007; 164: 505-513.
- [13] Cagliari TC, Tiroli AO, Borges JC, Ramos CHI. Identification and in silico expression analysis of eucalyptus expressed sequencing tags (ESTs) encoding molecular chaperones. *Gen Mol Biol* 2005; 28: 520-8.
- [14] Csermely P. Chaperone overload is a possible contributor to 'civilization diseases'. *Trends Genet* 2001; 17: 701-4.
- [15] Chaduri TK, Paul S. Protein-misfolding diseases and chaperone-base therapeutic approaches. *FEBS J* 2006; 273: 1331-49.
- [16] Söti C, Nagy E, Giricz Z, Víg L, Csermely P, Ferdinandy P. Heat shock proteins as emerging therapeutic targets. *Br J Pharmacol* 2005; 146: 769-80.
- [17] Macario AJL, de Macario EC. Chaperonopathies and chaperonotherapy. *FEBS Lett* 2007; 581: 3681-8.
- [18] Powers MV, Workman P. Inhibitors of the heat shock response: Biology and pharmacology. *FEBS Lett* 2007; 581: 3758-69.
- [19] Turbyville TJ, Wijeratne EM, Whitesell L, Gunatilaka AA. The anticancer activity of the fungal metabolite terreicylic acid A is associated with modulation of multiple cellular stress response pathways. *Mol Cancer Ther* 2005; 4: 1569-76.
- [20] Westerheide SD, Bosman JD, Mbadugha BN, *et al.* Celastrols as inducers of the heat shock response and cytoprotection. *J Biol Chem* 2004; 279: 56053-60.
- [21] Nagai N, Nakai A, Nagata K. Quercetin suppresses heat shock response by down regulation of HSF1. *Biochem Biophys Res Commun* 1995; 208: 1099-1105.
- [22] Dechsupa S, Kothan S, Vergote J, *et al.* Quercetin, Siamois 1 and Siamois 2 induce apoptosis in human breast cancer MDA-MB-435 cells xenograft *in vivo*. *Cancer Biol Ther* 2007; 6: 56-61.
- [23] Prodromou C, Pearl LH. Structure and functional relationships of Hsp90. *Curr Cancer Drug Targets* 2003; 3: 301-23.
- [24] Prodromou C, Roe SM, O'Brien R, Ladbury JE, Piper PW, Pearl LH. Identification and structural characterization of the ATP/ADP-binding site in the Hsp90 molecular chaperone. *Cell* 1997; 90: 65-75.
- [25] Stebbins CE, Russo AA, Schneider C, Rosen N, Hartl FU, Pavletich NP. Crystal structure of an Hsp90-geldanamycin complex: targeting of a protein chaperone by an antitumor agent. *Cell* 1997; 89: 239-50.
- [26] Marcu MG, Chadli A, Bouhouche I, Catelli M, Neckers LM. The heat shock protein 90 antagonist novobiocin interacts with a previously unrecognized ATP-binding domain in the carboxyl terminus of the chaperone. *J Biol Chem* 2000; 275: 37181-6.
- [27] Garnier C, Lafitte D, Tsvetkov PO, *et al.* Binding of ATP to heat shock protein 90: evidence for an ATP-binding site in the C-terminal domain. *J Biol Chem* 2002; 277: 12208-14.
- [28] Soti C, Racz A, Csermely P. A nucleotide-dependent molecular switch controls ATP binding at the C-terminal domain of Hsp90. N-terminal nucleotide binding unmasks a C-terminal binding pocket. *J Biol Chem* 2002; 277: 7066-75.
- [29] Obermann WM, Sondermann H, Russo AA, Pavletich NP, Hartl FU. *In vivo* function of Hsp90 is dependent on ATP binding and ATP hydrolysis. *J Cell Biol* 1998; 143: 901-10.
- [30] Jez JM, Chen JC, Rastelli G, Stroud RM, Santi DV. Crystal Structure and Molecular Modeling of 17-DMAG in Complex with Human Hsp90. *Chem Biol* 2003; 10: 361-8.
- [31] Boston RS, Viitanen PV, Vierling E. Molecular chaperones and protein folding in plants. *Plant Mol Biol* 1996; 32: 191-222.
- [32] Sreedhar AS, Kalmár E, Csermely P, Shen YF. Hsp90 isoforms: functions, expression and clinical importance. *FEBS Lett* 2004; 562: 11-5.
- [33] Eustace BK, Sakurai T, Stewart JK, *et al.* Functional proteomic screens reveal an essential extracellular role for hsp90 alpha in cancer cell invasiveness. *Nat Cell Biol* 2004; 6: 507-14.
- [34] Wegele H, Müller L, Buchner J. Hsp70 and Hsp90 – a relay team for protein folding. *Rev Physiol Biochem Pharmacol* 2004; 151: 1-44.
- [35] Wandinger SK, Richter K, Buchner J. The Hsp90 chaperone machinery. *J Biol Chem* 2008; 283: 18473-7.
- [36] Chiosis G, Vilenchik M, Kim J, Solit D. Hsp90: the vulnerable chaperone. *Drug Discov Today* 2004; 9: 881-8.
- [37] Russell LC, Whitt SR, Chen MS, Chinkers M. Identification of conserved residues required for the binding of a tetratricopeptide repeat domain to heat shock protein 90. *J Biol Chem* 1999; 274: 20060-3.
- [38] Panaretou B, Siligardi G, Meyer P, *et al.* Activation of the ATPase activity of hsp90 by the stress-regulated cochaperone aha1. *Mol Cell* 2002; 10: 1307-18.
- [39] Kamal A, Thao L, Sensintaffar J, *et al.* A high-affinity conformation of Hsp90 confers tumour selectivity on Hsp90 inhibitors. *Nature* 2003; 425: 407-10.
- [40] Zhao R, Davey M, Hsu YC, *et al.* Navigating the chaperone network: an integrative map of physical and genetic interactions mediated by the hsp90 chaperone. *Cell* 2005; 120: 715-27.
- [41] Whitesell L, Lindquist SL. HSP90 and the chaperoning of cancer. *Nat Rev Cancer* 2005; 5: 761-72.
- [42] Pratt WB. The hsp90-based chaperone system: involvement in signal transduction from a variety of hormone and growth factor receptors. *Proc Soc Exp Biol Med* 1998; 217: 420-34.
- [43] Nardai G, Végh EM, Prohászka Z, Csermely P. Chaperone-related immune dysfunction: an emergent property of distorted chaperone networks. *Trends Immunol* 2006; 27: 74-9.
- [44] Citri A, Harari D, Shohat G, *et al.* Hsp90 recognizes a common surface on client kinases. *J Biol Chem* 2006; 281: 14361-9.
- [45] Pearl LH, Prodromou C, Workman P. The Hsp90 molecular chaperone: an open and shut case for treatment. *Biochem J* 2008; 410: 439-53.
- [46] Csermely P, Schnaider T, Soti C, Prohászka Z, Nardai G. The 90-kDa molecular chaperone family: structure, function, and clinical applications. A comprehensive review. *Pharmacol Ther* 1998; 79: 129-68.
- [47] Buchner J. Hsp90 & Co. a holding for folding. *Trends Biochem Sci* 1999; 24: 136-41.
- [48] Hanahan D, Weinberg RA. The hallmarks of cancer. *Cell* 2000; 100: 57-70.
- [49] Workman P. Combinatorial attack on multistep oncogenesis by inhibiting the Hsp90 molecular chaperone. *Cancer Lett* 2004; 206: 149-57.
- [50] Sharp S, Workman P. Inhibitors of the HSP90 molecular chaperone: current status. *Adv Cancer Res* 2006; 95: 323-48.
- [51] Neckers L. Heat shock protein 90: the cancer chaperone. *J Biosci* 2007; 32: 517-30.
- [52] Fortugno P, Beltrami E, Plescia J, *et al.* Regulation of survivin function by Hsp90. *Proc Natl Acad Sci* 2003; 100: 13791-6.
- [53] Becker B, Multhoff G, Farkas B, *et al.* Induction of Hsp90 protein expression in malignant melanomas and melanoma metastases. *Exp Dermatol* 2004; 13: 27-32.
- [54] Eustace BK, Jay DG. Extracellular roles for the molecular chaperone, hsp90. *Cell Cycle* 2004; 3: 1098-100.
- [55] Sreedhar AS, Csermely P. Heat shock proteins in the regulation of apoptosis: new strategies in tumor therapy: a comprehensive review. *Pharmacol Ther* 2004; 101: 227-57.
- [56] Munster PN, Basso A, Solit D, Norton L, Rosen N. Modulation of Hsp90 function by ansamycins sensitizes breast cancer cells to chemotherapy-induced apoptosis in an RB- and schedule-dependent manner. *Clin Cancer Res* 2001; 7: 2228-36.
- [57] Munster PN, Marchion DC, Basso AD, Rosen N. Degradation of HER2 by ansamycins induces growth arrest and apoptosis in cells with HER2 overexpression *via* a HER3, phosphatidylinositol 3'-kinase-AKT-dependent pathway. *Cancer Res* 2002; 62: 3132-7.
- [58] Basso AD, Solit DB, Chiosis G, Giri B, Tschlis P, Rosen N. Akt forms an intracellular complex with heat shock protein 90 (Hsp90) and Cdc37 and is destabilized by inhibitors of Hsp90 function. *J Biol Chem* 2002; 277: 39858-66.
- [59] Sreedhar AS, Mihaly K, Pato B, *et al.* Hsp90 inhibition accelerates cell lysis. Anti-Hsp90 ribozyme reveals a complex mechanism of Hsp90 inhibitors involving both superoxide- and Hsp90-dependent events. *J Biol Chem* 2003; 278: 35231-40.
- [60] Sreedhar AS, Nardai G, Csermely P. Enhancement of complement-induced cell lysis: a novel mechanism for the anticancer effects of Hsp90 inhibitors. *Immunol Lett* 2004; 92: 157-61.

- [61] Csermely P, Agoston V, Pongor S. The efficiency of multi-target drugs: the network approach might help drug design. *Trends Pharmacol Sci* 2005; 26: 178-82.
- [62] Neckers L, Neckers K. Heat-shock protein 90 inhibitors as novel cancer chemotherapeutics – an update. *Expert Opin Emerg Drugs* 2005; 10: 137-49.
- [63] Janin YL. Heat shock protein 90 inhibitors. A text book example of medicinal chemistry? *J Med Chem* 2005; 48: 7503-12.
- [64] Solit DB, Chiosis G. Development and application of Hsp90 inhibitors. *Drug Discov Today* 2008; 13: 38-43.
- [65] Wehrli W. Ansamycins. Chemistry, biosynthesis and biological activity. *Top Curr Chem* 1977; 72: 21-49.
- [66] Prodromou C, Roe SM, O'Brien R, Ladbury JE, Piper PW, Pearl LH. Identification and structural characterization of the ATP/ADP-binding site in the Hsp90 molecular chaperone. *Cell* 1997; 90: 65-75.
- [67] Sasaki K, Yasuda H, Onodera K. Growth inhibition of virus transformed cells *in vitro* and antitumor activity *in vivo* of geldanamycin and its derivatives. *J Antibiot* 1979; 32: 849-51.
- [68] Whitesell L, Mimnaugh EG, De Costa B, Myers CE, Neckers LM. Inhibition of heat shock protein HSP90-pp60v-src heteroprotein complex formation by benzoquinone ansamycins: essential role for stress proteins in oncogenic transformation. *Proc Natl Acad Sci* 1994; 91: 8324-8.
- [69] Bagatell R, Paine-Murrieta GD, Taylor CW, *et al.* Induction of a heat shock factor 1-dependent stress response alters the cytotoxic activity of hsp90-binding agents. *Clin Cancer Res* 2000; 6: 3312-8.
- [70] Sittler A, Lurz R, Lueder G, *et al.* Geldanamycin activates a heat shock response and inhibits huntingtin aggregation in a cell culture model of Huntington's disease. *Hum Mol Genet* 2001; 10: 1307-15.
- [71] Neckers L, Ivy SP. Heat shock protein 90. *Curr Opin Oncol* 2003; 15: 419-24.
- [72] Supko JG, Hickman RL, Grever MR, Malspeis L. Preclinical pharmacologic evaluation of geldanamycin as an antitumor agent. *Cancer Chemother Pharmacol* 1995; 36: 305-15.
- [73] Egorin MJ, Zuhowski EG, Rosen DM, Sentz DL, Covey JM, Eise-man JL. Plasma pharmacokinetics and tissue distribution of 17-(allylamino)-17-demethoxygeldanamycin (NSC 330507) in CD2F1 mice1. *Cancer Chemother Pharmacol* 2001; 47: 291-302.
- [74] Patel K, Piagentini M, Rascher A, *et al.* Engineered biosynthesis of geldanamycin analogs for Hsp90 inhibition. *Chem Biol* 2004; 11: 1625-33.
- [75] Xie Q, Gao CF, Shinomiya N, *et al.* Geldanamycins exquisitely inhibit HGF/SF-mediated tumor cell invasion. *Oncogene* 2005; 24: 3697-707.
- [76] Schulte TW, Neckers LM. The benzoquinone ansamycin 17-allylamino-17-demethoxygeldanamycin binds to HSP90 and shares important biologic activities with geldanamycin. *Cancer Chemother Pharmacol* 1998; 42: 273-279.
- [77] Chiosis G, Huezio H, Rosen N, Mimnaugh E, Whitesell L, Neckers L. 17AAG: low target binding affinity and potent cell activity – finding an explanation. *Mol Cancer Ther* 2003; 2: 123-9.
- [78] Workman P. Auditing the pharmacological accounts for Hsp90 molecular chaperone inhibitors: unfolding the relationship between pharmacokinetics and pharmacodynamics. *Mol Cancer Ther* 2003; 2: 131-8.
- [79] Banerji U, O'donnell A, Scurr M, *et al.* Phase I pharmacokinetic and pharmacodynamic study of 17-allylamino,17-demethoxygeldanamycin in patients with advanced malignancies. *J Clin Oncol* 2005; 23: 4152-61.
- [80] Sausville EA, Tomaszewski JE, Ivy P. Clinical development of 17-allylamino, 17-demethoxygeldanamycin. *Curr Cancer Drug Targets* 2003; 3: 377-83.
- [81] Modi S, Stopeck AT, Gordon MS, *et al.* Combination of trastuzumab and tanespimycin (17-AAG, KOS-953) is safe and active in trastuzumab-refractory HER-2 overexpressing breast cancer: a phase I dose-escalation study. *J Clin Oncol* 2007; 25: 5410-7.
- [82] Powers MV, Workman P. Inhibitors of the heat shock response: biology and pharmacology. *FEBS Lett* 2007; 581: 3758-69.
- [83] Banerji U, Affolter A, Judson I, Marais R, Workman P. BRAF and NRAS mutations in melanoma: potential relationships to clinical response to HSP90 inhibitors. *Mol Cancer Ther* 2008; 7: 737-9.
- [84] De Candia P, Solit DB, Giri D, *et al.* Angiogenesis impairment in Id-deficient mice cooperates with an Hsp90 inhibitor to completely suppress HER2/neu-dependent breast tumors. *Proc Natl Acad Sci* 2003; 100: 12337-42.
- [85] Bisht KS, Bradbury CM, Mattson D. Geldanamycin and 17-allylamino-17-demethoxygeldanamycin potentiate the *in vitro* and *in vivo* radiation response of cervical tumor cells via the heat shock protein 90-mediated intracellular signalling and cytotoxicity. *Cancer Res* 2003; 63: 8984-95.
- [86] Smith V, Sausville EA, Camalier RF, Fiebig HH, Burger AM. Comparison of 17-dimethylaminoethylamino-17-demethoxygeldanamycin (17DMAG) and 17-allylamino-17-demethoxygeldanamycin (17AAG) *in vitro*: effects on Hsp90 and client proteins in melanoma models. *Cancer Chemother Pharmacol* 2005; 56(2): 126-37.
- [87] Egorin MJ, Lagattuta TF, Hamburger DR, *et al.* Pharmacokinetics, tissue distribution, and metabolism of 17-(dimethylaminoethylamino)-17-demethoxygeldanamycin (NSC 707545) in CD2F1 mice and Fischer 344 rats. *Cancer Chemother Pharmacol* 2002; 49(1): 7-19.
- [88] Phillips JJ, Yao ZP, Zhang W, *et al.* Conformational dynamics of the molecular chaperone Hsp90 in complexes with a co-chaperone and anticancer drugs. *J Mol Biol* 2007; 372(5): 1189-203.
- [89] Delmotte P, Delmotte-Plaque J. A new antifungal substance of fungal origin. *Nature* 1953; 171: 344.
- [90] Kwon HJ, Yoshida M, Abe K, Horinouchi S, Beppu T. Radicol, an agent inducing the reversal of transformed phenotypes of src-transformed fibroblasts. *Biosci Biotechnol Biochem* 1992; 56(3): 538-9.
- [91] Soga S, Neckers LM, Schulte TW, *et al.* KF25706, a novel oxime derivative of radicol, exhibits *in vivo* antitumor activity via selective depletion of Hsp90 binding signaling molecules. *Cancer Res* 1999; 59(12): 2931-8.
- [92] Agatsuma T, Ogawa H, Akasaka K, *et al.* Halohydrin and oxime derivatives of radicol: synthesis and antitumor activities. *Bioorg Med Chem* 2002; 10(11): 3445-54.
- [93] Soga S, Shiotsu Y, Akinaga S, Sharma SV. Development of radicol analogues. *Curr Cancer Drug Targets* 2003; 3(5): 359-69.
- [94] Marcu MG, Schulte TW, Neckers L. Novobiocin and related coumarins and depletion of heat shock protein 90-dependent signaling proteins. *J Natl Cancer Inst* 2000; 92(3): 242-8.
- [95] Yu XM, Shen G, Neckers L, *et al.* Hsp90 inhibitors identified from a library of novobiocin analogues. *J Am Chem Soc* 2005; 127(37): 12778-9.
- [96] Llauger L, He H, Kim J, *et al.* Evaluation of 8-arylsulfanyl, 8-arylsulfoxyl, and 8-arylsulfonyl adenine derivatives as inhibitors of the heat shock protein 90. *J Med Chem* 2005; 48(8): 2892-905.
- [97] He H, Zatorska D, Kim J, *et al.* Identification of potent water soluble purine-scaffold inhibitors of the heat shock protein 90. *J Med Chem* 2006; 49(1): 381-90.
- [98] Sharp SY, Prodromou C, Boxall K, *et al.* Inhibition of the heat shock protein 90 molecular chaperone *in vitro* and *in vivo* by novel, synthetic, potent resorcinyl pyrazole/isoxazole amide analogues. *Mol Cancer Ther* 2007; 6(4): 1198-211.
- [99] Eccles SA, Massey A, Raynaud FL, *et al.* NVP-AUY922: a novel heat shock protein 90 inhibitor active against xenograft tumor growth, angiogenesis, and metastasis. *Cancer Res* 2008; 68(8): 2850-60.
- [100] Martin CJ, Gaisser S, Challis IR, *et al.* Molecular characterization of macbecin as an hsp90 inhibitor. *J Med Chem* 2008; 51(9): 2853-7.
- [101] Modi S, Stopeck AT, Gordon MS, *et al.* Combination of trastuzumab and tanespimycin (17-AAG, KOS-953) is safe and active in trastuzumab-refractory HER-2 overexpressing breast cancer: a phase I dose-escalation study. *J Clin Oncol* 2007; 25(34): 5410-7.
- [102] Sydor JR, Normant E, Pien CS, *et al.* Development of 17-allylamino-17-demethoxygeldanamycin hydroquinone hydrochloride (IPI-504), an anti-cancer agent directed against Hsp90. *Proc Natl Acad Sci* 2006; 103(46): 17408-13.
- [103] Onodera H, Kaneko M, Takahashi Y, *et al.* Conformational significance of EH21A1-A4, phenolic derivatives of geldanamycin, for Hsp90 inhibitory activity. *Bioorg Med Chem Lett* 2008; 18(5): 1577-80.
- [104] Banerji U, Sain N, Sharp SY, *et al.* An *in vitro* and *in vivo* study of the combination of the heat shock protein inhibitor 17-allylamino-17-demethoxygeldanamycin and carboplatin in human ovarian cancer models. *Cancer Chemother Pharmacol* 2008; 62(5): 769-78.
- [105] Chandralapaty S, Sawai A, Ye Q, *et al.* SNX2112, a synthetic heat shock protein 90 inhibitor, has potent antitumor activity against

- HER kinase-dependent cancers. *Clin Cancer Res* 2008; 14(1): 240-48.
- [106] Yu X, Guo ZS, Marcu MG, *et al.* Modulation of p53, ErbB1, ErbB2, and Raf-1 expression in lung cancer cells by depsipeptide FR901228. *J Natl Cancer Inst* 2002; 94(7): 504-13.
- [107] Aoyagi S, Trevor K. Archer Modulating molecular chaperone Hsp90 functions through reversible acetylation. *Trends in Cell Biology* 2005; 15(11): 565-7.
- [108] Martínez-Ruiz A, Villanueva L, González de Orduña C, *et al.* S-nitrosylation of Hsp90 promotes the inhibition of its ATPase and endothelial nitric oxide synthase regulatory activities. *Proc Natl Acad Sci* 2005; 102(24):8525-30.
- [109] Legagneux V, Morange M, Bensaude O. Heat shock increases turnover of 90 kDa heat shock protein phosphate groups in HeLa cells. *FEBS Lett* 1991; 291(2): 359-62.
- [110] Zhao YG, Gilmore R, Leone G, Coffey MC, Weber B, Lee PW. Hsp90 phosphorylation is linked to its chaperoning function. Assembly of the reovirus cell attachment protein. *J Biol Chem* 2001; 276(35): 32822-7.
- [111] Kurokawa M, Zhao C, Reya T, Kornbluth S. Inhibition of apoptosome formation by suppression of Hsp90 β phosphorylation in tyrosine kinase-induced leukemias. *Mol Cell Biol* 2008; 28(17): 5494-506.
- [112] Beere H. Death versus survival: functional interaction between the apoptotic and stress-inducible heat shock protein pathways. *J Clin Invest* 2005; 115: 2633-9.
- [113] Gorre ME, Ellwood-Yen K, Chiosis G, Rosen N, Sawyers CL. BCRABL point mutants isolated from patients with imatinib mesylate-resistant chronic myeloid leukemia remain sensitive to inhibitors of the BCR-ABL chaperone heat shock protein 90. *Blood* 2002; 100: 3041-4.
- [114] Srivastava PK, Maki RG. Stress-induced proteins in immune response to cancer. *Curr Top Microbiol Immunol* 1991; 167: 109-23.
- [115] Ishii T, Udono H, Yamano T, *et al.* Isolation of MHC class I-restricted tumor antigen peptide and its precursors associated with heat shock proteins hsp70, hsp90, and gp96. *J Immunol* 1999; 162(3):1303-9.
- [116] Callahan MK, Garg M, Srivastava PK. Heat-shock protein 90 associates with N-terminal extended peptides and is required for direct and indirect antigen presentation. *Proc Natl Acad Sci* 2008; 105(5):1662-7.
- [117] Brodsky JL, Chiosis G. Hsp70 molecular chaperones: emerging roles in human disease and identification of small molecule modulators. *Curr Top Med Chem* 2006; 6: 1215-25.
- [118] Johnson JL, Beito TG, Krco CJ, Toft DO. Characterization of a novel 23-kilodalton protein of unactive progesterone receptor complexes. *Mol Cell Biol* 1994; 14: 1956-63.
- [119] Kimura Y, Rutherford SL, Miyata Y. Cdc37 is a molecular chaperone with specific functions in signal transduction. *Genes Dev* 1997; 14: 1775-85.
- [120] Mayer MP, Nikolay R, Bukau B. Aha, another regulator for hsp90 chaperones. *Mol Cell* 2002; 6: 1255-6.
- [121] Perdeu GH, Whitelaw ML. Evidence that the 90-kDa heat shock protein (HSP90) exists in cytosol in heteromeric complexes containing HSP70 and three other proteins with Mr of 63,000,56,000, and 50,000. *J Biol Chem* 1991; 266: 6708-13.
- [122] Johnson BD, Schumacher RJ, Ross ED, Toft DO. Hop modulates Hsp70/Hsp90 interactions in protein folding. *J Biol Chem* 1998; 6: 3679-86.
- [123] Young JC, Hoogenraad NJ, Hartl FU. Molecular chaperones Hsp90 and Hsp70 deliver preproteins to the mitochondrial import receptor Tom70. *Cell* 2003; 1: 41-50.
- [124] Catlett MG, Kaplan KB. Sgt1p is a unique co-chaperone that acts as a client adaptor to link Hsp90 to Skp1p. *J Biol Chem* 2006; 44: 33739-48.
- [125] Liu L, Srikakulam R, Winkelmann DA. Unc45 activates Hsp90-dependent folding of the myosin motor domain. *J Biol Chem* 2008; 19: 13185-93.
- [126] Pirkel F, Buchner J. Functional analysis of the Hsp90-associated human peptidyl prolyl cis/trans isomerases FKBP51, FKBP52 and Cyp40. *J Mol Biol* 2001; 4: 795-806.
- [127] Warth R, Briand PA, Picard D. Functional analysis of the yeast 40 kDa cyclophilin Cyp40 and its role for viability and steroid receptor regulation. *Biol Chem* 1997; 5: 381-91.
- [128] Silverstein AM, Galigniana MD, Chen MS, Owens-Grillo JK, Chinkers M, Pratt WB. Protein phosphatase 5 is a major component of glucocorticoid receptor.hsp90 complexes with properties of an FK506-binding immunophilin. *J Biol Chem* 1997; 26: 16224-30.
- [129] Connell P, Ballinger CA, Jiang J, *et al.* The co-chaperone CHIP regulates protein triage decisions mediated by heat-shock proteins. *Nat Cell Biol* 2001; 3: 93-6.
- [130] Rosser MF, Washburn E, Muchowski PJ, Patterson C, Cyr DM. Chaperone functions of the E3 ubiquitin ligase CHIP. *J Biol Chem* 2007; 31: 22267-77.

1.8. Objetivos

1.8.1 Objetivo geral

Estudar o sistema chaperona Hsp90 humano, pela caracterização do domínio C-terminal da Hsp90 humana (C-Hsp90), de suas co-chaperonas humanas Hop e Tom70, e pela interação do C-Hsp90 com a Tom70.

1.8.2 Objetivos Específicos

Produzir as proteínas humanas recombinantes, C-Hsp90, Hop e Tom70 na forma solúvel e enovelada;

Avaliar a estrutura secundária e terciária local das proteínas aplicando técnicas de dicroísmo circular (CD) e fluorescência intrínseca do triptofano (Trp);

Caracterizar o estado oligomérico da C-Hsp90, aplicando as técnicas ultracentrifugação analítica (UCA) e gel filtração acoplada a espalhamento de luz em multi-ângulos (SEC-MALS);

Caracterizar o estado oligomérico da Hop, aplicando as técnicas de UCA, gel filtração analítica e gel nativo azul (BNPAGE);

Caracterizar o estado oligomérico da Tom70, aplicando as técnicas de UCA e SEC-MALS;

Caracterizar a interação da C-Hsp90 e Tom70, determinando estequiometria e parâmetros termodinâmicos da interação, por meio das técnicas de *pull-down*, SEC-MALS e calorimetria de titulação isotérmica (ITC).

CAPÍTULO 2

ARTIGO CIENTÍFICO:

Human Hsp70/Hsp90 Organizing Protein (Hop) D456G is a Mixture of Monomeric and Dimeric Species

Publicado na revista *Protein & Peptide Letters*, 2010, 17 (4), 492-498.

DANIELI CRISTINA GONÇALVES*, **LISANDRA MARQUES GAVA*** & **CARLOS HENRIQUE INÁCIO RAMOS** (* Esses autores contribuíram igualmente para o trabalho).

A Hop é uma co-chaperona do sistema Hsp70-Hsp90, está envolvida em importantes processos celulares. Nesse artigo, apresentamos a Hop humana recombinante D456G, que apresenta uma mutação de um resíduo de aspartato para glicina no domínio TPR2B. Estão reportadas nesse artigo a clonagem, purificação e caracterização estrutural da proteína. Foram aplicadas técnicas de dicróismo circular e fluorescência intrínseca do triptofano para caracterização inicial. Para determinação das propriedades hidrodinâmicas da proteína foram utilizadas as técnicas de ultracentrifugação analítica, gel filtração analítica e espalhamento dinâmico de luz. A técnica de gel nativo também foi utilizada na caracterização do estado oligomérico da proteína. Em suma, a Hop D456G é uma mistura de espécies monoméricas e outras de mais alta massa molecular, apresenta forma alongada e bastante hidratada.

Human Hsp70/Hsp90 Organizing Protein (Hop) D456G Is a Mixture of Monomeric and Dimeric Species

Danieli C. Gonçalves^{1,2,#}, Lisandra M. Gava^{1,2,#} and Carlos H.I. Ramos^{1,3,*}

¹Institute of Chemistry and ²Institute of Biology, University of Campinas-UNICAMP. P.O. Box 6154, 13083-970, Campinas, SP, Brazil. ³Instituto Nacional de Ciência e Tecnologia em Biologia Estrutural e Bioimagem, Brazil

Abstract: Hop is a tetratricopeptide repeat domain (TPR)-containing co-chaperone that is able to directly associate with both Hsp70 and Hsp90. Previous data showed that the TPR2A-domain is the primary site for dimerization and that the TPR2B-domain may also play a role in dimerization. We present Hop-D456G, a mutant within the TPR2B-domain, that is a mixture of monomeric and dimeric species.

Keywords: Heat shock protein, Hop, TPR domain, Protein folding, protein-protein interaction, Hsp90.

1. INTRODUCTION

Hsp90 is a molecular chaperone that is responsible for maintaining the folding, stability and function of many proteins involved with signal-transduction pathways, cell-cycle regulation and apoptosis [1,2]. Hsp90 collaborates with Hsp70 to form a multifunctional multicomponent chaperone machine that plays a pivotal role in protecting the cell from environmental and genetic stresses [1]. Hop (Hsp70/Hsp90 Organizing Protein) was first identified in yeast as STI1 (for stress-inducible protein 1 [3]), and it is able to directly associate with both Hsp70 and Hsp90 [4,5]. In fact, Hop appears to be involved in several important processes, including recruitment of Hsp90 to preexisting steroid receptor-Hsp70 complexes, thus promoting the assembly and functional maturation of the receptor [4-6], and acting as a receptor for prion proteins [7].

The binding of Hop to Hsps is mediated by multiple tetratricopeptide repeat (TPR) domains, each formed by three TPR motifs, which are antiparallel α -helical hairpins (helix-turn-helix) that are 34 amino acids in length [6,8,9]. The Hop TPR1 and TPR2A domains, which have known crystallographic structures, consist of an antiparallel α -helical stack that forms a large groove along one surface of the domain [10-14]. The TPR domain has side chains projecting into the groove solvent space that can readily specify interactions with side chains from a bound polypeptide and thus facilitate specific protein-protein interactions. Two other domains containing aspartic acid-proline (DP) repeats complete the domain structure of Hop, which has the following arrangement: TPR1-DP1-TPR2A-TPR2B-DP2 (Fig. 1). TPR domains link chaperones and other protein systems into cooperative networks and participate in the action of Hsp90 as a stabilizer of the cancer phenotype thus TPR-Hsp90 com-

plexes are potential drug targets. Additionally, the presence of multiple domains gives Hop the ability to simultaneously bind the EEVD sites of both Hsp70 and Hsp90.

Although a structure for full-length Hop does not exist, it has been shown that the protein is dimeric in solution and binds as a dimer to Hsp90 [10]. Many lines of evidence show that the TPR2A-domain, which contains the Hsp90-binding site, is the primary site for dimerization [13,15]. Proteins deleted for the TPR2A-domain are monomers, but deletion of the TPR2B-domain, whose structure is unknown, causes a mixture of monomeric and dimeric species, suggesting the existence of residues within TPR2B that may also play a role in dimerization [15]. Also, there is evidence that the isolated TPR2B-domain is a dimer [16]. We report here on human Hop-D456G, which has a single mutation within the TPR2B-domain, that is a mixture of monomeric and dimeric species.

2. MATERIALS AND METHODS

2.1. Protein Preparation and Characterization

The molecular biology assays of *Homo sapiens* Hop cDNA (NCBI - BC002987), including cloning and site-directed mutagenesis, and protein production using the pET system (pET28a) were performed by standard methods [17,18]. A three-step chromatography procedure was used to purify Hop-D456G, which had a 6xHis-tag to facilitate purification, from the soluble fraction of *E. coli* lysate. The first step was affinity chromatography using a HiTrap Chelating 5 ml column (GE) on an ÄKTA FPLC instrument (GE) equilibrated in 20 mM sodium phosphate (pH 7.4), 500 mM NaCl and 20 mM imidazole, in which the protein was eluted by a 20-500 mM linear gradient of imidazole. The second step was ion exchange chromatography carried out in a DEAE 26/20 45 mL column (GE) previously equilibrated with 25 mM Tris-HCl (pH 7.5), 10 mM NaCl and 2 mM EDTA, in which the protein was eluted by a 10-1000 mM linear gradient of NaCl. The third step was a HiLoad Superdex 200 pg 26/60 size exclusion column (GE) previously equilibrated in 25 mM Tris-HCl (pH 7.5), 200 mM NaCl and 2 mM EDTA.

*Address correspondence to this author at the Institute of Chemistry, University of Campinas-UNICAMP. P.O. Box 6154, 13083-970, Campinas, SP, Brazil and Instituto Nacional de Ciência e Tecnologia em Biologia Estrutural e Bioimagem, Brazil; Tel: 55-19-3521-3144; Fax: 55-19-3521-3023; E-mail: cramos@iqm.unicamp.br

[#]These two authors contributed equally to this work.

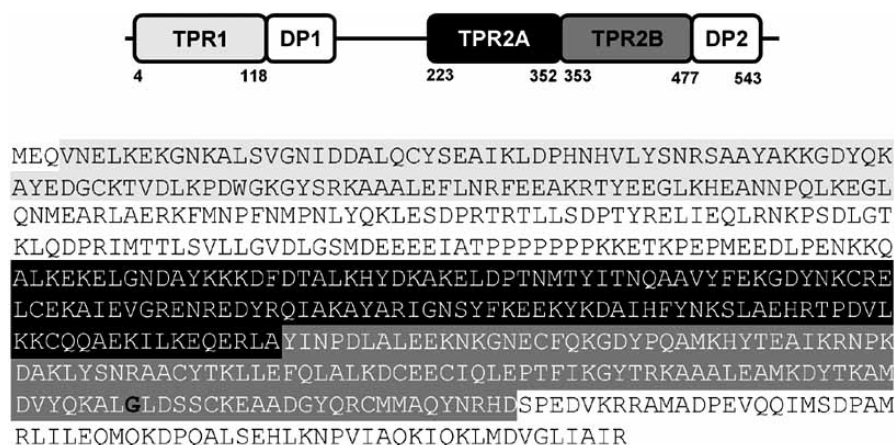


Figure 1. Hop-D456G structural arrangement. Top: Hop-D456G is composed of three tetratricopeptide repeat (TPR) domains and two other domains containing aspartic acid-proline (DP) repeats and has the following arrangement: TPR1-DP1-TPR2A-TPR2B-DP2. Bottom: The amino acid sequence is shown and TPR domains are labeled as in the top. Residue G456 is labeled in bold.

Protein purification was analyzed by sodium dodecyl sulfate-polyacrylamide gel electrophoresis (SDS-PAGE).

2.2. Spectroscopic Experiments

Protein concentration was 2.5 $\mu\text{g/ml}$ for circular dichroism (CD) and 3 $\mu\text{g/ml}$ for emission fluorescence experiments, in buffer 25 mM Tris-HCl (pH 7.5), 200 mM NaCl and 2 mM EDTA. A JASCO model J-810 CD spectropolarimeter (Jasco, Japan) equipped with a thermoelectric sample temperature controller (Peltier system) was used to record CD spectra as previously described [19]. Measurements were taken from 260 to 200 nm, unfolding was monitored at 222 nm, and the average of at least three independent experiments is reported. Measurements were performed at a temperature rate of 1°C/min using a 1 mm pathlength cell. The prediction of secondary structure content was performed as previously described [19]. Emission fluorescence was measured using a Multifrequency Cross-Correlation and Modulation Fluorometer K2™ - ISS (ISS, Champaign, IL, USA) using quartz cuvettes of 1 cm x 1 cm optical pathlength with excitation at 295 nm and emission was from 300 to 450 nm. Fluorescence data were analyzed by their maximum wavelength (λ_{max}) and center of spectral mass ($\langle\lambda\rangle$), as described by the equation:

$$\langle\lambda\rangle = \frac{\sum \lambda_i F_i}{\sum F_i} \quad 1$$

where λ_i is each wavelength and F_i is the fluorescence intensity at λ_i [19].

2.3. Hydrodynamic Experiments

Analytical ultracentrifugation (AUC) sedimentation equilibrium (SE) experiments were performed using a Beckman Optima XL-A analytical ultracentrifuge and analyzed as previously described [20,21]. Briefly, experiments were conducted from 4,000 to 10,000 rpm at 20°C with scan data acquisition at 279 nm and protein concentration of 800-1,200 $\mu\text{g/mL}$ in 25 mM Tris-HCl (pH 7.5), 200 mM NaCl and 2

mM EDTA. SE analyses involved fitting a model of absorbance versus cell radius data using nonlinear regression. The Self-Association method was used to analyze the experiments using several models of association for Hop-D456G. Distribution of the protein along the cell was fitted with the following equation [21]:

$$C = C_0 e^{\left[\frac{M(1 - V\bar{\rho})\omega^2(r^2 - r_0^2)}{2RT} \right]} \quad 2$$

Dynamic light scattering (DLS) experiments were performed on a DynaPro-MS800 instrument (Protein Solutions Inc.) that monitors the scattered light at 90°, equipped with a temperature controlled microsampler and used to obtain the diffusion coefficient parameter, D , at 20°C. Hop-D456G concentration was 0.5-1.6 $\mu\text{g/ml}$ in 25 mM Tris-HCl (pH 7.5), 200 mM NaCl and 2 mM EDTA. The software Sednterp (www.jphilo.mailway.com/download.htm) was used to estimate protein partial specific volume at 20°C ($V\bar{\rho}$), buffer density (ρ) and buffer viscosity (η), and D_{sphere} for a globular protein of 66.4 kDa.

2.4. Blue-Native Polyacrylamide Gel Electrophoresis (BN-PAGE)

BN-PAGE is a “charge shift” method for assessing the oligomeric form, molecular mass and homogeneity of native proteins in which the electrophoretic mobility of the proteins is mainly determined by the negative charges of the bound Coomassie dye. The molecular sieving effect of the acrylamide gradient gel is the separation principle because the migration ceases when areas of appropriate pore size are reached [22]. BN-PAGE was performed as previously described [22-24]. Briefly, 5 to 16% linear gradient gels were poured into a protean II minigel system (Bio-Rad) and 5 μg of Hop-D456G (monomer 66.4 kDa; pI 6.9), Bovine Serum Albumin (BSA, 66 and 132 kDa, monomer and dimer respectively; pI 4.9), Conalbumin (Co, 78 kDa; pI 5.9), and unfolded Hop-D456G (4 M urea, 90 °C, 15 min) were loaded as monomer standards. Runs started with anode buffer (50 mM Bis-Tris, pH 7.0) and blue cathode buffer (15 mM Bis-Tris (pH 7.0), 50 mM tricine, 0.02% Coomassie-Blue G250) at 4°C and 80 V until the separating gel was reached, and

then conditions were switched to 200 V and colorless cathode buffer (15 mM Bis-Tris, pH 7.0, 50 mM tricine).

2.5. Gel Filtration Chromatography

Gel filtration chromatography was used to estimate the hydrodynamic or Stokes radius (R_s) at different temperatures. Gel filtration chromatography was performed on a Superdex™ 200 10/300 molecular exclusion (GE) pre-equilibrated with 25 mM Tris-HCl (pH8.0), 2mM EDTA, and 150 mM NaCl. Experiments were performed at a flow rate of 0.5 ml.min⁻¹, at room temperature. Hop-D456G (30 μM) and a mixture of proteins with known Stokes radii (standard: Ribonuclease A (16.4 Å, 3.0 mg/mL), ovalbumin (30.5 Å, 3.5 mg/mL), aldolase (48.1 Å, 3.5 mg/mL) and apoferritin (61.0 Å, 0.4 mg/mL) (Sigma)) were centrifuged at 12,000 g for 10 min and then loaded onto the column. Elution profiles were monitored by measuring absorbance at 280 nm. Hop-D456G Stokes radius was estimated by a linear fit of the Stokes radii of the standard proteins versus the partition coefficient K_{av} as described by the following equation:

$$K_{av} = \frac{V_e - V_0}{V_t - V_0} \quad 3$$

where V_e is the elution volume of the protein, V_0 is the void volume and V_t is the total volume of the column. All data were analyzed with Origin software (Microcal).

3. RESULTS AND DISCUSSION

3.1. Hop-D456G: Purification and Initial Characterization

Longshaw *et al.* [16] showed that two regions disrupted the alignment of TPR1, TPR2A and TPR2B domains (Fig. 1A in their paper). These regions correspond to the first 3 residues of helix 3A and residue 12 of helix 3B. To answer whether specific residues where involved in the role of TPR2B in dimerization we studied Hop-D456G. Residue D456 (residue 12 in helix 3B of TPR2B) mutated to Glycine may disrupt any possible interaction in that particular position (Fig. 1). Human Hop-D456G was produced pure (Fig. 2) and analyzed in solution. Circular dichroism spectroscopy showed that Hop-D456G was natively folded and predominantly α -helical (Fig. 3A), with an estimated α -helical content of $64 \pm 4\%$ (Table 1). The CD spectrum had minima at 210 nm, with a signal of about $-24,800 \text{ deg.cm}^2.\text{dmol}^{-1}$, and at 221 nm, with a signal of about $-28,100 \text{ deg.cm}^2.\text{dmol}^{-1}$ (Table 1). These values were within the margin of error of those reported for the wild-type (WT) protein [25]. Hop-D456G has one tryptophan residue located in the TPR1 domain, and its emission fluorescence spectrum had a maximum intensity at $339 \pm 1 \text{ nm}$ and a spectral center of mass at $345 \pm 1 \text{ nm}$ (Fig. 3B). These results suggested that the single tryptophan residue was well-buried into the protein structure. Thermal-induced unfolding measurements showed that Hop-D456G unfolded reversibly through a sigmoidal transition curve with a T_m of $53 \pm 1^\circ\text{C}$ (Table 1). This value was within the margin of error reported for the WT protein [25]. Altogether, these results indicated that Hop-D456G had secondary structure and thermal stability similar to that of WT.

3.2. Hop-D456G is a Mixture of Monomeric and Dimeric Species

Upon sedimentation equilibrium (SE) analytical ultracentrifugation (AUC), Hop-D456G was mainly a single species with a molecular mass of $66 \pm 2 \text{ kDa}$ (Fig. 4 and Table 2), similar to that of 66.4 kDa predicted for a monomer from the amino acid sequence. The random distribution of the residuals (top panel in Fig. 4) indicated that the fit had very good quality and was in good agreement with a single species.

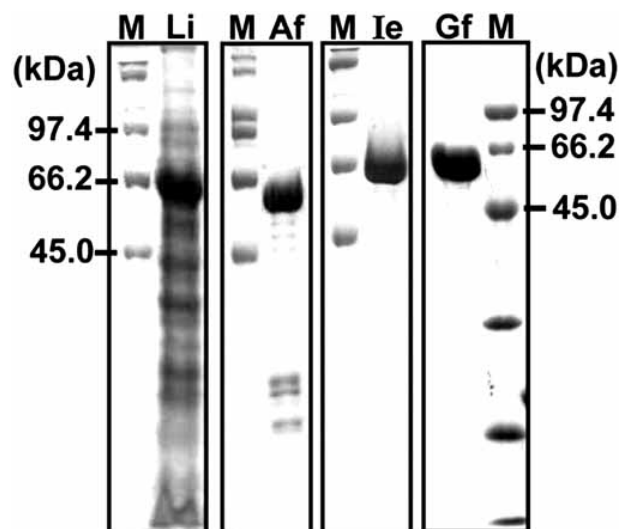


Figure 2. Protein purification. SDS-polyacrylamide gel electrophoresis was used to monitor protein purification. Hop-D456G (main band in Li, Af, Ie and Gf) was produced pure. M, molecular standards (mass in kDa are shown); Li, soluble fraction after bacterial lyses; Af, after Affinity chromatography; Ie, after Ion-exchange chromatography; Gf, after Gel filtration chromatography.

Blue-native polyacrylamide gels electrophoresis (BN-PAGE) is a “charge shift” method for assessing the oligomeric form, molecular mass and homogeneity of native proteins [22]. In this experiment, folded Hop-D456G migrated mainly as a monomer as compared to the standards: the unfolded Hop-D456G (by high urea concentration and heat), a standard for monomer migration, BSA a monomer-dimer protein with 66 and 132 kDa respectively, and Conalbumin with 78 kDa (Fig. 5). The folded Hop-D456G also had some oligomeric species, probably dimer and higher species. The participation of the TPR2B-domain in dimerization has been suggested before. Onuhua *et al.* [15] showed that Hop lacking the DP2 domain (1-477) is a dimer, Hop lacking the TPR2B domain (1-352) is converted into a monomer-dimer and additional deletion of the TPR2A-domain (1-211) converts the protein into a monomer. In their work [15] Hop lacking the TPR2B domain was a monomer at 5 μM, a concentration similar to that used in our AUC experiments, and a dimer at 50 μM, a concentration similar to that used in our BN-PAGE experiments. Therefore, our results indicate that Hop-D456G was converted into a monomer-dimer, a result also verified with mutants deleted for the TPR2B-domain [14]. Previous mutations within the TPR2B-domain of full-length Hop (K429E, K429A, R433E, R433A [10], K364A-N368A and K429A-R433A [16]) have not showed any effect on dimerization.

Table 1. Spectroscopy and Stability Parameters

	Circular Dichroism at 210 nm (deg.cm ² .dmol ⁻¹)	Circular Dichroism at 221 nm (deg.cm ² .dmol ⁻¹)	Estimated α -Helical Content	T _m of Unfolding (°C)
Hop	-25,000 ± 600 ^a	-29,000 ± 600 ^a	65 ± 6%	54 ± 2 ^a
Hop-D456G	-24,800 ± 400	-28,100 ± 300	64 ± 4%	53 ± 1

^a from reference [27];

3.3. Hydrodynamic Properties of the Monomer

We investigated the hydrodynamic characteristics of Hop-D456G to gain insight about its overall shape. Analytical gel filtration chromatography experiments were used to calculate the Stokes radius (R_S), also known as the hydrodynamic radius (R_h). The results showed that Hop-D456G eluted as a homogeneous species (Fig. 6, inset) with an R_S of 44 ± 2 Å (Fig. 6 and Table 2). It is important to mention that these results are not caused by Hop-D456G being misfolded, as this hypothesis is ruled out by CD (Fig. 3A), tryptophan emitted fluorescence (Fig. 3B) and thermal-induced unfolding experiments (Table 1).

The value of R_S was used to calculate the so-called Perrin or shape factor F [26], which is informative of the shape of the molecule. The Perrin factor is a ratio of the measured frictional coefficient f to the frictional coefficient f_0 of a hypothetical sphere for which a hypothetical radius is calculated using its molecular mass. For the theoretical calculations, the subunits were treated as globular proteins (both equatorial, a , and polar, b , radii are equal). In this way, the Perrin factor (f/f_0 ratio) provides information about the shape of the particle because the closer it is to 1, the more spherical (globular) the shape is. Mutant Hop was an asymmetric protein with an f/f_0 ratio (Perrin factor) of about 1.6.

In addition, dynamic light scattering experiments were used to measure the diffusion coefficient D of Hop-D456G at several protein concentrations (Fig. 7). Then, the standard diffusion coefficient ($D_{20,w}$) at each protein concentration was calculated and plotted in order to estimate the $D_{20,w}$ at a 0 mg/mL protein concentration ($D_{20,w}^0$) by extrapolation (Fig. 7). The measurements revealed that $D_{20,w}^0 = 6.2 \times 10^{-7} \pm 0.2$ cm²/s (Fig. 7 and Table 2). Otherwise, the Perrin factor can be estimated by $D_{sphere}/D_{20,w}^0$. A hard sphere with the mass of a monomeric Hop-D456G will have a theoretical R_S of 27 Å, a theoretical $D_{20,w}^0$ of 8.0×10^{-7} cm²/s and thus a Perrin factor of about 1.3. The disagreement of Perrin factor values estimated from the two independent experiments may be explained by the effect of hydration, which can increase the effective volume of the proteins and thus increase the R_S and affect the results. In any case, our results indicate that Hop-D456G is a monomeric protein that appears to be elongated and hydrated. An elongated monomer is in good agreement with the estimated conformation of Hop from the SAXS experiments [15].

3.4. Is Hop an Adaptor Capable of Switching from Monomer to Dimer?

Hop is a versatile protein that is capable of binding to Hsp70 and Hsp90 but also to other chaperones. Hop is in-

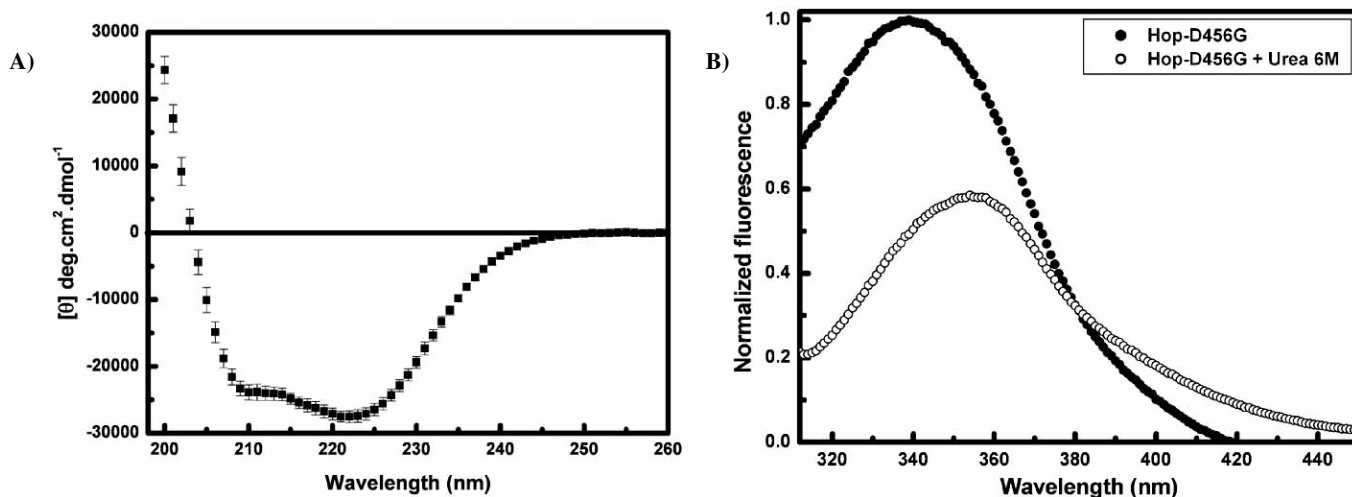


Figure 3. Hop-D456G is folded. A) *Circular dichroism spectrum.* Residual molar ellipticity $[\theta]$ was measured from 200 to 260 nm with protein in a solution of 25 mM Tris-HCl (pH 7.5), 200 mM NaCl and 2 mM EDTA. The spectrum profile is characteristic of α -helical protein. B) *Emission fluorescence spectrum.* Excitation was at 295 nm and emission was from 300 to 450 nm in 25 mM Tris-HCl (pH 7.5), 200 mM NaCl and 2 mM EDTA, in the absence or in the presence of 6M urea. Fluorescence spectra revealed that the tryptophan is well-buried in the protein structure. λ_{max} was 339 ± 1 and spectral center of mass was 345 ± 1 nm. In the presence of 6 M urea, λ_{max} was 354 ± 1 and spectral center of mass was 361 ± 1 .

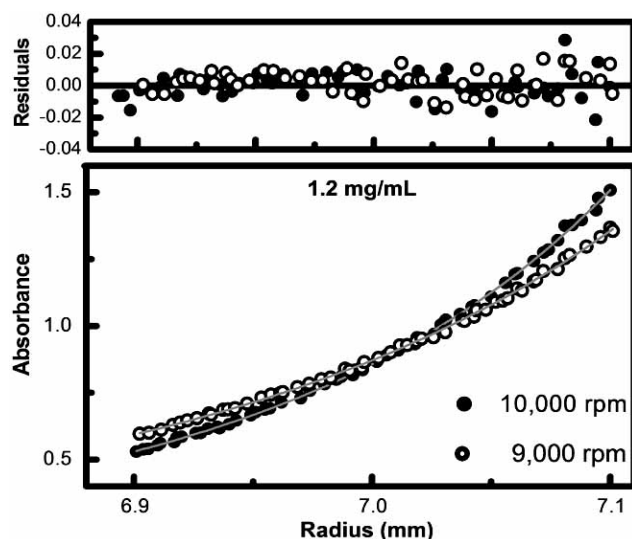


Figure 4. Sedimentation equilibrium experiments. The data analysis involved fitting a model of absorbance versus cell radius data using nonlinear regression using the Origin software package (Microcal). The best fit was determined by the randomness of the residuals and by minimization of variance (5×10^{-5}), and the random distribution of the residuals (top panel) indicated a good quality fit in good agreement with a single species with molecular mass of 66 ± 2 kDa. Experiments were conducted from 4,000 to 10,000 rpm at 20°C with scan data acquisition at 279 nm. The best fits of the experimental data for 1200 $\mu\text{g/mL}$ at 9,000 and 10,000 rpm are shown.

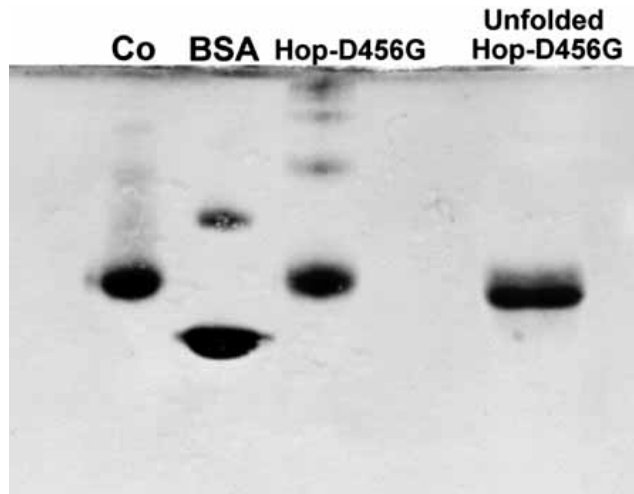


Figure 5. Blue native electrophoresis. BN-PAGE is a “charge shift” method for assessing oligomeric form, molecular mass and homogeneity of native proteins, and the electrophoretic mobility of the proteins is mainly determined by the negative charge of the bound coomassie dye. Hop-D456G (monomer 66.4 kDa; pI 6.9), Bovine Serum Albumin (BSA, 66 and 132 kDa, monomer and dimer respectively; pI 4.9), Conalbumin (Co, 78 kDa; pI 5.9), and unfolded Hop-D456G (as the standard for monomer migration; urea 4 M, 90 °C, 15 min).

involved in many cellular processes, acts in many cellular compartments and may have other partners. To accomplish all these functions, the protein may have to be promiscuous,

a property facilitated by the large amount of TPR domains. However, Hop's promiscuity may also be facilitated by an ability to switch from monomer to dimer depending on the partner or some other factor. In fact, it has been proposed that full-length Hop associates with Hsp70 in a monomer-monomer interaction [27,28]. Our results indicated that the switch from monomer to dimer could be mediated by an intervention in the TPR2B domain. However more experiments will be necessary to show whether this residue is really involved in a possible dimer to monomer mechanism.

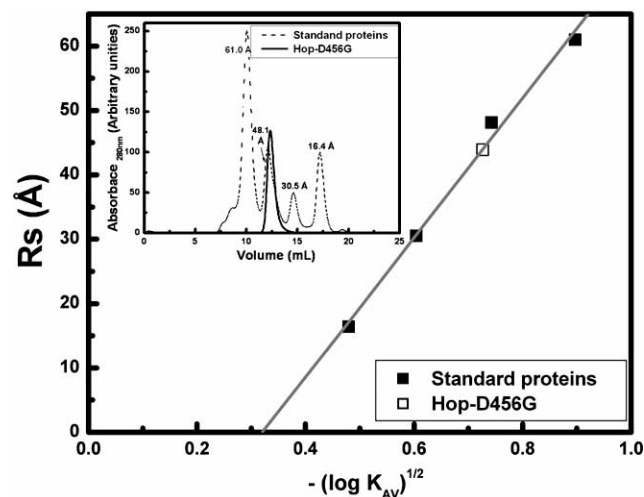


Figure 6. Analytical gel filtration. Analytical gel filtration chromatography experiments were used to calculate the Stokes radius (R_s), also known as the hydrodynamic radius (R_h). Standard proteins with known R_s were loaded onto a gel filtration column (Inset; dashed line) and their elution volume ($-\sqrt{\log K_{av}}$) was calculated to create a plot of elution volume versus R_s . The Hop-D456G elution volume (inset; solid line) was inserted into the plot (white square) and corresponded to a Stokes radius of $44 \pm 2 \text{ \AA}$.

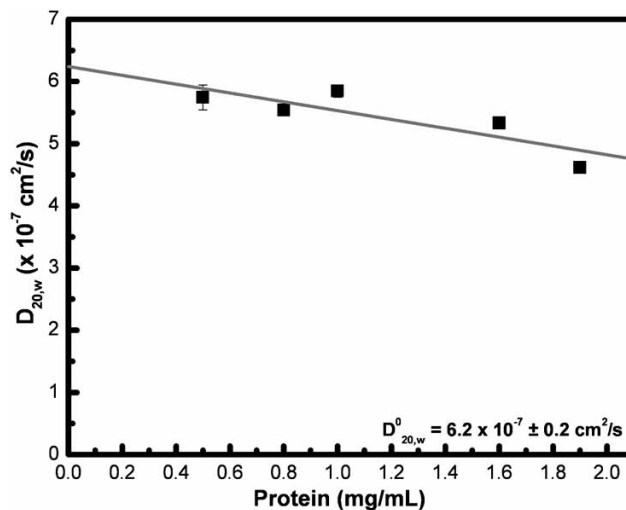


Figure 7. Plot of $D_{20,w}$ versus protein concentration. The diffusion coefficient $D_{20,w}$, calculated by dynamic light scattering versus protein concentration, was fit with linear regression to calculate $D_{20,w}^0$. Hop-D456G had a $D_{20,w}^0 = 6.2 \times 10^{-7} \text{ cm}^2/\text{s}$.

Table 2. Hydrodynamic Parameters of Hop-D456G

Molecular mass by analytical ultracentrifugation (kDa)	Stokes radius by gel filtration chromatography (Å)	Diffusion coefficient ($D_{20,w}^0$) by dynamic light scattering (cm^2/s)
66±2	44 ± 2 ^a	6.2x10 ⁻⁷ ±0.2 ^b

a, Perrin factor=1.3; b, Perrin factor=1.6;

In conclusion, we have shown for the first time that Hop-D456G, a mutation within the TPR2B-domain, is a mixture of monomer and higher species. Although no structure for full-length Hop exists previous works have characterized the wild-type protein using biophysical tools, established the role of the TPR2A-domain in dimerization and opened up the possibility that the TPR2B-domain might also be involved in dimerization. It may be possible that Hop is regulated between monomeric and dimeric states to facilitate its adaptor functions.

Additional indication that Hop-D456G is primarily monomeric at low concentrations is shown on Fig. S1 (Supplementary data) using SEC-MALS (size exclusion chromatography- multi-angle light scattering).

ACKNOWLEDGEMENTS

Research in the laboratory of CHIR is supported by grants from Fundação de Amparo a Pesquisa do Estado de São Paulo (FAPESP), Conselho Nacional de Pesquisa e Desenvolvimento (CNPq), and NIH-R03TW007437 funded by the Fogarty International Center. DCG and LMG thank CNPq and FAPESP for fellowships. We thank J.C. Borges and T.C. Cagliari for helpful discussion.

SUPPLEMENTARY MATERIAL

Supplementary material is available on the publishers Web site along with the published article.

ABBREVIATIONS

Hsp	=	Heat shock protein
Hop	=	Hsp70-Hsp90 organizing protein
AUC	=	Analytical ultracentrifugation
CD	=	Circular Dichroism
DLS	=	Dynamic Light Scattering
SDS-PAGE	=	Sodium dodecyl sulfate polyacrylamide gel electrophoresis
BN-PAGE	=	Blue native polyacrylamide gel electrophoresis
Rs	=	Stokes radius
TPR	=	Tetratricopeptide repeat
WT	=	Wild-type

REFERENCES

- [1] Wegele, H.; Müller, L.; Buchner, J. Hsp70 and Hsp90 - a relay team for protein folding. *Rev. Physiol. Biochem. Pharmacol.*, **2004**, *151*, 1-44.

- [2] Gava, L.M.; Ramos, C.H.I. Human 90 kDa Heat Shock Protein Hsp90 as a Target for Cancer Therapeutics. *Curr. Chem. Biol.*, **2009**, *3*(1), 10-21.
- [3] Nicoletti, C.M.; Craig, E.A. Isolation and characterization of STI1, a stress-inducible gene from *Saccharomyces cerevisiae*. *Mol. Cell. Biol.*, **1989**, *9*, 3638-3646.
- [4] Chen, S.; Smith, D.F. Hop as an Adaptor in the Heat Shock Protein 70 (Hsp70) and Hsp90 Chaperone Machinery. *J. Biol. Chem.*, **1998**, *273*, 35194-35200.
- [5] Johnson, D.B.; Schumacher, R.J.; Ross, E.D.; Toft, D.O. Hop Modulates hsp70/hsp90 Interactions in Protein Folding. *J. Biol. Chem.*, **1998**, *273*, 3679-3686.
- [6] Smith, S.F. Tetratricopeptide repeat cochaperones in steroid receptor complexes. *Cell Stress Chaperones*, **2004**, *9*(2), 109-121.
- [7] Zanata, S.M.; Lopes, M.H.; Mercadante, A.F.; Hajj, G.N.; Chiarini, L.B.; Nomizo, R.; Freitas, A.R.; Cabral, A.L.; Lee, K.S.; Juliano, M.A.; de Oliveira, E.; Jachieri, S.G.; Burlingame, A.; Huang, L.; Linden, R.; Brentani, R.R.; Martins, V.R. Stress-inducible protein 1 is a cell surface ligand for cellular prion that triggers neuroprotection. *EMBO J.*, **2002**, *21*(13), 3307-3316.
- [8] Das, A.K.; Cohen, P.W.; Barford, D. The structure of the tetratricopeptide repeats of protein phosphatase 5: implications for TPR-mediated protein-protein interactions. *EMBO J.*, **1998**, *17*(5), 1192-1199.
- [9] Blatch, G.L.; Lässle, M. The tetratricopeptide repeat: a structural motif mediating protein-protein interactions. *Bioessays*, **1999**, *21*(11), 932-939.
- [10] Carrigan, P.E.; Nelson, G.M.; Roberts, P.J.; Stoffer, J.; Riggs, D.L.; Smith, D.F. Multiple domains of the co-chaperone Hop are important for Hsp70 binding. *J. Biol. Chem.*, **2004**, *279*, 16185-16193.
- [11] Odunuga, O.O.; Longshaw, V.M.; Blatch, G.L. Hop: more than an Hsp70/Hsp90 adaptor protein. *Bioessays*, **2004**, *26*(10), 1058-1068.
- [12] Song, Y.; Marison, D.C. Independent regularization of Hsp70 and Hsp90 chaperones by Hsp70/Hsp90-organizing protein Sti1 (Hop1). *J. Biol. Chem.*, **2005**, *280*, 34178-34185.
- [13] Flom, G.; Behal, R.H.; Rosen, L.; Cole, D.G.; Johnson, J.L. Definition of the minimal fragments of Sti1 required for dimerization, interaction with Hsp70 and Hsp90 and *in vivo* functions. *Biochem. J.*, **2007**, *404*, 159-167.
- [14] Scheufler, C.; Brinker, A.; Bourenkov, S.; Pegoraro, L.; Moroder, L.; Bartunik, H.; Hartl, F.; Moarefi, I. Structure of TPR domain-peptide complexes: critical elements in the assembly of the Hsp70-Hsp90 multichaperone machine. *Cell*, **2000**, *101*(2), 199-210.
- [15] Onuoha, S.C.; Coulstock, E.T.; Grossman, J.G.; Jackson, S.E. Structural studies on the co-chaperone Hop and its complexes with Hsp90. *J. Mol. Biol.*, **2008**, *379*(4), 732-744.
- [16] Longshaw, V.M.; Stephens, L.L.; Daniel, S.; Blatch, G.L. The TPR2B domain of the Hsp70/Hsp90 organizing protein (Hop) may contribute towards its dimerization. *Prot. Pep. Lett.*, **2009**, *16*, 402-407.
- [17] Sambrook, J.; Russel, D. *Molecular Cloning: A Laboratory Manual*, 3rd ed.; Cold Spring Harbor Laboratory Press: New York, **2001**.
- [18] Borges, J.C.; Fischer, H.; Craievich, A.F.; Hansen, L.D.; Ramos, C.H.I. Free human mitochondrial GrpE is a symmetric dimer in solution. *J. Biol. Chem.*, **2003**, *278*, 35337-35344.
- [19] Corrêa, D.H.A.; Ramos, C.H.I. The use of circular dichroism spectroscopy to study protein folding, form and function. *Afr. J. Biochem.*, **2009**, *3*(5), 164-173.
- [20] Tiroli, A.O.; Ramos, C.H.I. Biochemical and biophysical characterization of small heat shock proteins from sugarcane. Involvement of a specific region located at the N-terminus with substrate specificity. *Int. J. Biochem. Cell Biol.*, **2007**, *39*, 818-831.

- [21] Borges, J.C.; Ramos, C.H.I. Characterization of nucleotide-induced changes on the structure of human 70 kDa heat shock protein Hsp70.1 by analytical ultracentrifugation. *BMB Reports.*, **2009**, *42*, 166-171.
- [22] Schägger, H.; Cramer, W.A.; von Jagow, G. Analysis of molecular masses and oligomeric states of protein complexes by blue native electrophoresis and isolation of membrane protein complexes by two-dimensional native electrophoresis. *Anal. Biochem.*, **1994**, *217*(2), 220-230.
- [23] Schägger, H.; von Jagow, G. Tricine-sodium dodecyl sulfate-polyacrylamide gel electrophoresis for the separation of proteins in the range from 1 to 100 kDa. *Anal. Biochem.*, **1987**, *166*(2), 368-379.
- [24] Schägger, H.; von Jagow, G. Blue native electrophoresis for isolation of membrane protein complexes in enzymatically active form. *Anal. Biochem.*, **1991**, *199*(2), 223-231.
- [25] Carrigan, P.E.; Sikkink, L.A.; Smith, D.F.; Ramirez-Alvarado, M. Domain:domain interactions within Hop, the Hsp70/Hsp90 organizing protein, are required for protein stability and structure. *Prot. Sc.*, **2006**, *15*, 522-532.
- [26] Cantor, C.R.; Schimmel, P.R. Size and shape of macromolecules. *Biophysical Chemistry; Part II: Techniques for the Study of Biological Structure and Function*, W. H. Freeman and Company: New York, **1980**.
- [27] Prodromou, C.; Siligardi, G.; O'Brien, R.; Woolfson, D.N.; Regan, L.; Panaretou, B.; Ladbury, J.E.; Piper, P.W.; Pearl, L.H. Regulation of Hsp90 ATPase activity by tetratricopeptide repeat (TPR)-domain co-chaperones. *EMBO J.*, **1999**, *18*(3), 754-762.
- [28] van der Spuy, J.; Cheetham, M.E.; Dirr, H.W.; Blatch, G.L. The cochaperone murine stress-inducible protein 1: overexpression, purification, and characterization. *Protein Expr. Purif.*, **2001**, *21*(3), 462-469.

SUPPLEMENTARY DATA

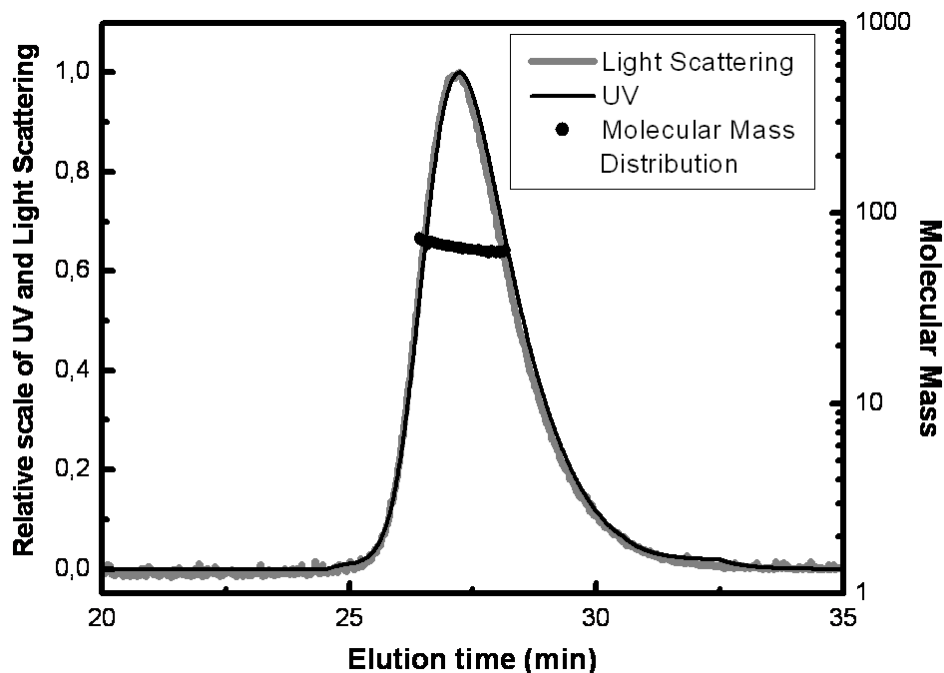


Figure S1: SEC-MALS experiment. The chromatogram shows the UV absorbance, light scattering intensity (90° detector) and Mass distribution of Hop-D456G protein. Protein was eluted with 25 mM Tris-HCl (pH 7.5), 150 mM NaCl, 2mM EDTA, at room temperature and flow rate of 0.5 mL/min.

MATERIAL AND METHODS

SEC-MALS (Size Exclusion Chromatography – Multi-angle Light Scattering) is a robust technique, which provides absolute molecular weight without need of size calibration, as traditional SEC (Yi et al, 2009). SEC-MALS was performed using a Superdex 200 10/300 column (GE) connected to an ÄKTA FPLC system, equipped sequentially with a MALS detector (miniDAWN- TREOS – Wyatt). An amount of 400 µg of purified protein were loaded, filtered on a 0.1 µm microfilter and centrifuged (10 000 g / 20 minutes) before loading. ASTRA software (Wyatt) was used for data acquisition and analysis.

RESULTS

Sample was isocratically eluted with 25 mM Tris-HCl (pH 7.5), 150 mM NaCl, 2mM EDTA, at room temperature and flow rate of 0.5 mL/min. The UV absorbance and light scattering intensity (90° detector) are well aligned indicating the same species were detected by both methods. The peak contains a major population at around 65 kDa, wich is in agreement with the monomeric molecular mass.

REFERENCE

Li, Yi; Weiss IV, W.F.; Roberts C.J. (2009) Characterization of High-Molecular-Weight Nonnative Aggregates and Aggregation Kinetics by Size Exclusion Chromatography With Inline Multi-Angle Laser Light Scattering. *Journal of Pharmaceutical Sciences*, Vol. 98, n.11.

CAPÍTULO 3

ARTIGO CIENTÍFICO:

Human mitochondrial import receptor Tom70 functions as a monomer

Publicado na revista *Biochemical Journal* (2010) 429, 553–563

**ANA C.Y. FAN, LISANDRA MARQUES GAVA, CARLOS HENRIQUE INÁCIO
RAMOS & JASON C. YOUNG**

A Tom70, um receptor de importação mitocondrial da membrana externa de mitocôndria interage com complexos (chaperona/proteína precursora) por meio de dois domínios estruturais: o primeiro liga a chaperona molecular (Hsp70/Hsp90) e um segundo liga as proteínas precursoras. A definição do estado oligomérico da Tom70 tem sido controversa, com evidência para ambas as formas: monomérica e homodimérica. Nesse trabalho, a Tom70 é apresentada como um monômero funcional, com implicações na sua atividade de importação de proteínas para a mitocôndria. Os dados de dicroísmo circular e ultracentrifugação analítica (velocidade de sedimentação e sedimentação em equilíbrio) são os resultados produzidos nessa tese de doutorado.



Human mitochondrial import receptor Tom70 functions as a monomer

Anna C. Y. FAN*, Lisandra M. GAVA†‡, Carlos H. I. RAMOS† and Jason C. YOUNG*¹

*Department of Biochemistry, McGill University, 3649 Promenade Sir William Osler, Montreal, Quebec, Canada H3G 0B1, †Institute of Chemistry, University of Campinas (UNICAMP), Campinas, SP, Brazil, and ‡Institute of Biology, University of Campinas (UNICAMP), Campinas, SP 13083-970, Brazil

The mitochondrial import receptor Tom70 (translocase of the mitochondrial outer membrane 70) interacts with chaperone–preprotein complexes through two domains: one that binds Hsp70 (heat-shock protein 70)/Hsc70 (heat-shock cognate 70) and Hsp90, and a second that binds preproteins. The oligomeric state of Tom70 has been controversial, with evidence for both monomeric and homodimeric forms. In the present paper, we report that the functional state of human Tom70 appears to be a monomer with mechanistic implications for its function in mitochondrial protein import. Based on analytical ultracentrifugation, cross-linking, size-exclusion chromatography and multi-angle light scattering, we found that the soluble cytosolic fragment of human Tom70 exists in equilibrium between monomer and dimer. A point mutation introduced at the predicted

dimer interface increased the percentage of monomeric Tom70. Although chaperone docking to the mutant was the same as to the wild-type, the mutant was significantly more active in preprotein targeting. Cross-linking also demonstrated that the mutant formed stronger contacts with preprotein. However, cross-linking of full-length wild-type Tom70 on the mitochondrial membrane showed little evidence of homodimers. These results indicate that the Tom70 monomers are the functional form of the receptor, whereas the homodimers appear to be a minor population, and may represent an inactive state.

Key words: chaperone, dimerization, heat-shock protein (Hsp), mitochondrion, protein structure, translocase of the mitochondrial outer membrane complex (Tom complex).

INTRODUCTION

Mitochondria are double-membrane-bound organelles that are crucial to many physiological functions, such as cellular respiration, metabolism of lipids, amino acids and iron, and regulation of apoptosis. There are 1000–2000 proteins in mitochondria but few of them (eight in budding yeast *Saccharomyces cerevisiae*, 13 in humans) are encoded by the mitochondrial genome [1]. The vast majority of mitochondrial proteins are encoded in the nucleus, translated by cytosolic ribosomes and subsequently imported into mitochondria. The Tom (translocase of the mitochondrial outer membrane) complex includes two integral membrane import receptors, Tom20 and Tom70, and a GIP (general import pore) complex. Many proteins destined for the matrix and intermembrane space are synthesized with N-terminal amphipathic presequences, which are recognized by Tom20 via hydrophobic interactions [2–4]. In contrast, Tom70 preferentially recognizes preproteins with internal hydrophobic targeting sequences, many of which are inner membrane metabolite carriers [2,3,5]. Tom70 has also been implicated in the import of several large hydrophobic matrix proteins [6,7] and Tom40 [8], and the insertion of some outer membrane proteins [9–11]. After binding by the Tom70 or Tom20 receptors, precursor proteins are then transferred to the GIP for translocation across the outer mitochondrial membrane and sorted to their appropriate sub-compartments [2].

The Tom70-mediated import pathway is chaperone-dependent. Prior to import, Tom70-dependent preproteins are bound by Hsp (heat-shock protein) chaperones, notably Hsp70/Hsc70 (heat-shock cognate 70) and Hsp90, as well as the human (mammalian)

DNAJA1 and DNAJA2 co-chaperones [12–15]. Tom70 contains an N-terminal transmembrane domain followed by a cytosolic TPR (tetratricopeptide repeat) clamp domain similar to those first structurally characterized in the cytosolic co-chaperone Hop [16]. This TPR clamp domain serves as a docking site for Hsc70 and Hsp90 and thus for the multi-chaperone complexes that contain preprotein. Preproteins are then thought to interact with Tom70 directly via a C-terminal domain separate from the TPR clamp [12,17,18]. Cross-linking experiments showed direct contacts between preproteins and chaperones, as well as contacts between preproteins and Tom70 itself [12,13]. Progression of preproteins from the Tom70 complex to the GIP is dependent on ATP and the Tim9 (translocase of the mitochondrial inner membrane 9)/Tim10 components in the intermembrane space [5,19,20]. Geldanamycin, an ATP-mimetic for Hsp90, blocks progression of preproteins from the receptor-bound state to the GIP complex, suggesting that ATP-dependent cycling by Hsp90 and, most probably, Hsc70 assists the subsequent translocation step [13]. However, the mechanism by which Tom70 co-ordinates interactions with preproteins and chaperones remains unresolved.

The oligomeric state in which Tom70 functions is controversial, based on experiments with the receptor from *S. cerevisiae*. Cross-linking of translocation intermediates of the Tom70-dependent preprotein AAC (ADP/ATP carrier) produced high-molecular-mass species consistent with binding to two Tom70 molecules [20,21]. Tom70 from isolated yeast mitochondria was also shown to generate a cross-linked dimer [19]. Targeting of AAC to the outer membrane led to the recruitment of up to three homodimers of yeast Tom70 in higher-molecular-mass complexes, by analysis on BN-PAGE (blue native PAGE) [19]. As a result of these original

Abbreviations used: AAC, ADP/ATP carrier; AUC, analytical ultracentrifugation; BMH, bismaleimidohexane; BN-PAGE, blue native PAGE; DTT, dithiothreitol; GIP, general import pore; Hsc70, heat-shock cognate 70; Hsp, heat-shock protein; MALS, multi-angle light scattering; MBS, *m*-maleimidobenzoyl-*N*-hydroxysulfosuccinimide ester; OGC, oxoglutarate carrier; PiC, phosphate carrier; SAXS, small-angle X-ray scattering; SEC, size-exclusion chromatography; SMCC, succinimidyl-4-(*N*-maleimidomethyl) cyclohexane-1-carboxylate; s-SMCC, sulfo-SMCC; SE, sedimentation equilibrium; SV, sedimentation velocity; Tim, translocase of the mitochondrial inner membrane; Tom, translocase of the mitochondrial outer membrane; TPR, tetratricopeptide repeat; WT, wild-type.

¹ To whom correspondence should be addressed (email jason.young2@mcgill.ca).

studies, the functional state of yeast Tom70 on the membrane was believed to be a dimer. The crystal structure of the soluble cytosolic fragment of yeast Tom70 also suggested a homodimeric model [22], in which each molecule has a 'closed' arrangement with the TPR clamp and C-terminal domains tightly packed so that the chaperone binding sites were not readily accessible. On the contrary, biophysical studies with a similar fragment of yeast Tom70 suggested a very different conclusion. AUC (analytical ultracentrifugation) and SEC (size-exclusion chromatography) indicated that soluble yeast Tom70 was monomeric [23], and measurements of its unfolding transitions suggested that the domains within Tom70 were relatively independent of each other [23,24]. SAXS (small-angle X-ray scattering) data, when fitted to predicted profiles by various methods, also indicated a monomeric yeast Tom70 with an 'open' end-to-end arrangement of the domains, and with a small fraction in a more flexible state with its domains dissociated. Peptide ligands corresponding to Hsc70 in yeast (Ssa1) and preprotein bound to soluble Tom70 readily without changing its overall shape [18]. Most recently, the crystal structure of a close Tom70 homologue, *S. cerevisiae* Tom71, was solved. Despite more than 50% sequence identity and a similar domain arrangement with yeast Tom70, the crystal structure of yeast Tom71 depicted a monomer with an elongated conformation resembling the open model. Structures of Tom71 in complex with C-terminal peptides of yeast Hsc70 (Ssa1) and Hsp90 (Hsp82) further suggested that chaperone docking induced opening of the preprotein binding site of the monomeric receptor [25]. These conflicting models of Tom70 imply different mechanisms of function.

The mammalian homologue of Tom70 was identified by Suzuki et al. [26], but structural data are not yet available and its biophysical properties remain uncharacterized up to now. In humans, there is only one gene encoding Tom70, which is equally divergent from yeast Tom70 and Tom71. Human Tom70 shares only 24% sequence identity with yeast Tom70 and, despite having the same overall domain architecture and chaperone-dependent mechanism, it cannot substitute functionally for its yeast homologue [12]. This suggests that there are significant differences between the fungal and mammalian import systems at the functional, and perhaps even structural, level.

Here, we demonstrate that the cytosolic fragment of human Tom70 exists in equilibrium between monomer and dimer. Mutagenesis of the predicted dimerization interface shifts the equilibrium to the monomeric form and increases the level of pre-protein targeting, but not chaperone docking. Cross-linking of endogenous human Tom70 on mitochondria isolated from HeLa cells failed to generate homodimeric cross-links, although other cross-linked forms were observed. Taken together, these results show that the functional state of human Tom70 is monomeric.

EXPERIMENTAL

Materials

The expression vectors pGEM4 and pGEM4Z were purchased from Promega, pET11a and pET15b from Novagen and pPro-ExHTa from Invitrogen. The QuikChange® mutagenesis kit was from Stratagene, the TNT™-coupled reticulocyte lysate system was from Promega and [³⁵S]methionine/cysteine labelling mix was from GE Healthcare. Cross-linkers SMCC [succinimidyl-4-(*N*-maleimidomethyl) cyclohexane-1-carboxylate], BMH (bismaleimidohexane) and s-SMCC (sulfo-SMCC) were from Pierce. Unless stated otherwise, all chemical reagents were from Sigma or BioShop Canada.

Plasmids

Sequences encoding bovine PiC (phosphate carrier) and bovine OGC (oxoglutarate carrier) were in pGEM4 [27,28], rat Hsc70 was in pET11a and human Hsp90α was in pET15b [29]. The full-length human Tom70 was in pGEM4Z and the cytosolic fragment (residues 111–608) was in pProExHTa [12]. The mutation R192A in the TPR clamp of human Tom70 was previously introduced by PCR [12] and the mutation YS585AA in the predicted dimerization interface was introduced using the QuikChange® mutagenesis kit.

Proteins and antibodies

The His-tagged cytosolic fragments of human Tom70 [denoted WT_{Δ110} (where WT is wild-type), YS585AA_{Δ110} and R192A_{Δ110}] were purified as described previously [13]. Briefly, the proteins were expressed in *Escherichia coli* BL21(DE3) cells and induced with 0.2 mM isopropyl β-D-thiogalactoside at 37°C for 2 h. The cells were lysed by extrusion in a French press and the cell debris was removed by centrifugation. The His-tagged proteins were bound to a nickel–Sepharose high-performance column (GE Healthcare) equilibrated in 20 mM KH₂PO₄, pH 7.5, 500 mM NaCl and 20 mM imidazole, and eluted with 20 mM KH₂PO₄, pH 7.5, and 300 mM imidazole. The protein purity was assayed by SDS/PAGE (12% gels), and the yield was determined by absorbance at 280 nm. Specific rabbit polyclonal antibodies were raised against Tom70 WT_{Δ110}.

Biophysical analysis

CD measurements were recorded in a JASCO J-810 spectropolarimeter, using a 1 mm pathlength cuvette and protein concentration from 1.9 to 7.8 μM in 20 mM Tris/HCl, pH 8.5, and 150 mM NaCl. CDNN deconvolution software [30] was used to predict the secondary structure content.

SV (sedimentation velocity) and SE (sedimentation equilibrium) experiments were carried out using a Beckman Optima XL-A ultracentrifuge and an AN-60Ti rotor at 20°C [31]. Scan data acquisition were taken at 280 nm, in buffer containing 20 mM Tris/HCl, pH 8.5, 150 mM NaCl and 5 mM magnesium acetate at 9000 to 11 000 rev./min and protein concentrations from 150 to 1500 μg/ml for SE and at 30 000 rev./min and protein concentrations from 500 to 1500 μg/ml for SV experiments. SE data were analysed by nonlinear regression using the Origin software package (MicroCal) and a self-association method, applying either a monomer model (fixed molecular mass of 60 kDa) or a monomer–dimer model (fixed molecular mass of 60 kDa and N₂ equals 2, which corresponds to a dimer). Protein distribution was fitted to the following equation [32]:

$$C = C_{\text{monomer},r_0} e^{\left[\frac{M(1 - V_{\text{bar}}\rho)\omega^2(r^2 - r_0^2)}{2RT} \right]} + KB * (C_{\text{monomer},r_0})^n e^{\left[\frac{M(1 - V_{\text{bar}}\rho)\omega^2(r^2 - r_0^2)}{2RT} \right]}$$

where C is the protein concentration at radial position r , C_{monomer,r_0} is the protein concentration at radial position r_0 (initial radial position), ω is the centrifugal angular velocity, KB is the binding constant and n is the stoichiometry. The software Sednterp (<http://www.jphilo.mailway.com/download.htm>) was applied to estimate the partial specific volume at 20°C (0.7327 ml/g), buffer density and buffer viscosity. SV data were analysed with SedFit

software [33] using the continuous sedimentation distribution model to yield the sedimentation coefficient and frictional ratio.

SEC-MALS (SEC and multi-angle light scattering) experiments were performed using an analytical Superdex 200 10/300 column (GE Healthcare) or BioSuite 250 4 μm UHR SEC column (Waters) equilibrated in buffer CG (20 mM Hepes/KOH, pH 7.5, 100 mM potassium acetate and 5 mM magnesium acetate), combined with online static light scattering by absorbance and differential refractive index detectors (miniDawn TREOS and Optilab rEX, Wyatt Technology). Recombinant human Tom70 WT $_{\Delta 110}$ and YS585AA $_{\Delta 110}$ were loaded at 2000 $\mu\text{g/ml}$ (unless otherwise indicated) with a sample size of 50 μl , and experiments were performed at room temperature (22°C). Data were analysed with the ASTRA software package (Wyatt Technology).

Cross-linking and co-precipitation

Purified proteins were incubated at 10 μM in buffer CG with 1% DMSO or 100 μM SMCC at 4°C for 15 min. The reactions were quenched with 100 mM DTT (dithiothreitol) and 10 mM ethanolamine, pH 8, at 4°C for 15 min and analysed by SDS/PAGE (8% gels) and immunoblots. For SEC, 200 μl of WT $_{\Delta 110}$ was cross-linked and quenched at the above conditions and then resolved by a Superdex 200 10/300 column (GE Healthcare) equilibrated in buffer CG. Eluted protein was collected in 0.3 ml fractions, precipitated by trichloroacetic acid, and then analysed by SDS/PAGE (8% gels) and Coomassie Blue staining.

Co-precipitation with nickel–Sepharose was performed [13] with radiolabelled OGC, PiC, Hsc70 or Hsp90 at a final concentration of 5 μM WT $_{\Delta 110}$, YS585AA $_{\Delta 110}$ or R192A $_{\Delta 110}$ as indicated, and analysed by autoradiography.

For cross-linking, the co-precipitated OGC or PiC complex was resuspended in 100 μl of buffer CG, and then incubated with 1% DMSO or 100 μM BMH at 4°C for 15 min. The reaction was quenched by 200 mM DTT and, where indicated, washed by denaturing buffer containing 250 mM NaCl, 20 mM Tris/HCl, pH 8, and 1% SDS.

Mitochondrial targeting

Mitochondria were isolated as described previously [11,13], except that HeLa cells were used. HeLa cells were maintained in DMEM (Dulbecco's modified Eagle's medium) containing 4.5 g/l glucose, 36 mg/l pyruvate, 2 mM glutamine and 10% fetal bovine serum (Invitrogen). The cells were washed with PBS, collected by scraping in PBS and centrifugation, resuspended in buffer B (10 mM Hepes/KOH, pH 7.5, 220 mM mannitol, 70 mM sucrose and 1 mM EDTA) containing 2 mg/ml BSA and Complete Mini Protease Inhibitors (Roche), and lysed by seven passes through a 27-gauge needle. Mitochondria were recovered from the postnuclear supernatant by centrifugation at 12000 g for 5 min and resuspended at 2 mg/ml in buffer containing 20 mM Hepes/KOH, pH 7.5, 250 mM sucrose, 80 mM potassium acetate, 5 mM magnesium acetate, 10 mM succinate, 2 mM ADP and 2 mM DTT. The isolated mitochondria were competent for import, dependent on the inner membrane potential, and potential-independent insertion into the outer membrane. The targeting of cell-free translated proteins to mitochondria was performed as described [13]. After targeting, mitochondria were resuspended in buffer B at 1 mg/ml and incubated with 1% DMSO or 1 mM s-SMCC at 4°C for 15 min. The reactions were quenched with 100 mM DTT and 10 mM ethanolamine, pH 8, at 4°C for 15 min and analysed by SDS/PAGE and autoradiography.

BN-PAGE

BN-PAGE analysis was performed as described previously [5,13]. Purified proteins (WT $_{\Delta 110}$ or YS585AA $_{\Delta 110}$) were resolved in buffer CG containing 1% digitonin (Calbiochem), 10% glycerol and 0.5% Coomassie Blue G-250 (EMD Chemicals). HeLa mitochondria were solubilized in buffer containing 20 mM Hepes/KOH (pH 7.5), 50 mM potassium acetate, 1% digitonin and 10% glycerol at 4°C. After a clarifying spin, Coomassie Blue G-250 was added to 0.5% for loading. Samples were loaded on to 6–16.5% gradient gels. Purified proteins were visualized by Coomassie Blue staining, for endogenous Tom70 by immunoblotting against Tom70, and for radiolabelled full-length human Tom70 (WT or YS585AA) by autoradiography. For two-dimensional PAGE, purified recombinant WT $_{\Delta 110}$ and YS585AA $_{\Delta 110}$ were cross-linked with 100 μM SMCC and quenched as described, and then resolved by BN-PAGE in the presence of 1% digitonin, 10% glycerol and 0.5% Coomassie Blue G-250 as above. After that, gel strips were loaded on to SDS/PAGE (8% gels) and resolved in the presence of 1% agarose containing 5% SDS, 50 mM Tris/HCl, pH 6.8, 25 mM DTT and 5% glycerol, followed by immunoblotting against Tom70.

RESULTS

The cytosolic region (residues 111–608) of His-tagged human Tom70 (Tom70 WT $_{\Delta 110}$) was purified as described previously [13]. CD spectroscopy indicated that it was natively folded and largely α -helical ($66 \pm 4\%$) by deconvolution analysis (Figure 1A), which is similar to that predicted by homology to yeast Tom70. To examine its oligomeric state in solution, we performed AUC. SV analyses (Figure 1B) were performed at concentrations from 500 $\mu\text{g/ml}$ (dashed line) to 1500 $\mu\text{g/ml}$ (solid line.) The $c(s)$ distribution of the recombinant Tom70 WT $_{\Delta 110}$ yielded two species, in major and minor fractions, seen most clearly in the plot for the highest concentration. The majority had a sedimentation coefficient of 3.8 S, in agreement with the values of 3.9 S and 3.6 S observed for yeast Tom70 by Beddoe et al. [23] and Mills et al. [18] respectively. In addition, the $c(s)$ distribution of Tom70 WT $_{\Delta 110}$ showed a minor peak with a sedimentation coefficient of 6.2 S containing at least 15% of total protein, indicating that some of the protein is present in a higher oligomeric state. The 3.8 S and 6.2 S sedimentation coefficients were consistent with molecular masses of approx. 60 kDa and 120 kDa respectively.

To further investigate this, SE experiments, shown in Figure 1(C), were performed at concentrations of 150 $\mu\text{g/ml}$ (left panels) and 1500 $\mu\text{g/ml}$ (right panels). Notably, concentration distributions shown by absorbance scans (Figure 1C, lower panels) could not be fitted to a single species model, as seen by the biased distribution of residuals (Figure 1C, upper panels). Instead, the concentration distributions fit best to a self-association model as shown by residuals that were evenly distributed over the regression line (Figure 1C, middle panels) with an estimated equilibrium dissociation constant of approx. 10^{-5} M. So, the SE velocity results were in agreement, suggesting that a single species model could not account for the full behaviour of the human Tom70 soluble fragment. A higher-order oligomer with a sedimentation coefficient consistent with a homodimer appeared to make up a minor, but appreciable, fraction of the population.

To address this further and study potential functional consequences, we performed site-directed mutagenesis to disrupt the putative homodimerization of Tom70. Although an earlier crystal structure by Wu and Sha [22] depicted yeast Tom70 as a compact homodimer with a dimerization interface that is

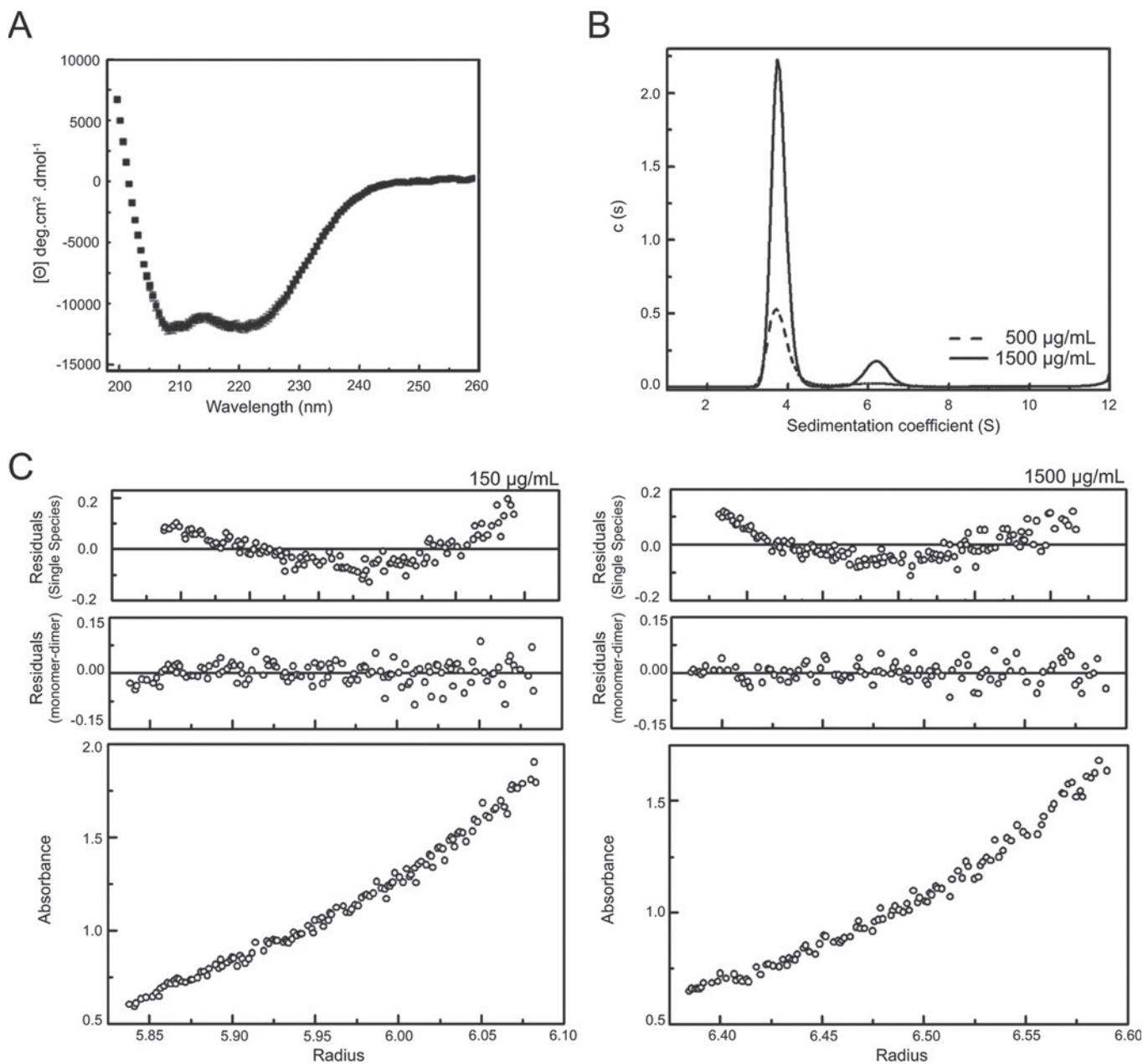


Figure 1 Biophysical analysis of Tom70 $_{\Delta 110}$

(A) To obtain the CD spectrum of Tom70 $_{\Delta 110}$, the residual molar ellipticity (Θ) was measured from 260 to 200 nm at 20 °C. Deconvolution indicated a percentage of $66 \pm 4\%$ of α -helix. (B) $c(s)$ distribution from SV analyses performed with Tom70 $_{\Delta 110}$ at 500 $\mu\text{g/ml}$ (broken line) and 1500 $\mu\text{g/ml}$ (continuous line). Peaks had sedimentation coefficients of 3.8 S and 6.2 S, consistent with molecular masses of approx. 60 kDa and 120 kDa with $f/\rho_0 = 1.4$. (C) SE analyses were carried out at 150 $\mu\text{g/ml}$ (left panels) and 1500 $\mu\text{g/ml}$ (right panels) at 10 000 rev/min at 20 °C.

almost flat, Mills et al. [18] characterized Tom70 as an elongated open monomer in solution by SAXS and proposed an alternate interpretation of the crystal structure with two intertwining molecules of the open Tom70. Therefore, we performed homology modelling of human Tom70 using Swiss-Model [34] with the homodimeric structures as templates, and the model was depicted in an open monomeric conformation by alternate pairing of N- and C-terminal domains, as proposed by Mills et al. [18] (Figure 2A). Although the SAXS-refined monomer model in the study by Mills et al. [18] was not available as a template, a homology model of open monomeric human Tom70 was also generated using the unliganded monomeric structure of

yeast Tom71 [25] as a template (Supplementary Figure S1A at <http://www.BiochemJ.org/bj/429/bj4290553add.htm>). In all models, hydrophobic contacts were predicted between helices of the TPR clamp and C-terminal domains: between domains from different subunits in the dimeric model, and from the same polypeptide in the monomeric models. In particular, Tyr⁵⁸⁵ and neighbouring Ser⁵⁸⁶ interacted closely with residues Gly²³⁶, Ala²⁴⁰ and Lys²⁴³. We therefore created a double mutation, YS585AA (Figure 2A, black spheres) at the predicted domain interface and purified the mutant protein, YS585AA $_{\Delta 110}$, as a recombinant fusion protein. The mutation was expected to disturb intersubunit contacts in a dimeric form of Tom70, as well as promoting

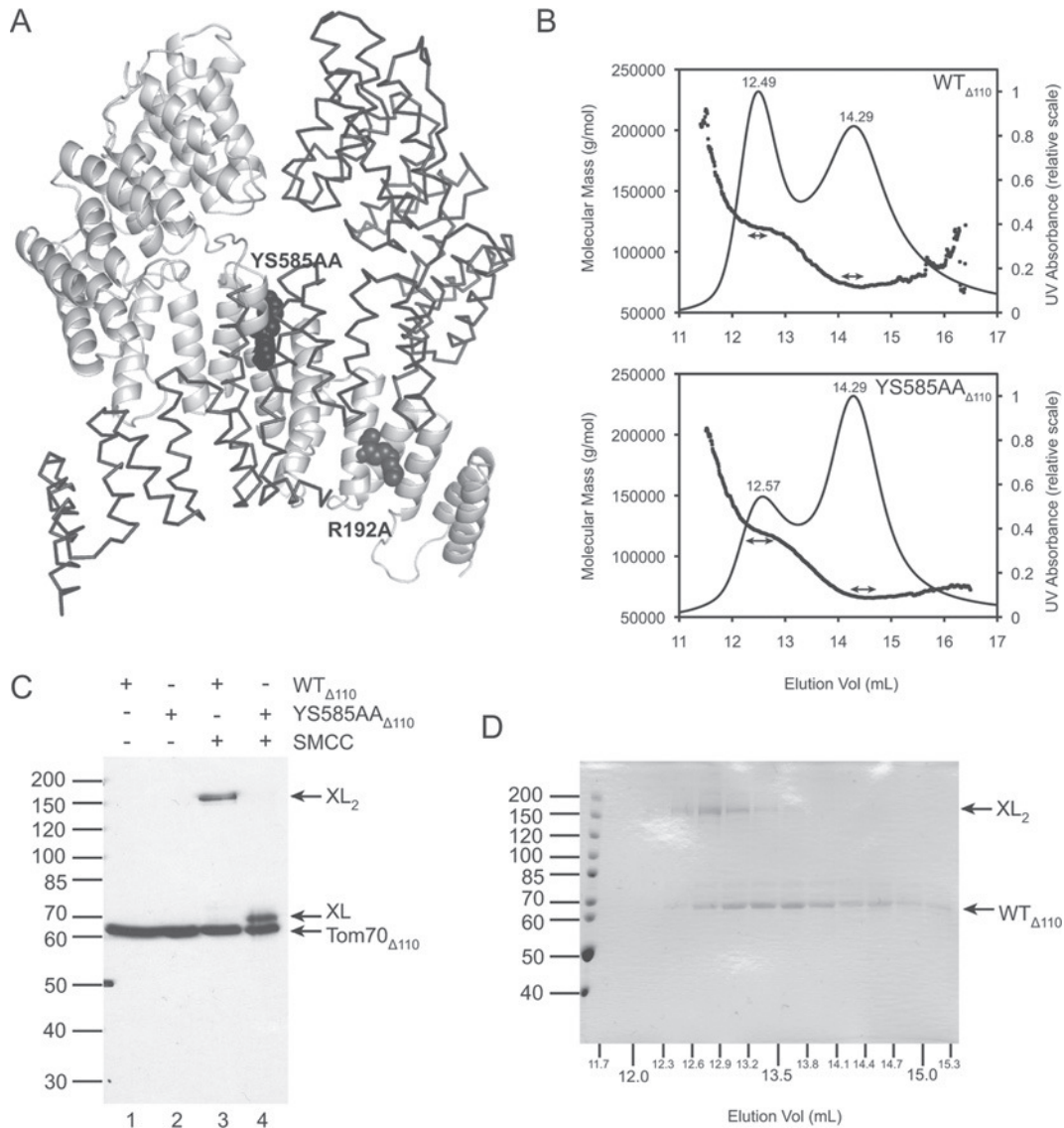


Figure 2 The mutation YS585AA disrupts homodimerization of Tom70_{Δ110}

(A) An intertwined dimeric model of Tom70 was generated with the human homology model (ribbon structure) superimposed on to the yeast Tom70 crystal structure (PDB: 2GW1) used as template (stick structure). A double mutation at the dimerization interface, YS585AA (black spheres), was generated in human Tom70. Mutation R192A (dark grey spheres) in the TPR clamp is also indicated in the structure. (B) Recombinant Tom70 WT_{Δ110} (upper panel) and YS585AA_{Δ110} (lower panel) were analysed by SEC-MALS. The elution profile from a Superdex 200 10/300 column (straight line) is plotted with the corresponding molecular masses (squares). Elution volumes of the peaks are indicated. Double arrows denote areas under the peaks selected for molecular mass estimations. (C) Cross-linking of recombinant WT_{Δ110} and YS585AA_{Δ110} performed with 1% DMSO control (lanes 1 and 2) or 100 μ M SMCC (lanes 3 and 4). The higher molecular mass cross-link was observed at approx. 150 kDa (arrow XL₂) for WT_{Δ110} (lane 3) but not for YS585AA_{Δ110} (lane 4). (D) WT_{Δ110} was cross-linked with 100 μ M SMCC and then resolved on a Superdex 200 10/300 column. Fractions between 11.7 and 15.3 ml were pooled, trichloroacetic acid precipitated and analysed by SDS/PAGE and Coomassie Blue staining. The homodimeric cross-link (arrow XL₂) eluted in earlier fractions, whereas in later fractions only un-cross-linked Tom70 was present.

a domain-dissociated and more flexible state of monomeric protein.

To confirm the effect of the mutation, the purified proteins WT_{Δ110} and YS585AA_{Δ110} were subjected to SEC followed by in-line MALS with concentration determination by refractive index (Figure 2B). Tom70 WT_{Δ110} eluted in two peaks at 12.5 ml and 14.3 ml, and the proportion of early peak to late peak was estimated to be 50:50. Although the mutant YS585AA_{Δ110} also eluted in two peaks at 12.6 ml and 14.3 ml, the proportion of early peak to late peak was significantly reduced to 30:70. The molecular masses of protein in the early peaks were unambiguously determined by MALS to be 120 kDa for both WT_{Δ110} and YS585AA_{Δ110} (119.5 kDa and 119.9 kDa respectively, rounded

up), indicating that the peaks were dimeric human Tom70 species. The molecular masses of the protein in the late peaks were calculated to be 71.8 kDa for WT_{Δ110} and 66.2 kDa for YS585AA_{Δ110}, which should correspond to the monomeric forms with predicted molecular masses of 59.6 kDa and 59.5 kDa respectively. The molecular mass estimations for the late peaks were probably skewed upwards because of co-eluting dimeric species trailing from the early peaks, a common chromatographic occurrence that did not affect analysis of the early peaks. In addition, SEC analysis of WT_{Δ110} at progressively lower concentrations produced increasingly higher late peaks, in agreement with a monomer–dimer equilibrium in solution (see Supplementary Figure S1B). Although there was no evidence of different monomeric conformations

between the open elongated and the domain-dissociated flexible states, the difference in physical and structural characteristics may be too small to be resolved by the SEC separation. Overall, SEC-MALS provided firm evidence that human recombinant Tom70 can exist as monomer and dimer, consistent with our AUC experiments (Figures 1B and 1C), and that the YS585AA mutation shifts the monomer–dimer equilibrium towards the monomeric form.

In addition to the biophysical methods, we also characterized the effect of the YS585AA mutation by chemical cross-linking for comparison with the earlier yeast Tom70 studies. We treated the purified proteins with the heterobifunctional cross-linking reagent SMCC, followed by immunoblotting against Tom70 (Figure 2C). SMCC is amine- and sulfhydryl-reactive and similar to the cross-linking reagent MBS (*m*-maleimidobenzoyl-*N*-hydroxysulfosuccinimide ester) used in previous studies [19,21]. Immunoblotting following SDS/PAGE showed that both WT_{Δ110} and YS585AA_{Δ110} migrated at 60 kDa in the absence of cross-linker. In the presence of SMCC, WT_{Δ110} formed a strong homodimeric cross-link band at approx. 150 kDa (Figure 2C, XL₂), which was not observed with YS585AA_{Δ110}. Instead, YS585AA_{Δ110} formed a cross-link band slightly above 60 kDa (Figure 2C, XL). We interpret this cross-link as an internal cross-link of the monomeric protein as it clearly migrates too rapidly to be any type of cross-linked dimer. It is possible that a more flexible monomeric conformation of the mutant could favour an internal cross-link, but it is highly unlikely that a more rigid WT monomer could produce the 150 kDa cross-link. We tested our result further by analysing cross-linked WT_{Δ110} by SEC (Figure 2D). The 150 kDa cross-link band eluted in a single peak between 12.3 and 13.5 ml (Figure 2D, XL₂), identical to the early peak in the SEC-MALS experiments. In contrast, the 60 kDa band spanned a wider range between 12.6 and 14.7 ml, in which both un-cross-linked dimeric Tom70 as well as monomeric Tom70 may be present. Taken together, we have clear evidence, from AUC, SEC-MALS and cross-linking, of dimeric as well as monomeric soluble human Tom70, and furthermore that our YS585AA mutant disrupts the homodimerization and shifts the equilibrium towards the monomer.

We thus proceeded to test the effect of the oligomeric state of human Tom70 on preprotein targeting and chaperone docking. Previously established co-precipitation assays were used [13], including the R192A mutation in the TPR clamp domain (Figure 2A, grey spheres) as a negative control. This mutation was shown to abolish chaperone-docking and preprotein targeting to human Tom70 [12]. The Tom70-dependent preproteins, OGC and PiC, were radiolabelled by cell-free translation and incubated with His-tagged Tom70 WT_{Δ110}, YS585AA_{Δ110} or R192A_{Δ110} as indicated. Stable complexes were isolated on nickel–Sepharose beads and analysed by SDS/PAGE and autoradiography. OGC was clearly pulled down by Tom70 WT_{Δ110} (Figure 3A, lane 3). Remarkably, YS585AA_{Δ110} increased the level of OGC recovered to approx. 140% of WT_{Δ110} (**P* = 0.039, Figure 3A, lane 4). In contrast, the level of OGC recovered by R192A_{Δ110} was reduced practically to the negative control without Tom70 (Figure 3A, lanes 2 and 5). Pull-down of the preprotein PiC showed a similar pattern (Figure 3B), with the amount of PiC recovered by YS585AA_{Δ110} increased to approx. 120% of WT_{Δ110} (***P* = 0.0013). The mutant was therefore more efficient at preprotein targeting than WT Tom70.

Tom70 is thought to directly contact preproteins after the chaperone-docking step. We asked whether this increase in preprotein targeting was a direct result of increased preprotein interaction with the import receptor, or an indirect effect from increased chaperone docking. We used the same co-precipitation assay except with radiolabelled Hsc70 (Figure 3C) and Hsp90

(Figure 3D) to monitor the level of chaperone docking on to Tom70 [13]. Radiolabelled chaperones Hsc70 (Figure 3C) and Hsp90 (Figure 3D) were recovered by WT_{Δ110} and YS585AA_{Δ110} to the same extent, whereas the mutant R192A_{Δ110} abolished chaperone docking to the level of the empty beads control. This indicates that our dimerization mutant, YS585AA_{Δ110}, binds chaperones as efficiently as WT_{Δ110}. We thus provide clear evidence that monomeric human Tom70 has higher levels of preprotein targeting via a mechanism that is separate from chaperone docking.

The oligomeric status may also affect the affinity of Tom70–preprotein interaction. Previous work using co-precipitation, cross-linking and resistance to denaturants revealed direct interactions between PiC and purified Tom70 [12]. We studied the preprotein–Tom70 contacts by co-precipitating the radiolabelled preproteins PiC and OGC with WT_{Δ110} or YS585AA_{Δ110} as above. The stably recovered complexes were then treated with a homobifunctional sulfhydryl-reactive cross-linker BMH, washed with buffer containing SDS and analysed by SDS/PAGE and autoradiography. Upon cross-linking of the isolated PiC complexes with WT_{Δ110} or YS585AA_{Δ110}, three SDS-resistant bands appeared at the higher-molecular-mass range 100–200 kDa (Figure 4A). In particular, cross-linked band ‘a’ was significantly stronger in PiC–YS585AA_{Δ110} than in PiC–WT_{Δ110} complexes (Figure 4A, compare arrow XL_a, lanes 3 to 4 and 6 to 7). The resistance of the enhanced band ‘a’ to SDS confirmed that it represented a direct contact between preprotein and Tom70. Furthermore, a stronger cross-link band was also observed in OGC–YS585AA_{Δ110} complexes (Figure 4B, compare arrow XL_a, lanes 3 and 6). The appearance of the stronger cross-links suggested that the YS585AA mutation enhanced direct contacts between the preprotein and Tom70, and that preprotein–Tom70 interactions are stabilized in the monomeric form of the receptor. Taken together, the monomeric Tom70 binds preproteins, but not chaperones, more efficiently, thus increasing preprotein targeting.

We concluded from our co-precipitation and cross-linking of stable preprotein–Tom70 complexes that the functional form of human Tom70 is monomeric, which led us to investigate human Tom70 in its endogenous membrane context. In experiments with isolated yeast mitochondria, cross-linking with 1 mM MBS led to a dimeric Tom70 species [19,21]. The same result is observed with the recombinant human Tom70 using a related cross-linker SMCC (Figure 2C). Therefore, we isolated mitochondria from HeLa cells and performed cross-linking with the membrane-impermeable cross-linker, s-SMCC. Mitochondria were incubated with 1% DMSO or s-SMCC in concentrations of 1–1000 μM and then analysed by SDS/PAGE and immunoblotting for Tom70 (Figure 5A). Surprisingly, human Tom70 did not form a homodimeric cross-link species at any of the cross-linker concentrations tested. Instead, a Tom70-adduct was observed at approx. 85 kDa in the presence of 500 μM and 1 mM s-SMCC (Figure 5A, lanes 2 and 3). The cross-link could represent an internal contact as observed with purified YS585AA_{Δ110}, or some other interaction on the membrane, but in any case it is too small to be homodimeric Tom70. This first report of cross-linking endogenous human Tom70 shows that human Tom70 exists predominantly as a monomer on the outer mitochondrial membrane. Human Tom70 is therefore distinct from its yeast homologue, which cross-links as dimers on the membrane [19,21].

We also compared endogenous human Tom70 on BN-PAGE, which had been applied to its yeast counterpart [19]. We solubilized the HeLa cell mitochondria in 1% digitonin, separated the lysate on BN-PAGE and then detected Tom70 by immunoblotting. Human Tom70 migrated in a wide band slightly above 140 kDa on BN-PAGE, larger than expected for monomers

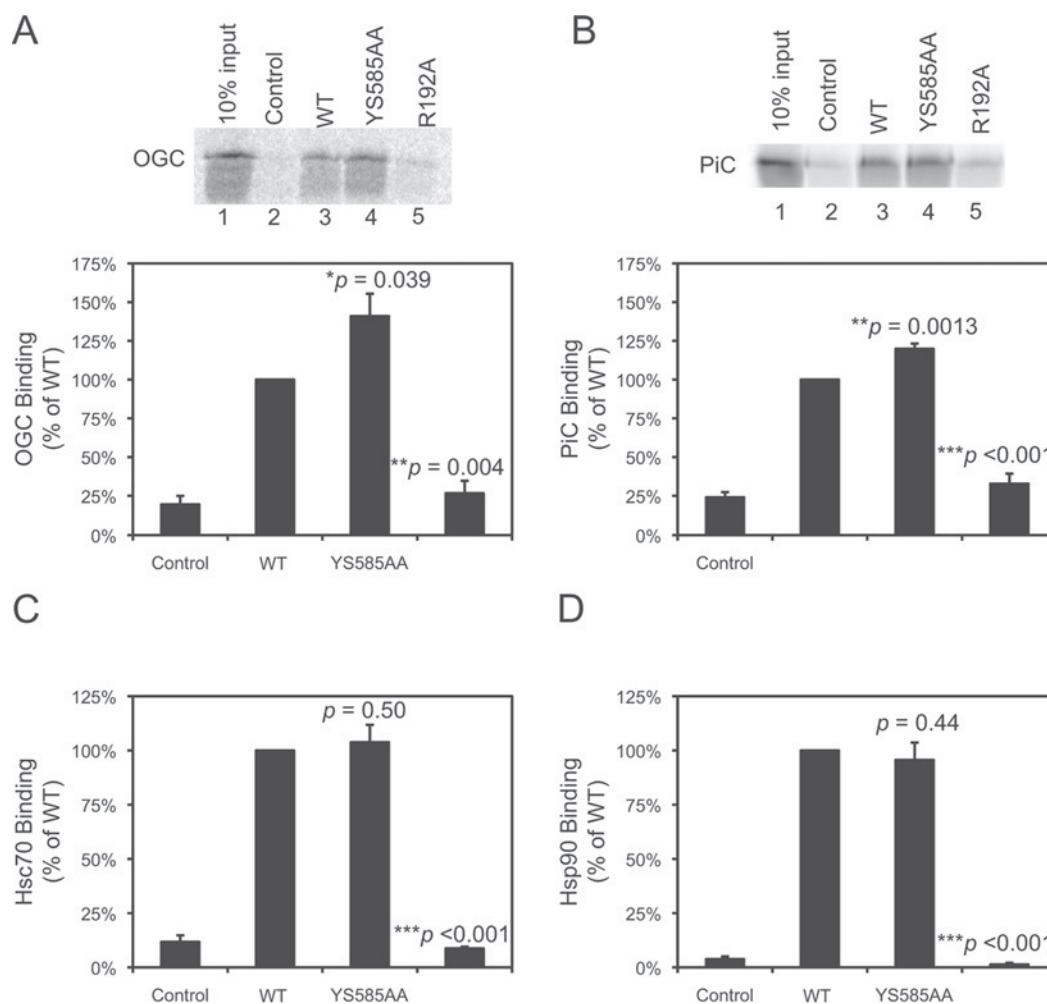


Figure 3 Co-precipitation of Tom70_{Δ110} with preproteins and chaperones

(A) OGC was radiolabelled by cell-free translation (lane 1) and then co-precipitated with nickel–Sepharose in the absence (lane 2) or presence of the His-tagged cytosolic domain of human Tom70 WT_{Δ110}, YS585AA_{Δ110} or R192A_{Δ110} (lanes 3–5). The final concentration of the His-tagged proteins was 5 μM, which was within the biological concentration range of Hsp90 and its co-chaperones. Quantification of the OGC band showed OGC bound by YS585AA_{Δ110} was increased to 140% of WT_{Δ110} at 5% level of significance. (B) Similarly, radiolabelled PiC was recovered by YS585AA_{Δ110} and the amount bound was increased to 120% of WT_{Δ110} at 1% level of significance. Co-precipitation of radiolabelled Hsc70 (C) and Hsp90 (D) showed no significant difference in chaperone docking between WT_{Δ110} and YS585AA_{Δ110}. Significance level (*P*) was calculated based on the Student's *t* test with a minimum of three independent experiments (*n* ≥ 3).

(Figure 5B), but similar to the migration of the yeast homologue. However, addition of the cross-linker *s*-SMCC had no effect on the migration of human Tom70 on BN-PAGE (results not shown), and such treatment had been shown not to produce a homodimeric cross-link (Figure 5A). This led us to believe that monomeric full-length Tom70 may migrate abnormally slowly on BN-PAGE.

To address this using a different approach, we compared the WT Tom70 in its native environment with the YS585AA mutant form that favoured the monomeric state. Full-length WT and YS585AA Tom70 were radiolabelled by cell-free translations (Figure 5C, lanes 1 and 4). After integration into isolated HeLa cell mitochondria, the mitochondria containing Tom70 WT or YS585AA were treated with 1% DMSO or 1 mM *s*-SMCC and analysed by electrophoresis and autoradiography (Figure 5C, lanes 2, 3, 5 and 6). Again, a lower-molecular-mass adduct was present at 85 kDa on SDS/PAGE, but no homodimeric cross-link was observed for radiolabelled human Tom70 WT and YS585AA. In parallel experiments, radiolabelled WT and YS585AA Tom70 integrated into HeLa cell mitochondria were analysed by BN-PAGE (Figure 5D), and both migrated identically

with endogenous Tom70 (Figure 5B). These results also suggested a slow abnormal migration of monomeric Tom70.

Furthermore, we investigated the behaviour of our purified recombinant Tom70 WT_{Δ110} and YS585AA_{Δ110} on BN-PAGE. We had already shown that WT_{Δ110} exists in equilibrium between monomer and dimer, whereas YS585AA_{Δ110} is mostly monomeric. Nonetheless, when subjected to BN-PAGE under the same conditions used for endogenous HeLa cell Tom70, both of them migrated slightly below 140 kDa (Figure 5E), and the addition of the cross-linker SMCC had no apparent effect on such migration (results not shown). This result was in reasonable agreement with the full-length forms (Figures 5B and 5D), given that the recombinant proteins have smaller molecular masses. This was also intriguing because a difference in migrations on BN-PAGE between monomeric and dimeric Tom70 populations was not detected. To investigate this more closely, we treated WT_{Δ110} and YS585AA_{Δ110} with SMCC (Figure 2C, lanes 3 and 4), and resolved them on BN-PAGE in the first dimension followed by SDS/PAGE in the second dimension (Figure 5F). In addition to the main band in the centre, WT_{Δ110} formed a homodimeric

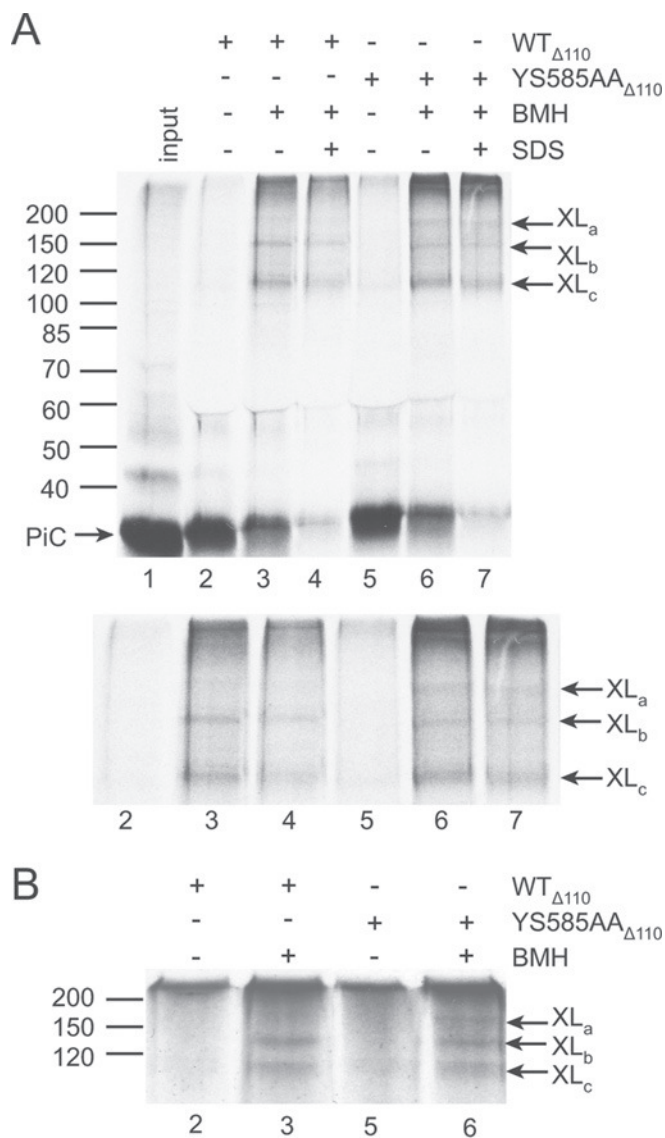


Figure 4 Cross-linking of preprotein-Tom70_{Δ110} complexes

(A) Upper panel: radiolabelled PiC (lane 1) was co-precipitated with His-tagged WT_{Δ110} (lane 2) or YS585AA_{Δ110} (lane 5) and recovered by nickel–Sepharose as described in Figure 3. After incubation with BMH, stable complexes were washed in the absence (lanes 3 and 6) or presence of SDS (lanes 4 and 7). Bands that are SDS-resistant represent direct interactions (XL arrows). A cross-link of particular interest in YS585AA_{Δ110} is marked (XL_a). Lower panel: a magnified view of the cross-linked bands at the higher molecular masses. (B) Radiolabelled OGC was co-precipitated and cross-linked with BMH (XL arrows). A magnified view of the cross-linked bands is shown. Lanes are numbered as in (A).

cross-link at approx. 150 kDa on SDS/PAGE (Figure 5F, XL₂, left panel). Although this homodimeric cross-link was well separated in the second dimension, it migrated only slightly slower than the non-cross-linked Tom70 on the BN-PAGE first dimension. In agreement with this, YS585AA_{Δ110} mainly resolved as a spot in the centre similar to that of WT (Figure 5F, right panel), with only a trace amount of homodimeric cross-link visible on overexposure of the immunoblot. We conclude that the monomeric and dimeric forms of Tom70 had similar and overlapping migrations in BN-PAGE. This may be due to the asymmetric shape of the monomer, or the flexibility of different monomer conformations [18,25].

Taken together, our results suggest that cross-linking rather than BN-PAGE migration is the more reliable test of Tom70 homo-

dimerization. By this measure, we showed that the conditions on the outer mitochondrial membrane are normally unfavourable for dimer formation, perhaps because the concentration of human Tom70 on the membrane is too low. Our co-precipitation and cross-linking experiments of stable preprotein–Tom70 complexes also suggest that the monomer is the functional state capable of binding both chaperones and preproteins. However, Tom70 oligomerization under transiently high local concentrations at subsequent import steps is still possible.

DISCUSSION

The present study provides the first experimental demonstration that the biological function of Tom70 is affected by its oligomeric state. Previous biophysical studies of recombinant yeast Tom70 provided convincing evidence that it was solely monomeric, and functional for binding peptides from chaperone and preprotein. Yet, because dimers of yeast Tom70 could only be observed by cross-linking of endogenous protein on membranes, the relative activity of the putative dimers could not be directly tested [18,19,23]. In the present study, we find that dimers of recombinant human Tom70 can in fact be detected, but that human Tom70 monomers are more active than dimers in interacting with preproteins. This is consistent with the predominantly monomeric form of Tom70 observed on human mitochondria. Overall, our results support the idea that Tom70 is functionally monomeric [18], with higher-order oligomers formed only transiently or under particular conditions.

Human Tom70 diverges from its yeast homologue in many regions of primary sequence, and it is not surprising that aspects of its biochemical mechanism also differ. Functional surfaces including the TPR clamp domain are moderately, not absolutely, conserved between the proteins, and it has been shown that specificity of chaperone binding is different between human and yeast Tom70 [12]. The surface of human Tom70 that is predicted to form the interdomain and/or intersubunit contact is also divergent from the yeast protein, with the critical Tyr⁵⁸⁵–Ser⁵⁸⁶ residues being identical only in metazoan Tom70s (the equivalent residues are isoleucine and threonine in *S. cerevisiae* Tom70 and threonine and threonine in Tom71). Differences in oligomer formation between human and yeast Tom70 may also be expected. Indeed, AUC SV and SE experiments (Figures 1B and 1C) and SEC-MALS data (Figure 2B) established that, although soluble human Tom70 monomers were the majority of the population, dimers were unambiguously evident. The double YS585AA mutation in the predicted interdomain interface disrupted homodimerization of recombinant human Tom70, as shown by SEC-MALS and cross-linking (Figures 2B and 2C). This provided us with a means of testing the effect of dimerization on Tom70 function. Preprotein targeting to Tom70 was more efficient with the monomeric form of the receptor, but not by changing Tom70 interaction with chaperones. Instead, stronger preprotein–Tom70 cross-links were observed, indicating greater contact between the molecules. These results suggest that human Tom70 receives and interacts with preproteins in a monomeric state. Therefore, the monomeric mechanism of Tom70 characterized by Mills et al. [18] is fundamentally conserved from yeast to humans.

In monomeric Tom70, the YS585AA mutation could also promote dissociation of the TPR clamp and C-terminal domains and increase the overall flexibility of the protein. We were unable to directly observe conformational differences within the monomer populations, as the bulk biophysical properties of the conformers were apparently too similar. It can still be speculated that the domain-dissociated monomer is more efficient

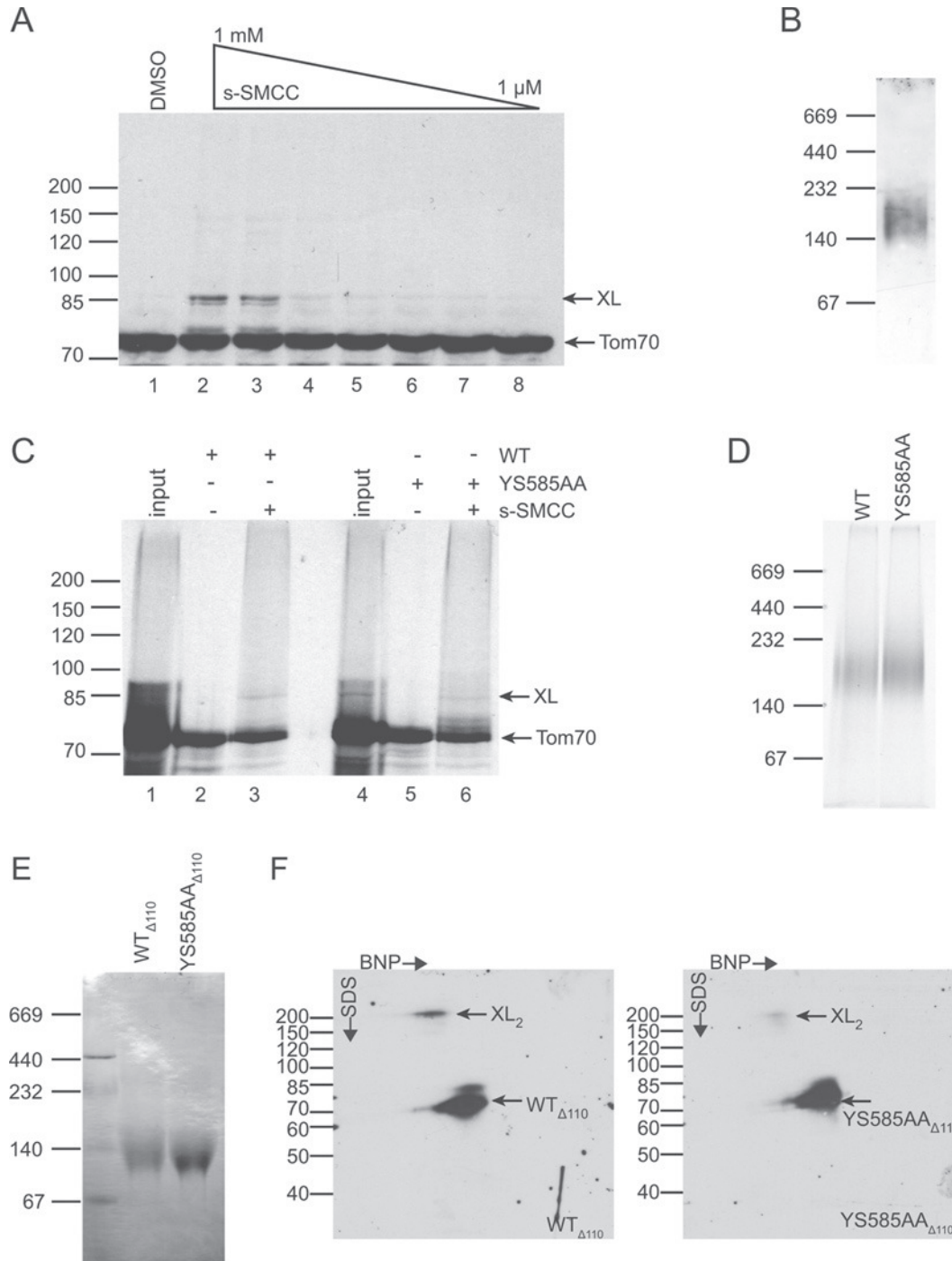


Figure 5 The native state of human Tom70

(A) Mitochondria from HeLa cells were incubated with 1% DMSO (lane 1) or cross-linked with 1000, 500, 100, 50, 10, 5 or 1 μM s-SMCC (lanes 2–8) and then analysed by SDS/PAGE and immunoblotting against Tom70. (B) HeLa cell mitochondria were solubilized in 1% digitonin and resolved on 6–16.5% BN-PAGE gels. Endogenous Tom70 was visualized by immunoblotting. (C) Full-length human Tom70 WT or YS585AA were radiolabelled by cell-free translation (lanes 1 and 4). After insertion into HeLa cell mitochondria, reactions were incubated with 1% DMSO (lanes 2 and 5) or 1 mM s-SMCC (lanes 3 and 6) and analysed by SDS/PAGE and autoradiography. (D) Radiolabelled human Tom70 WT or YS585AA was inserted into HeLa cell mitochondria, solubilized in 1% digitonin and analysed on BN-PAGE and autoradiography as described. (E) WT_{Δ110} and YS585AA_{Δ110} were resolved on BN-PAGE in the presence of 1% digitonin and then visualized by Coomassie Blue staining. Native molecular mass markers are indicated. (F) WT_{Δ110} (left panel) and YS585AA_{Δ110} (right panel) were cross-linked with 100 μM SMCC, resolved on BN-PAGE and SDS/PAGE (8% gels) in the second dimension, followed by immunoblotting against Tom70. The homodimeric cross-link (XL₂) was well separated on SDS-PAGE but not on BN-PAGE.

at contacting preprotein than the domain-docked form, because the increased flexibility may allow the C-terminal domain to adapt its structure to that of the preprotein ligand. Also, we

cannot distinguish the domain arrangement within our observed dimers. Although it is possible that the subunits are in the closed conformation first proposed by Wu and Sha [22], it seems more

likely that the dimers are made up of subunits in the elongated open form, in the interpretation of Mills et al. [18]. The dimer would then resemble that depicted in Figure 2(A). The latter arrangement would allow dimer formation without major internal re-orientations of the domains for both human and yeast Tom70.

Recent structural studies of yeast Tom70 [18] and Tom71 [25] support our monomeric model of Tom70 function and outline a generally conserved mechanism. Nonetheless, given that human recombinant Tom70 can form homodimers, we cannot rule out the possibility that homodimeric Tom70 may be present on the outer mitochondrial membrane as a minor species. It was suggested that in a resting state, yeast Tom70 could exist in a homodimeric form to prevent non-specific interactions, and that chaperone docking may be involved in opening Tom70 into the monomeric state before preprotein binding [25]. We suggest an updated model in which human Tom70 interacts with chaperones and preproteins in the monomeric active form, and the homodimeric form may be involved in another mechanistic function perhaps unique to metazoan Tom70s. After preprotein binding, up to six active monomeric receptors may be recruited by one molecule of preprotein in order to proceed to the general import pore [19]. This creates a local environment where high concentrations of the receptor may drive transient homodimerization. The closed conformation of the homodimer could then provide a mechanism for the import receptor to release the preprotein for translocation across the outer mitochondrial membrane. It is also possible that dimerization of Tom70 is induced under certain cellular conditions, perhaps by post-translational modifications, as a means of down-regulating mitochondrial import. New approaches to study Tom70 in the process of preprotein translocation will be needed to establish or refute these ideas.

AUTHOR CONTRIBUTION

Experiments were performed by Anna Fan (Figures 2–5 and Supplementary Figure S1) and Lisandra Gava (Figure 1). The experimental strategy was directed by Jason Young and Carlos Ramos, in consultation with Anna Fan and Lisandra Gava. The manuscript was written by Anna Fan and Jason Young, with assistance from Carlos Ramos. Figures were prepared by Anna Fan, Lisandra Gava and Carlos Ramos. The project was initiated and supervised by Jason Young.

ACKNOWLEDGEMENTS

We thank Richard Marcellus, William Wittbold (Wyatt Technology) and the members of Jason Young's laboratory for technical assistance.

FUNDING

This work was supported by the Canadian Institutes of Health Research [grant number MOP-68825], and grants from Fundação de Amparo a Pesquisa do Estado de São Paulo (FAPESP) and Conselho Nacional de Pesquisa e Desenvolvimento (CNPq). J.C.Y. holds a Tier II Canada Research Chair in Molecular Chaperones. L.M.G. holds a FAPESP fellowship.

REFERENCES

- Westermann, B. and Neupert, W. (2003) 'Omics' of the mitochondrion. *Nat. Biotechnol.* **21**, 239–240
- Chacinska, A., Koehler, C. M., Milenkovic, D., Lithgow, T. and Pfanner, N. (2009) Importing mitochondrial proteins: machineries and mechanisms. *Cell* **138**, 628–644
- Brix, J., Dietmeier, K. and Pfanner, N. (1997) Differential recognition of preproteins by the purified cytosolic domains of the mitochondrial import receptors Tom20, Tom22, and Tom70. *J. Biol. Chem.* **272**, 20730–20735
- Abe, Y., Shodai, T., Muto, T., Mihara, K., Torii, H., Nishikawa, S., Endo, T. and Kohda, D. (2000) Structural basis of presequence recognition by the mitochondrial protein import receptor Tom20. *Cell* **100**, 551–560
- Ryan, M. T., Muller, H. and Pfanner, N. (1999) Functional staging of ADP/ATP carrier translocation across the outer mitochondrial membrane. *J. Biol. Chem.* **274**, 20619–20627
- Chan, N. C., Lick, V. A., Waller, R. F., Mulhern, T. D. and Lithgow, T. (2006) The C-terminal TPR domain of Tom70 defines a family of mitochondrial protein import receptors found only in animals and fungi. *J. Mol. Biol.* **358**, 1010–1022
- Yamamoto, H., Fukui, K., Takahashi, H., Kitamura, S., Shiota, T., Terao, K., Uchida, M., Esaki, M., Nishikawa, S. I., Yoshihisa, T. et al. (2009) Roles of TOM70 in import of presequence-containing mitochondrial proteins. *J. Biol. Chem.* **284**, 31635–31646
- Humphries, A. D., Streimann, I. C., Stojanovski, D., Johnston, A. J., Yano, M., Hoogenraad, N. J. and Ryan, M. T. (2005) Dissection of the mitochondrial import and assembly pathway for human Tom40. *J. Biol. Chem.* **280**, 11535–11543
- Chou, C. H., Lee, R. S. and Yang-Yen, H. F. (2006) An internal EELD domain facilitates mitochondrial targeting of Mcl-1 via a Tom70-dependent pathway. *Mol. Biol. Cell* **17**, 3952–3963
- Otera, H., Taira, Y., Horie, C., Suzuki, Y., Setoguchi, K., Kato, H., Oka, T. and Mihara, K. (2007) A novel insertion pathway of mitochondrial outer membrane proteins with multiple transmembrane segments. *J. Cell Biol.* **179**, 1355–1363
- Rone, M. B., Liu, J., Blonder, J., Ye, X., Veenstra, T. D., Young, J. C. and Papadopoulos, V. (2009) Targeting and insertion of the cholesterol-binding translocator protein into the outer mitochondrial membrane. *Biochemistry* **48**, 6909–6920
- Young, J. C., Hoogenraad, N. J. and Hartl, F. U. (2003) Molecular chaperones Hsp90 and Hsp70 deliver preproteins to the mitochondrial import receptor Tom70. *Cell* **112**, 41–50
- Fan, A. C., Bhargoo, M. K. and Young, J. C. (2006) Hsp90 functions in the targeting and outer membrane translocation steps of Tom70-mediated mitochondrial import. *J. Biol. Chem.* **281**, 33313–33324
- Bhargoo, M. K., Tzankov, S., Fan, A. C., Deigaard, K., Thomas, D. Y. and Young, J. C. (2007) Multiple 40-kDa heat-shock protein chaperones function in Tom70-dependent mitochondrial import. *Mol. Biol. Cell* **18**, 3414–3428
- Zara, V., Ferramosca, A., Robitaille-Foucher, P., Palmieri, F. and Young, J. C. (2009) Mitochondrial carrier protein biogenesis: role of the chaperones Hsc70 and Hsp90. *Biochem. J.* **419**, 369–375
- Scheuffler, C., Brinker, A., Bourenkov, G., Pegoraro, S., Moroder, L., Bartunik, H., Hartl, F. U. and Moarefi, I. (2000) Structure of TPR domain-peptide complexes: critical elements in the assembly of the Hsp70-Hsp90 multichaperone machine. *Cell* **101**, 199–210
- Brix, J., Ziegler, G. A., Dietmeier, K., Schneider-Mergener, J., Schulz, G. E. and Pfanner, N. (2000) The mitochondrial import receptor Tom70: identification of a 25 kDa core domain with a specific binding site for preproteins. *J. Mol. Biol.* **303**, 479–488
- Mills, R. D., Trewella, J., Qiu, T. W., Welte, T., Ryan, T. M., Hanley, T., Knott, R. B., Lithgow, T. and Mulhern, T. D. (2009) Domain organization of the monomeric form of the Tom70 mitochondrial import receptor. *J. Mol. Biol.* **388**, 1043–1058
- Wiedemann, N., Pfanner, N. and Ryan, M. T. (2001) The three modules of ADP/ATP carrier cooperate in receptor recruitment and translocation into mitochondria. *EMBO J.* **20**, 951–960
- Truscott, K. N., Wiedemann, N., Rehling, P., Muller, H., Meisinger, C., Pfanner, N. and Guiard, B. (2002) Mitochondrial import of the ADP/ATP carrier: the essential TIM complex of the intermembrane space is required for precursor release from the TOM complex. *Mol. Cell Biol.* **22**, 7780–7789
- Sollner, T., Rassow, J., Wiedemann, M., Schlossmann, J., Keil, P., Neupert, W. and Pfanner, N. (1992) Mapping of the protein import machinery in the mitochondrial outer membrane by crosslinking of translocation intermediates. *Nature* **355**, 84–87
- Wu, Y. and Sha, B. (2006) Crystal structure of yeast mitochondrial outer membrane translocator member Tom70p. *Nat. Struct. Mol. Biol.* **13**, 589–593
- Beddoe, T., Bushell, S. R., Perugini, M. A., Lithgow, T., Mulhern, T. D., Bottomley, S. P. and Rossjohn, J. (2004) A biophysical analysis of the tetratricopeptide repeat-rich mitochondrial import receptor, Tom70, reveals an elongated monomer that is inherently flexible, unstable, and unfolds via a multistate pathway. *J. Biol. Chem.* **279**, 46448–46454
- Bushell, S. R., Bottomley, S. P., Rossjohn, J. and Beddoe, T. (2006) Tracking the unfolding pathway of a multirepeat protein via tryptophan scanning: evidence of localized instability in the mitochondrial import receptor Tom70. *J. Biol. Chem.* **281**, 24345–24350
- Li, J., Qian, X., Hu, J. and Sha, B. (2009) Molecular chaperone Hsp70/Hsp90 prepares the mitochondrial outer membrane translocator receptor Tom71 for preprotein loading. *J. Biol. Chem.* **284**, 23852–23859
- Suzuki, H., Maeda, M. and Mihara, K. (2002) Characterization of rat TOM70 as a receptor of the preprotein translocase of the mitochondrial outer membrane. *J. Cell Sci.* **115**, 1895–1905
- Palmisano, A., Zara, V., Honlinger, A., Voza, A., Dekker, P. J., Pfanner, N. and Palmieri, F. (1998) Targeting and assembly of the oxoglutarate carrier: general principles for biogenesis of carrier proteins of the mitochondrial inner membrane. *Biochem. J.* **333**, 151–158
- Zara, V., Rassow, J., Wachter, E., Tropschug, M., Palmieri, F., Neupert, W. and Pfanner, N. (1991) Biogenesis of the mitochondrial phosphate carrier. *Eur. J. Biochem.* **198**, 405–410

-
- 29 Young, J. C. and Hartl, F. U. (2000) Polypeptide release by Hsp90 involves ATP hydrolysis and is enhanced by the co-chaperone p23. *EMBO J.* **19**, 5930–5940
- 30 Bohm, G., Muhr, R. and Jaenicke, R. (1992) Quantitative analysis of protein far UV circular dichroism spectra by neural networks. *Protein Eng.* **5**, 191–195
- 31 Borges, J. C., Fischer, H., Craievich, A. F., Hansen, L. D. and Ramos, C. H. (2003) Free human mitochondrial GrpE is a symmetric dimer in solution. *J. Biol. Chem.* **278**, 35337–35344
- 32 Johnson, M. L., Correia, J. J., Yphantis, D. A. and Halvorson, H. R. (1981) Analysis of data from the analytical ultracentrifuge by nonlinear least-squares techniques. *Biophys. J.* **36**, 575–588
- 33 Brown, P. H. and Schuck, P. (2006) Macromolecular size-and-shape distributions by sedimentation velocity analytical ultracentrifugation. *Biophys. J.* **90**, 4651–4661
- 34 Schwede, T., Kopp, J., Guex, N. and Peitsch, M. C. (2003) SWISS-MODEL: an automated protein homology-modeling server. *Nucleic Acids Res.* **31**, 3381–3385
-

Received 7 December 2009/16 May 2010; accepted 26 May 2010

Published as BJ Immediate Publication 26 May 2010, doi:10.1042/BJ20091855

SUPPLEMENTARY ONLINE DATA

Human mitochondrial import receptor Tom70 functions as a monomer

Anna C. Y. FAN*, Lisandra M. GAVA†‡, Carlos H. I. RAMOS† and Jason C. YOUNG*¹

*Department of Biochemistry, McGill University, 3649 Promenade Sir William Osler, Montreal, Quebec, Canada H3G 0B1, †Institute of Chemistry, University of Campinas (UNICAMP), Campinas, SP, Brazil, and ‡Institute of Biology, University of Campinas (UNICAMP), Campinas, SP 13083-970, Brazil

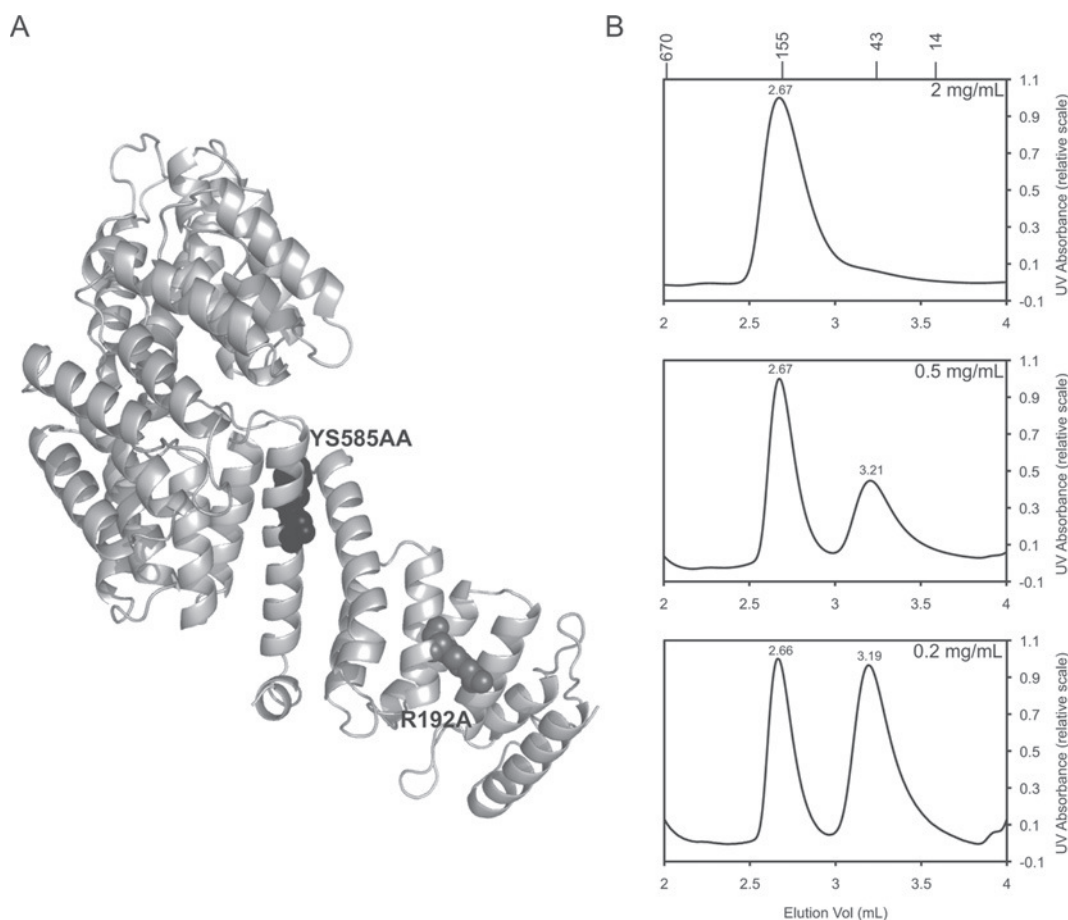


Figure S1 Concentration-dependent behaviour of Tom70_{Δ110} on SEC provides evidence for monomer–dimer equilibrium

(A) An alternative monomeric homology model of human Tom70 was generated with the unliganded yeast Tom71 crystal structure (PDB: 3FP3) as template. The dimerization mutant, YS585AA (black spheres), and the TPR clamp mutant, R192A (grey spheres), are also indicated. (B) The dimer populations of Tom70 WT_{Δ110} are concentration-dependent. Samples were loaded on to a Biosuite 250 4 μ m UHR SEC column at 2 mg/ml (upper panel), 0.5 mg/ml (middle panel) and 0.2 mg/ml (lower panel), with corresponding proportions of the early peak (2.5–3.0 ml) against the late peak (3.0–3.5 ml) being 90:10, 60:40 and 40:60 respectively. Elution volumes of the peaks and the molecular mass markers, including thyroglobulin (670 kDa), γ -globulin (155 kDa), ovalbumin (43 kDa) and ribonuclease A (14 kDa), are indicated.

Received 7 December 2009/16 May 2010; accepted 26 May 2010
 Published as BJ Immediate Publication 26 May 2010, doi:10.1042/BJ20091855

¹ To whom correspondence should be addressed (email jason.young2@mcgill.ca).

CAPÍTULO 4

ARTIGO CIENTÍFICO:

Stoichiometry and thermodynamics of the interaction between the C-terminus of human 90 kDa heat shock protein Hsp90 and the mitochondrial translocase of outer membrane Tom70.

Publicado na revista *Archives of Biochemistry and Biophysics* (2011) 513(2): 119-125.

LISANDRA MARQUES GAVA, DANIELI CRISTINA GONÇALVES, JÚLIO CÉSAR BORGES & CARLOS HENRIQUE INÁCIO RAMOS

A grande maioria das proteínas mitocondriais é codificada por genes nucleares e sintetizada como proteínas precursoras nos ribossomos no citosol. Essas proteínas precursoras contêm regiões sinalizadoras para sua translocação pela membrana mitocondrial. As translocases da membrana mitocondrial são capazes de reconhecer essas regiões, como a Tom70, por exemplo. A Tom 70 interage com complexos proteína precursora-chaperona molecular, a chaperona é responsável por manter a proteína precursora enovelada e estável até a sua translocação. Nesse sentido, estudamos a interação entre a Tom70 e a Hsp90 humanas, especificamente o domínio C-terminal da Hsp90 (C-Hsp90). Nesse artigo está reportada a interação entre Tom70 e C-Hsp90, com dados termodinâmicos e estequiometria de interação, determinadas por técnicas de pull-down, SEC-MALS e calorimetria de titulação isotérmica. Além disso, também está apresentada a caracterização da C-Hsp90 por dicroísmo circular, fluorescência intrínseca do triptofano, ultracentrifugação analítica e SEC-MALS.



Contents lists available at ScienceDirect

Archives of Biochemistry and Biophysics

journal homepage: www.elsevier.com/locate/yabbi

Stoichiometry and thermodynamics of the interaction between the C-terminus of human 90 kDa heat shock protein Hsp90 and the mitochondrial translocase of outer membrane Tom70

Lisandra M. Gava^{a,b,c}, Danieli C. Gonçalves^{a,b,c}, Júlio C. Borges^d, Carlos H.I. Ramos^{a,b,*}

^aInstitute of Chemistry, University of Campinas (UNICAMP), 13083-970 Campinas, SP, Brazil

^bInstituto Nacional de Ciência e Tecnologia em Biologia Estrutural e Bioimagem, Brazil

^cInstitute of Biology, University of Campinas (UNICAMP), 13083-970 Campinas, SP, Brazil

^dInstitute of Chemistry of São Carlos, University of São Paulo, São Carlos, SP, Brazil

ARTICLE INFO

Article history:

Received 23 May 2011
and in revised form 26 June 2011
Available online 14 July 2011

Keywords:

Hsp90
Tom70
Protein translocation into mitochondria
Protein–protein interaction
Analytical ultracentrifugation
Isothermal titration calorimetry

ABSTRACT

A large majority of the 1000–1500 proteins in the mitochondria are encoded by the nuclear genome, and therefore, they are translated in the cytosol in the form and contain signals to enable the import of proteins into the organelle. The TOM complex is the major translocase of the outer membrane responsible for preprotein translocation. It consists of a general import pore complex and two membrane import receptors, Tom20 and Tom70. Tom70 contains a characteristic TPR domain, which is a docking site for the Hsp70 and Hsp90 chaperones. These chaperones are involved in protecting cytosolic preproteins from aggregation and then in delivering them to the TOM complex. Although highly significant, many aspects of the interaction between Tom70 and Hsp90 are still uncertain. Thus, we used biophysical tools to study the interaction between the C-terminal domain of Hsp90 (C-Hsp90), which contains the EEVD motif that binds to TPR domains, and the cytosolic fragment of Tom70. The results indicate a stoichiometry of binding of one monomer of Tom70 per dimer of C-Hsp90 with a K_D of 360 ± 30 nM, and the stoichiometry and thermodynamic parameters obtained suggested that Tom70 presents a different mechanism of interaction with Hsp90 when compared with other TPR proteins investigated.

© 2011 Elsevier Inc. All rights reserved.

Introduction

Mitochondria, which are ubiquitous in eukaryotic cells types, are crucial to many physiological functions [1,2], and they have critical roles in physiological and pathological processes and act as cellular “powerhouses”. In addition to being vital for energy production and therefore for the survival of eukaryotic cells, mitochondria are implicated in a number of other essential functions, such as cellular respiration, metabolism of lipids, amino acids, iron homeostasis, and the regulation of intrinsic pathway of apoptosis [3–5].

Mitochondria are double-membrane bound organelles that include four compartments: the outer membrane, the inner membrane, the intermembrane space and the mitochondrial matrix. In the interior of the mitochondria, about 1000–1500 different proteins are present, of which only a small fraction are encoded by the mitochondrial genomic DNA [4,6]. The vast majority of mitochondrial proteins are encoded by the nuclear genome, translated by cytosolic ribosomes in the form of preproteins and thereafter

translocated into the mitochondria [6–8]. Preproteins targeted specifically to the mitochondria contain signals to localize to the correct compartments within the organelle. The signals are recognized by cytosol-exposed receptors located in the mitochondrial outer membrane [4]. Following recognition, these signals are decoded by mitochondrial translocases, which contain multifunctional components that coordinate the preprotein transfer to the translocation pore and that control the sorting and communication with subsequent translocases [1,6,8]. Thus, the machineries of importing and sorting proteins into the mitochondria are greatly important in maintaining proper mitochondrial function.

A major translocase of the outer membrane is the TOM complex. It consists of the general import pore (GIP) complex and two membrane import receptors, Tom20 and Tom70, with a single N-terminal transmembrane domain and a receptor domain exposed into the cytosol [5,8]. Tom20 recognizes the N-terminal mitochondrial targeting signals from the preproteins, via hydrophobic interactions, while Tom70 preferentially recognizes preproteins with internal hydrophobic targeting sequences, such as the inner membrane metabolite carriers [4,5,9–12]. The Tom70-mediated import pathway is chaperone dependent. Molecular chaperones Hsp70 and Hsp90 have important roles in targeting the preproteins to the TOM complex and in the protection of these

* Corresponding author at: Institute of Chemistry, University of Campinas (UNICAMP), 13083-970 Campinas, SP, Brazil. Fax: +55 19 3521 3023.

E-mail address: cramos@iqm.unicamp.br (C.H.I. Ramos).

preproteins from aggregation in the cytosol [13]. Tom70 contains a cytosolic TPR (tetratricopeptide repeat) clamp domain that serves as a docking site for the Hsp70 and Hsp90 C-terminal EEVD motifs and consequently for the multi-chaperone complexes that hold the preprotein. The C-terminal EEVD motif of the chaperones has been implicated in the binding of other proteins containing TPR regions, including Hop and CHIP co-chaperones [14–18]. The ATPase cycles of Hsp70/Hsp90 control interactions with substrates and client proteins and are also needed for the chaperones to assist in protein folding; in addition, preproteins are transferred in an ATP-dependent way to the TOM complex for translocation [19]. Specific Hsp90 inhibitors reduce the Tom-dependent import to a basal level, indicating that the chaperone has a significant role in protein import into the mitochondria via the TOM complex [19]; however, many aspects of the Tom70–Hsp90 interaction are still not clear. For instance, the details of the mechanism of interaction and the structure of the complex remain unclear. In a previous work, we showed that the functional state of human Tom70 is monomeric [5], and here, we present the stoichiometry and thermodynamic parameters of its interaction with the C-terminal domain of Hsp90, which is a dimer in solution.

Materials and methods

Plasmids, recombinant protein expression and purification

The coding sequences for the C-terminus fragment of human Hsp90 α , C-Hsp90, (NCBI Accession No.: AAI21063, residues 566–732) and the cytosolic fragment of human Tom70 (NCBI Accession No.: O94826.1, residues 111–608) cloned into a pProExHta (Invitrogen), which inserts a His-tag followed by a cleavage site for the TEV-protease, were a generous gift from Dr. Jason C. Young [14]. Both recombinant proteins were expressed in BL21(DE3) *Escherichia coli* cells and were induced with 0.8 mM isopropyl β -D-thiogalactoside at 37 °C for 4 h. His-tagged proteins were purified using a nickel–Sepharose 5 mL column (GE Healthcare) equilibrated in 20 mM sodium phosphate, pH 7.4, 500 mM NaCl and 20 mM imidazole, and they were eluted with 20 mM sodium phosphate, pH 7.4, 500 mM NaCl and 150 mM imidazole. Proteins were further purified over a Superdex 200 26/60 gel filtration column (GE Healthcare) in 20 mM Tris–HCl, pH 8.0, 150 mM NaCl using an ÄKTA FPLC instrument (GE). Protein purification was assessed by SDS–PAGE, and concentrations were determined using the absorbance at 280 nm.

Spectroscopic and hydrodynamic experiments of C-Hsp90

Circular dichroism (CD)¹ measurements were recorded on a Jasco J-810 spectropolarimeter (JASCO, Inc.) with temperature controlled by a Peltier-type system (PFD 425S). Data were collected at 20 °C using a 1 mm pathlength cuvette, in 20 mM Tris–HCl, pH 8.0, and 150 mM NaCl with a protein concentration of 10 μ M. Fluorescence measurements were done in a SLM AMINCO–Bowman Series 2 (AB2) spectrofluorimeter (Thermo Fisher Scientific, Inc.) using a 1 \times 1 cm pathlength cuvette with 10 μ M of C-Hsp90, in the same buffer as for the CD experiments. Excitation was at 295 nm and emission was measured from 300 to 420 nm (emission and excitation bandpass of 4 nm). Fluorescence data were evaluated by their emission maxima wavelength (λ_{max}) and by their spectral center of mass ($\langle \lambda \rangle$), as described by the equation:

$$\langle \lambda \rangle = \frac{\sum \lambda_i F_i}{\sum F_i} \quad (1)$$

where λ_i is each wavelength and F_i is the fluorescence intensity at λ_i .

Analytical ultracentrifugation experiments were conducted with a Beckman Optima XL-A analytical ultracentrifuge and an AN-60Ti rotor (for review, see [20]). Sedimentation equilibrium (SE) experiments were performed at protein concentrations from 200 to 600 μ g/mL (approximately 5–15 μ M of dimeric C-Hsp90), in a buffer containing 20 mM Tris–HCl, pH 8.0, and 150 mM NaCl at 20 °C, from 9000 to 13,000 rpm, and data acquisition was at 276 nm. The software SEDPHAT version 8.2 was applied to evaluate the SE data [21]. The partial specific volume of the protein, buffer density and viscosity were calculated with the program SEDNTERP [22]. The global fitting was accomplished with the “Species Analysis” model of the SEDPHAT program. All parameters were allowed to float freely, and then, the statistical analyses were performed. The statistical method used was the “Monte-Carlo non-linear regression” with at least 100 iterations and a confidence level of 0.68. Tom70 was similarly analyzed by CD, and fluorescence spectroscopy and analytical ultracentrifugation were performed as described in a previous work by some of the authors [5].

Pull-down experiments

The experiments were conducted at room temperature. The His-tag of C-Hsp90 was removed by the TEV-protease so that C-Hsp90 could be used as the prey in the pull-down assays, while the His-tag of Tom70 was maintained to be used as the bait. Pull-down experiments were performed in equilibrium buffer (50 mM sodium phosphate, 300 mM NaCl, pH 8.0), with 50 μ M of His₆–Tom70 and 25 μ M (dimer concentration) of cleaved C-Hsp90. Proteins were mixed and incubated for 2 h, and then, 100 μ L of nickel–agarose resin Ni–NTA (Qiagen) was added, and the mixture was further incubated for 2 h. The resin was washed four times with 200 μ L aliquots of equilibrium buffer added to 20 mM imidazole to release proteins bound nonspecifically to the resin. Proteins bound specifically to the resin and any proteins interacting with them were eluted with the equilibrium buffer added to 200 mM imidazole, precipitated with acetone, solubilized in sample buffer and analyzed by Coomassie-stained SDS–PAGE.

Size-exclusion chromatography–multiple angle light scattering (SEC–MALS)

The oligomeric states of Tom70, C-Hsp90 and their complex were estimated via SEC–MALS measurements on an ÄKTA FPLC system (GE Healthcare) connected to a triple-angle static light-scattering detector miniDAWN™ TREOS (Wyatt Technology, Santa Barbara, CA, USA). A Superdex 200 HR 10/300 GL column (GE Healthcare) was used in 20 mM Tris–HCl, pH 8.0, and 150 mM NaCl at a flow rate of 0.5 mL/min. Sample volumes of 250 μ L were injected at a concentration of approximately 100 μ M of Tom70 and 50 μ M of C-Hsp90 (dimer concentration). The data were recorded and processed using ASTRA V software (Wyatt Technology, Santa Barbara, CA, USA). To determine the detector delay volumes and normalization coefficients for the light scattering detector, a BSA sample (Sigma–Aldrich®) was used as a reference. SEC–MALS is an absolute method for molecular mass determination; it provides a direct measure of molecular mass without being limited by the molecular shape or hydrodynamic parameters. The signal from the light-scattering detector is directly proportional to the molecular mass of the protein multiplied by their concentrations (mg/mL). This signal and the concentration (determined by absorbance, for example) make it possible to measure the molecular

¹ Abbreviations used: C-Hsp90, Hsp90 C-terminal domain; CD, circular dichroism; ITC, isothermal titration calorimetry; K_D , dissociation constant; SEC–MALS, size-exclusion chromatography coupled to multi-angle light scattering; SE, sedimentation equilibrium; MM, molecular mass; Tom70, translocase of the outer membrane.

mass of each peak eluting from the column [23], so it is a reliable technique to determine the molecular mass and stoichiometry of protein–protein complexes. All elution peaks were collected in 0.5 mL aliquots and were assessed by Coomassie-stained SDS–PAGE.

Isothermal titration calorimetry

Isothermal titration calorimetry (ITC) experiments were performed at 20 °C using a VP-ITC calorimeter (Microcal, LLC, Northampton, MA, USA) running Origin version 5.0 software. All solutions were thoroughly degassed before use by stirring under vacuum, and protein samples were dialyzed against 20 mM Tris–HCl, pH 8.0, and 150 mM NaCl. Tris buffer was used to facilitate the comparison with previous works ([25] and references therein) and to eliminate possible artifactual results caused by the interaction of phosphate with a putative additional nucleotide binding site in the C-terminus of Hsp90 [25] (see also Results and discussion). Titrations consisted of 5 μ L injections of 109 μ M Tom70 every 300 s into 5 μ M C-Hsp90 solutions (dimer concentration). The enthalpy change for each injection was calculated by integrating the area under the peaks of the recorded time course of the change of power and then by subtracting that of the control titration. The control experiments were used to correct for heat effects of dilution and mixing, and they consisted of injections of buffer without protein into buffer. The heat of dilution was determined from the baseline at the end of titration and was negligible. The apparent enthalpy change of binding (ΔH_{app} , i.e. the sum of all events involved in the interaction), binding stoichiometry (n), and dissociation constant (K_D) were estimated from the best fit of the theoretical titration curve using a least squares fitting analysis (Origin 5.0).

Results and discussion

The C-terminus of Hsp90 was produced folded as a dimer in solution

The 90 kDa heat shock protein Hsp90 is one of the most important molecular chaperones, and it has only one homolog in prokaryotes, whereas in humans there are at least four homologs, two cytosolic, one in the mitochondria and one in the endoplasmic reticulum. Hsp90 is essential for survival in eukaryotes, and its client proteins are normally associated with cell cycling and signaling, and this association makes this chaperone a potential drug target [26–28]. Hsp90 is an elongated dimer in solution with the dimerization site located in the C-terminal domain [29–31], and it can be divided into specific domains, the N-terminal domain followed by a linker, the M or middle domain, and the C-terminal domain, which has the EEVD motif that is involved in the binding to proteins presenting the TPR domain. In the case of the inducible cytosolic Hsp90 α , the N-terminal domain comprises residues 1–210, the linker comprises residues 211–272, the M or middle domain comprises residues 273–629, and the C-terminal domain comprises residues 630–732 [26]. The EEVD motif is located at residues 729–732 and is essential for Hsp90 binding to its co-chaperone by the TPR domain present in these proteins. To gain insight into the mechanism by which Hsp90 interacts with Tom70, we purified a recombinant C-terminus fragment of human Hsp90 α (C-Hsp90) using a modified approach and characterized its folded state.

C-Hsp90 was pure and soluble (data not shown). Its CD spectrum is characteristic of a folded protein [32] with minima at 209 nm ($-10,840$ deg cm² dmol⁻¹) and 222 nm ($-10,670$ deg cm² dmol⁻¹) as shown in Fig. 1A. By applying the simple prediction methods proposed by Morriset et al. [33] and Greenfield

and Fasman [34], the percentage of α -helix and β -sheet were estimated to be of approximately 26% and 37%, respectively. These percentages are in good agreement with the crystal structure of the C-terminus of the Hsp90 homolog from *Saccharomyces cerevisiae* (PDB ID: 2CG9), in which the C-terminus comprises a three-stranded β -sheet positioned under a curved helix that faces a three-helix coil [35]. Emission fluorescence spectroscopy of tryptophan (Trp) is a reasonable method to access information regarding the environment where this residue is situated in a protein, because of its sensitivity to the polarity of this environment; thus, Trp is a local probe of the folded state of a protein [36]. C-Hsp90 has one Trp residue. The emission fluorescence spectrum had its maximum intensity at 343 ± 1 nm with a spectral center of mass at 341 ± 1 nm (Fig. 1B), suggesting that the residue was well-buried in the protein structure. This result is another indication that the protein was pure.

Sedimentation equilibrium analytical ultracentrifugation was used to determine the molecular mass (MM) and thus the oligo-

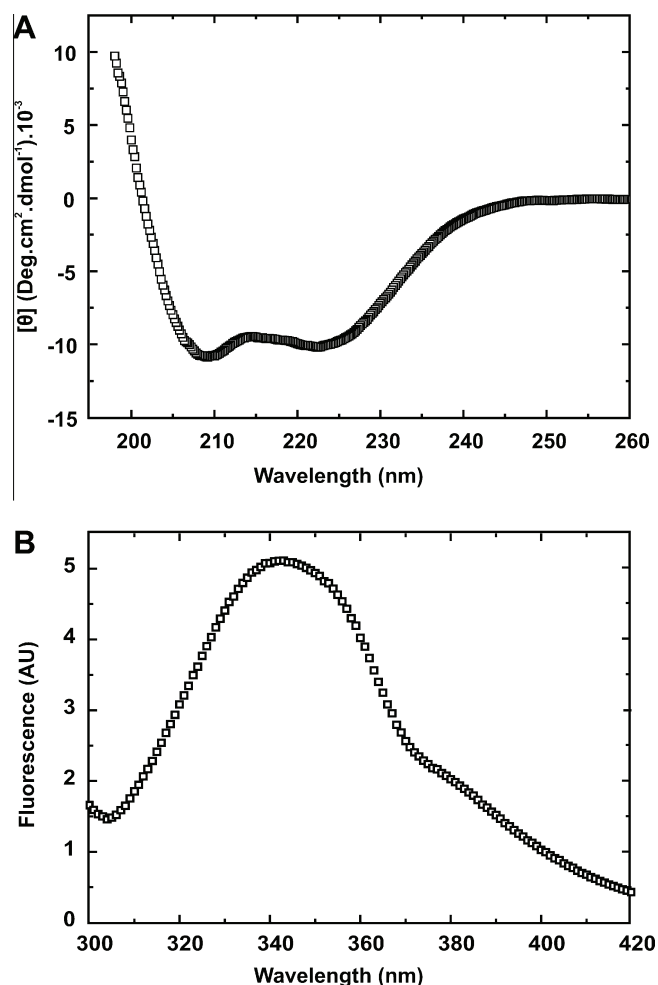


Fig. 1. (A) Circular dichroism spectrum of recombinant human C-Hsp90. Mean residue ellipticity ($[\theta]$) was measured from 198 to 260 nm at a protein concentration of 10 μ M, in 20 mM Tris–HCl, pH 8.0, with 150 mM NaCl at 20 °C, using a Jasco J-810 spectropolarimeter. The spectrum indicates that C-Hsp90 is folded and, by applying simple methods proposed by Morriset et al. [33] and Greenfield and Fasman [34], has about 26% and 37% α -helix and β -sheet content, respectively. (B) Emitted fluorescence spectrum of recombinant human C-Hsp90. Emission tryptophan fluorescence was measured from 300 to 420 nm; the excitation was at 295 nm at a protein concentration of 10 μ M, using a SLM AMINCO-Bowman Series 2 (AB2) spectrofluorimeter. C-Hsp90 has one Trp residue, and the emission fluorescence spectrum had a maximum intensity at 343 ± 1 nm with a spectral center of mass at 341 ± 1 nm suggesting that the residue was well-buried in the protein structure.

meric state of C-Hsp90. The results of three different protein concentrations at five different speeds were analyzed globally with SEDPHAT (see Materials and methods). Fig. 2 shows the results using 600 $\mu\text{g}/\text{mL}$ protein with the residuals from fitting shown in the upper panel. As determined by the fitting and the Monte-Carlo statistics analysis, C-Hsp90 has a molecular mass of 43 ± 1 kDa, which is consistent with a dimer in solution, since the MM predicted from the primary structure for the recombinant monomer is 21850.75 Da. Taken together, our results indicate that C-Hsp90 is properly folded and is a dimer.

Stoichiometry and thermodynamics of the interaction between C-Hsp90 and Tom70

The characterization of the folded conformation and oligomeric state of the recombinant cytosolic fragment of human Tom70 has been described previously [5], where we and our collaborators showed that the protein is purified in its natively folded state, has high α -helix content and is a functional monomer. Since both C-Hsp90 and Tom70 are well-behaved single species in solution, we undertook the measurement of their interaction. The interaction was initially studied by pull-down assays. For that examination, the Tom70 His-tagged construct was maintained intact to be used as bait in pull-down assays, since it was capable of binding to a nickel resin, whereas C-Hsp90 had its His-tag cleaved by TEV-protease. The results were assessed by PAGE in denaturing conditions by SDS (Fig. 3). The experiment showed that His-tagged Tom70 bound the resin as expected and free C-Hsp90, which has the His-tag removed did not (Fig. 3). However, when mixed with Tom70, C-Hsp90 remained bound to the resin even after two

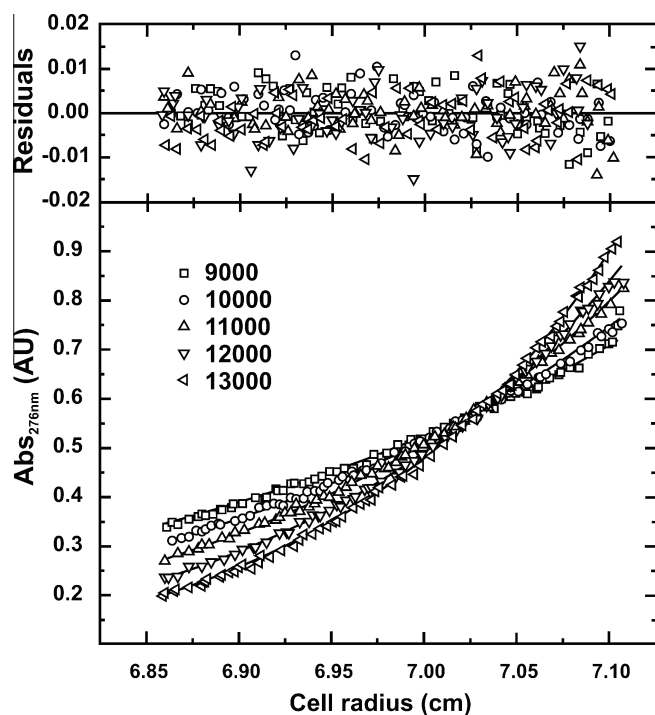


Fig. 2. Analytical ultracentrifugation sedimentation equilibrium of C-Hsp90. SE experiments were made at protein concentrations from 200 to 600 $\mu\text{g}/\text{mL}$ (approximately 5–15 μM of dimeric C-Hsp90), in 20 mM Tris-HCl, pH 8.0, and 150 mM NaCl at 20 $^{\circ}\text{C}$, from 9000 to 13,000 rpm, and data were acquired at 276 nm. The data analysis was performed with the software SEDPHAT version 8.2, and hydrodynamic parameters were calculated with SEDNTERP. Global reduced χ^2 was approximately 1.07, and the local rmsd was approximately 0.0052. The fitting and Monte-Carlo statistics indicated that C-Hsp90 is a dimer in solution, with a molecular mass of 43 ± 1 kDa, consistent with the known data for full-length Hsp90.

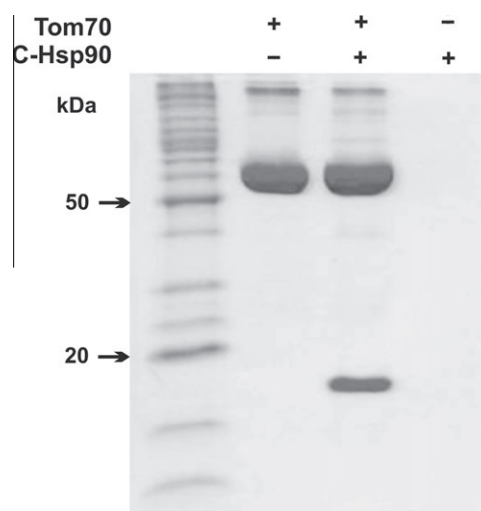


Fig. 3. Pull-down assays of Tom70 and C-Hsp90. The Tom70 His-tagged construct was maintained intact whereas C-Hsp90 had its His-tag cleaved by TEV-protease to be used as bait in pull-down assays. SDS-PAGE analysis of samples bound to the Ni-NTA resin that eluted in the presence of 200 mM imidazole (see Materials and methods). Lane 1, molecular mass marker (BenchMark™ Protein Ladder from Invitrogen); lane 2, Tom70 used as control; lane 3, Tom70 C-Hsp90 mixture; and lane 4, C-Hsp90 used as control. His-tagged Tom70 was capable of binding to C-Hsp90 and pulled it out of solution, confirming their interaction (lane 3).

washes and was released only when imidazole was used to decrease the affinity of His-tagged Tom70 for the resin (Fig. 3). Therefore, these results demonstrate that C-Hsp90 in fact interacted with Tom70. We then set out to determine the oligomeric state of the proteins in the complex by measuring the MM of the complex. We used size-exclusion chromatography combined with multi-angle static light scattering (SEC-MALS), a technique that provides a precise determination of MM independent of molecular shape or hydrodynamic parameters, to determine the MM of the complex (Fig. 4). Fig. 4A shows the SEC-MALS measurements of isolated proteins as normalized light scattering profiles and respective molecular mass distributions. Fig. 4B and C show the SDS-PAGE profiles of free Tom70 and free C-Hsp90 (B) and their mixture (C) from SEC-MALS, to confirm the presence of the proteins. As expected, free C-Hsp90 had a MM of ~ 43 kDa (Fig. 4A and B), which is in excellent agreement with the theoretically calculated MM of 43.7 kDa for a dimer, corroborating SE results (see above), and free Tom70 had a MM of ~ 62 kDa (Fig. 4A and B), consistent with the theoretical calculated MM of 59.7 kDa for a monomer, which is supported by previously analysis of its oligomeric state in solution [5]. Mixed Tom70 and C-Hsp90 eluted as a single peak with a MM of ~ 110 kDa (Fig. 4A and C), indicating a stoichiometry of one monomer of Tom70 to a dimer of C-Hsp90 in the complex.

The stoichiometry determined above by SEC-MALS was confirmed by isothermal titration calorimetry (ITC). In this experiment, the ΔH_{app} for the binding interaction is measured at a constant temperature, allowing for the determination of the binding stoichiometry (n) and the dissociation constant (K_D) by fitting of the titration curve. Both the sequence of injections and the differential heat plot are shown in Fig. 5. In accordance with the conclusion from the SEC-MALS results, the binding stoichiometry (n) was equal to 1.2 ± 0.1 , indicating that one monomer of Tom70 binds to a dimer of C-Hsp90. The K_D was determined to be 360 ± 30 nM, suggesting that the complex has high affinity. The ΔH_{app} of interaction was -2.6 ± 0.1 kcal/mol, and the apparent entropy of interaction was 21 ± 1 cal/mol K, indicating that the interaction is driven by both enthalpy and entropy. Interestingly, Hop and Cyp40, other TPR co-chaperones from human, bind the

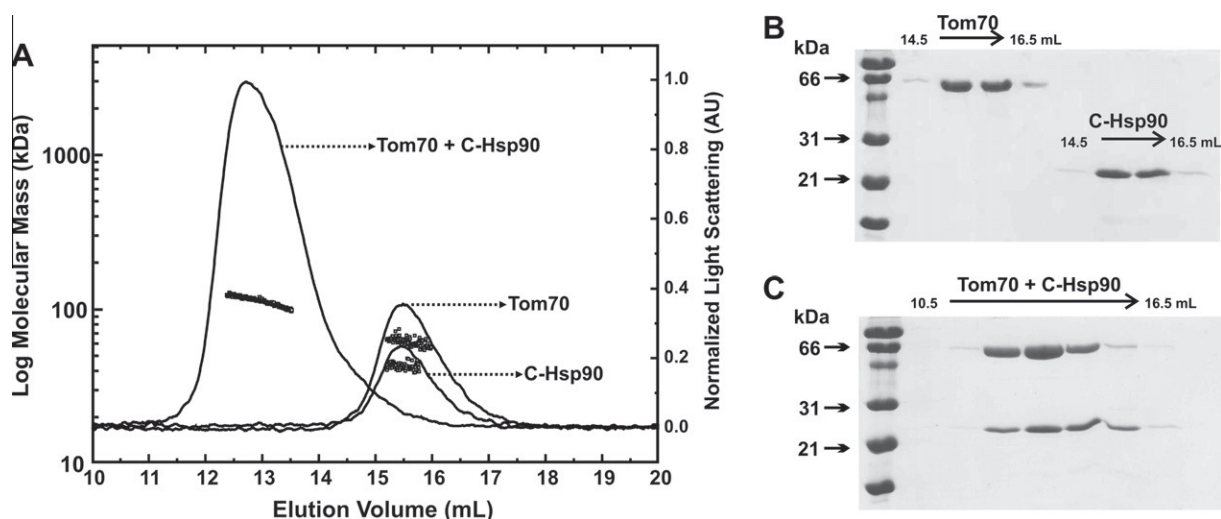


Fig. 4. SEC-MALS combined with SDS-PAGE for the determination of the molecular mass of the Tom70 C-Hsp90 complex. (A) SEC-MALS measurements of the isolated proteins and the complex are labeled. The graphic shows the representative normalized light scattering profiles recorded by detectors (continuous lines) and the molecular mass distributions (open squares) per elution volume unit (mL). Free C-Hsp90 had a MM of ~43 kDa (consistent with a dimer), free Tom70 had a MM of ~62 kDa (consistent with a monomer) and mixed Tom70 C-Hsp90 had a MM of ~110 kDa, indicating a stoichiometry of one monomer of Tom70 to a dimer of C-Hsp90 in the complex. (B and C) Fractions of 0.5 mL from free Tom70 and free C-Hsp90 (B) and complex (C) were collected and assessed by SDS-PAGE to confirm the presence of the proteins in the SEC-MALS measurements.

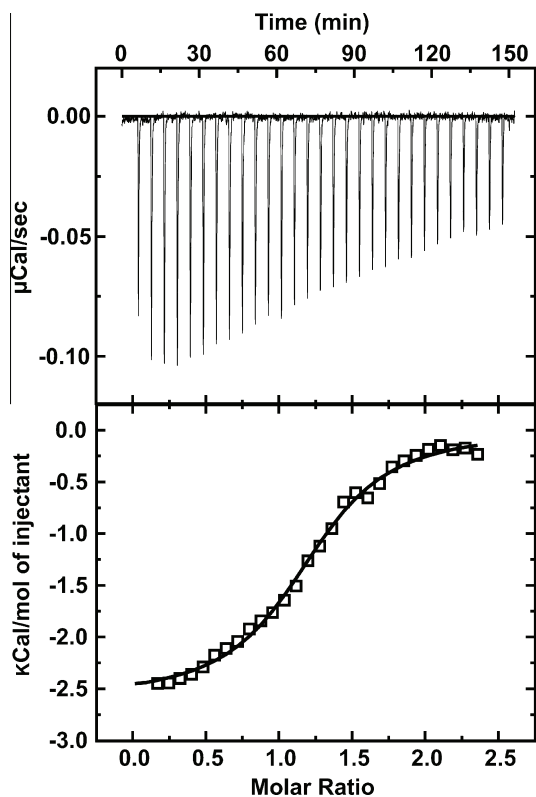


Fig. 5. Binding of Tom70 to C-Hsp90 monitored by ITC. Top, the experimental outline of the injections of Tom70 into the C-Hsp90 dimer showing thermal power, which is proportional to the heat of each injection, as a function of time. Bottom, the integrated heat plot. Heats of binding are represented by open squares, and the line represents the best fit of the data using the Origin 5.0 (Microcal). The binding stoichiometry (n) was equal to 1.2 ± 0.1 , indicating that one monomer of Tom70 binds to a dimer of C-Hsp90. Data analysis provided a K_D value of 360 ± 30 nM, suggesting that the complex has a high affinity. The binding ΔH measured from a single ITC experiment might include heat that is due to buffer ionization; therefore, the ΔH measured here is referred to as ΔH_{app} and was -2.6 ± 0.1 kcal/mol. The apparent entropy of interaction was 21 ± 1 cal/mol K indicating that the interaction is driven by both enthalpy and entropy.

C-terminus of human Hsp90- β with a K_D of about 10 times greater than that of Tom70, in an interaction that is also enthalpy driven, although the interaction with Cyp40 is driven by entropy [17,24]. It may be possible that there are slightly differences in the binding of different TPR co-chaperones with Hsp90. There are crystal structures of the Hsp90 MEEVD motif in complex with the TPR domains of human Hop [17] and yeast Tom 71 [4] (Fig. 6). Since the residues of Tom71 that interact with the MEEVD motif are conserved in human Tom70, the structure of the yeast ortholog can be used as a model for the interaction of Tom70 with Hsp90 [4]. First, one can observe general similarities. The interaction of the MEEVD with the TPR domains of both Hop and Tom71 involves mainly the dicarboxylate from the carboxy-terminal Asp residue from MEEVD and two basic lysines from the TPR domain (Fig. 6). At pH 8, the two lysines are positively charged while the MEEVD motif is negatively charged showing that the interaction between TPR co-chaperones and Hsp90 is electrostatic in nature. Second, slightly differences in binding can be observed when comparing Fig. 6A with B and C with D. The MEEVD motif appears to be more involved by the TPR domain when bound to Hop than when bound to Tom71, suggesting that the interaction between the MEEVD and Hop is more organized and thus has a higher entropic cost. In addition to that, the conformation of the MEEVD pentapeptide changes depending on the TPR co-chaperone to which it is bound (Fig. 6). Six residues from the Tom71 TPR domain are involved in seven electrostatic interactions with the MEEVD motif while seven residues from the Hop TPR domain are involved in ten electrostatic interactions with the MEEVD motif (Fig. 6A and B). The seventh residue is an Asn in position 308 of the TPR2a from Hop that has no equivalent in Tom71 and is hydrogen bonded to the first Glu residue of the MEEVD motif. A Tyr at position 236 of the TPR2a from Hop is hydrogen bonded to the carbonyl group of the peptide bond between the two Glu residues of the MEEVD motif (Fig. 6B), while the correspondent residue in Tom71, Phe138, does not make this kind of interaction (Fig. 6A). In contrast with the tight interactions when bound to Hop, the N-terminus of the MEEVD motif appears to be less restrained when bound to Tom71 (Fig. 6), indicating that although the interactions of this portion of the motif with Hop increase enthalpy they also have an entropic cost due to the organization of the complex. This observation is

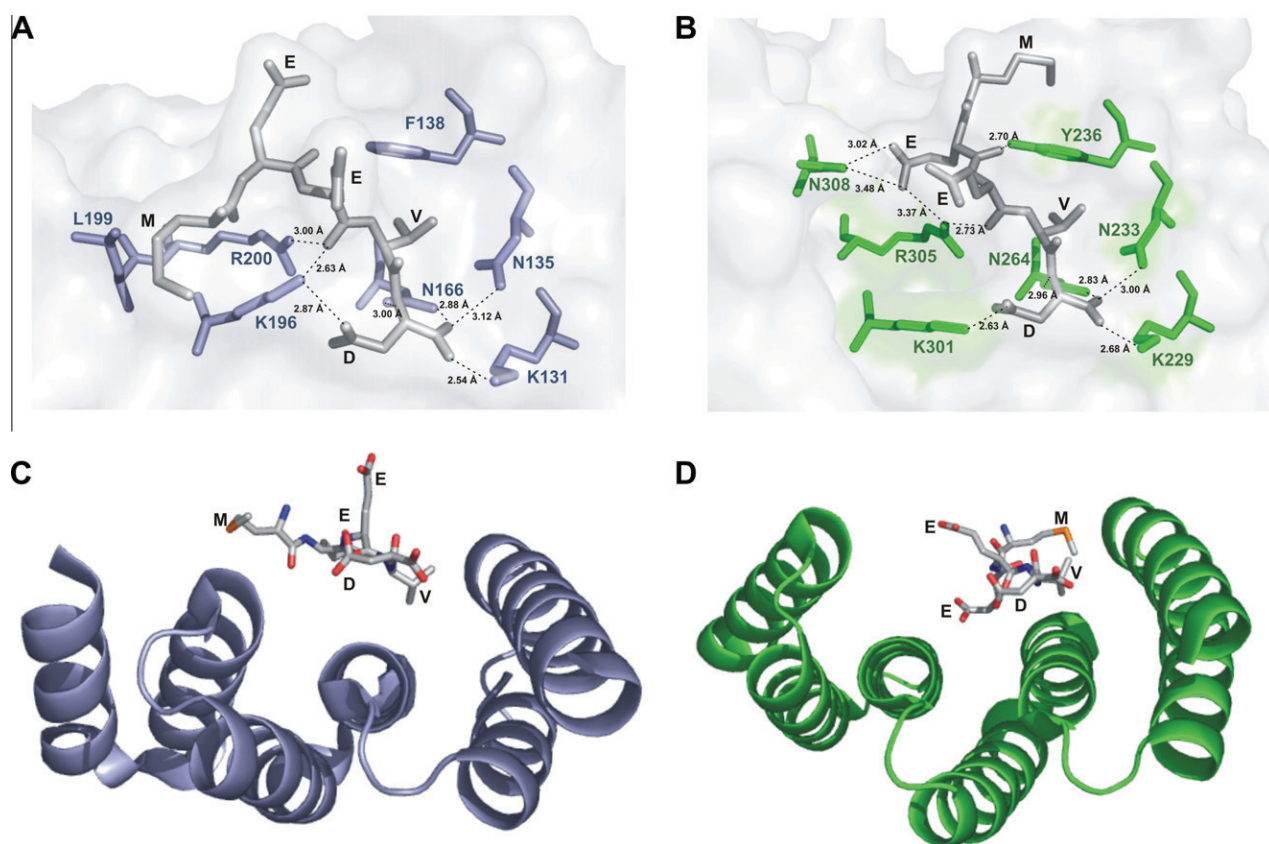


Fig. 6. The MEEVD motif from Hsp90 complexed with TPR domains. The structures of the MEEVD in complex with the TPR domains of yeast Tom71 (A and C) – PDB 3FP2; and human Hop (B and D) – PDB 1ELR) are shown. Electrostatic interactions and hydrogen bonds are highlighted in panels (A) and (B) while panels (C) and (D) present the front view of the complexes, highlighting the relative position of the dicarboxylate clamp (see text). Generated using Pymol (www.pymol.org).

supported by ITC experiments that measured the interaction of C-Hsp90 with Hop [24] and were performed in similar conditions to those reported in this work. Onuoha et al. [24] showed that the interaction between C-Hsp90 and Hop has a higher enthalpic contribution than that measured for Tom70 (this work) and a negative entropy value which is different from the interaction of C-Hsp90 with Tom70 that was entropy driven (this work). Additionally, when bound to the TPR domain of Tom71, the Met residue of the MEEVD motif makes hydrophobic interactions with a cleft formed by the protein residues Leu199 and Lys196 (Fig. 6A), indicating that the binding may have a lower apparent enthalpy of binding but also a positive entropic contribution. This observation is also in good agreement with our measurements on human Tom70 and is expected since hydrophobic interactions provide a higher degree of freedom.

Finally, the stoichiometry of binding for either Hop or Cyp40 is of one monomer per monomer of C-Hsp90- β [17,24], although some controversy exists regarding the oligomeric state of native Hop [37,38]. Therefore, the mode of interaction between Tom70 and C-Hsp90 appears to have specific characteristics that differ from those of other proteins containing TPR domains. Combined, these results suggest that the interaction of TPR proteins with Hsps may be more complex and diverse than previously expected. Moreover, it may be possible that the interaction with only one monomer of the C-Hsp90 motif allows the other to be available for additional interactions with other TPR co-chaperones, opening up the possibility for further functional modulation. However, more experimental evidence is necessary to support these hypotheses. Nevertheless, it is noteworthy that Tom70 also binds Hsp70, which is a monomer in solution [39,40].

These findings are potentially relevant because TPR–Hsp complexes have been a target of several investigations because of their potential as drug targets. Since Hsp90 is involved with the stabilization of the tumor phenotype, the interference with the interaction between the EEVD motif and TPR may inhibit the delivery of client proteins to Hsp90 [27]. Many hybrid peptides that mimic TPR domains are under investigation to substitute the general broad effect of small molecule inhibitors by a more specific inhibition strategy that will interfere with the interaction of Hsp90 with regulatory co-chaperones. We believe that the results presented here are an important step toward the design of such therapeutic strategies, and thus, they are of potential interest not only for those studying domain–domain interactions but also for those in the field of translational medicine.

Conclusion

Experiments using circular dichroism and intrinsic fluorescence spectroscopy were consistent with the purification of folded recombinant human proteins. Analytical sedimentation equilibrium showed that C-Hsp90 is a dimer in solution, a result corroborated by SEC–MALS experiments. As previously reported [5], Tom70 is a monomer in solution and interacts with C-Hsp90 forming a complex in which one monomer of Tom70 binds a dimer of C-Hsp90. The stoichiometry was confirmed by isothermal titration calorimetry, which also yielded the thermodynamic parameters of the interaction showing that human Tom70 has a high affinity for C-Hsp90 in comparison to other TPR proteins. The mode of binding between Tom70 and C-Hsp90 provides new information when

compared with what is currently known for the binding of other proteins that contain TPR domains. This information is potentially relevant for studies aiming to interfere with the interaction between the EEVD motif and TPR as this strategy may inhibit the delivery of client proteins to Hsp90.

Acknowledgments

This work was supported by the Fundação de Amparo à Pesquisa do Estado de São Paulo (FAPESP) and Conselho Nacional de Pesquisa e Desenvolvimento (CNPq). L.M.G. holds a FAPESP fellowship.

References

- [1] E. Schleiff, T. Becker, *Nat. Rev. Mol. Cell Biol.* 12 (2011) 48–59.
- [2] A.J. Perry, T. Lithgow, *Curr. Biol.* 15 (2005) R423–R425.
- [3] S. Fulda, L. Galluzzi, G. Kroemer, *Nat. Rev. Drug Discov.* 9 (2010) 447–464.
- [4] J.X. Li, X.G. Qian, J.B. Hu, B.D. Sha, *J. Biol. Chem.* 284 (2009) 23852–23859.
- [5] A.C.Y. Fan, L.M. Gava, C.H.I. Ramos, J.C. Young, *Biochem. J.* 429 (2010) 553–563.
- [6] A.C.Y. Fan, J.C. Young, *Protein Pept. Lett.* 18 (2011) 122–131.
- [7] P. Dolezal, V. Likic, J. Tachezy, T. Lithgow, *Science* 313 (2006) 314–318.
- [8] D. Mokranjac, W. Neupert, *Biochim. Biophys. Acta* 1793 (2009) 33–41.
- [9] A. Chacinska, C.M. Koehler, D. Milenkovic, T. Lithgow, N. Pfanner, *Cell* 138 (2009) 628–644.
- [10] J. Brix, K. Dietmeier, N. Pfanner, *J. Biol. Chem.* 272 (1997) 20730–20735.
- [11] Y. Abe, T. Shodai, T. Muto, K. Mihara, H. Torii, S. Nishikawa, T. Endo, D. Kohda, *Cell* 100 (2000) 551–560.
- [12] M.T. Ryan, H. Muller, N. Pfanner, *J. Biol. Chem.* 274 (1999) 20619–20627.
- [13] T. Beddoe, T. Lithgow, *Biochim. Biophys. Acta* 1592 (2002) 35–39.
- [14] J.C. Young, N.J. Hoogenraad, F.U. Hartl, *Cell* 112 (2003) 41–50.
- [15] R.D. Mills, J. Trehwella, T.W. Qiu, T. Welte, T.M. Ryan, T. Hanley, R.B. Knott, T. Lithgow, T.D. Mulhern, *J. Mol. Biol.* 388 (2009) 1043–1058.
- [16] J. Brix, G.A. Ziegler, K. Dietmeier, J. Schneider-Mergener, G.E. Schulz, N. Pfanner, *J. Mol. Biol.* 303 (2000) 479–488.
- [17] C. Scheffler, A. Brinker, G. Bourenkov, S. Pegoraro, L. Moroder, H. Bartunik, F.U. Hartl, I. Moarefi, *Cell* 101 (2000) 199–210.
- [18] P. Connell, C.A. Ballinger, J.H. Jiang, Y.X. Wu, L.J. Thompson, J. Hohfeld, C. Patterson, *Nat. Cell Biol.* 3 (2001) 93–96.
- [19] A.C.Y. Fan, M.K. Bhangoo, J.C. Young, *J. Biol. Chem.* 281 (2006) 33313–33324.
- [20] J.C. Borges, C.H.I. Ramos, *Curr. Med. Chem.* 18 (2011) 1276–1285.
- [21] J. Vistica, J. Dam, A. Balbo, E. Yikilmaz, R.A. Mariuzza, T.A. Rouault, P. Schuck, *Anal. Biochem.* 326 (2004) 234–256.
- [22] T.M. Laue, B.D. Shah, T.M. Ridgeway, S.L. Pelletier, in: S.E. Harding et al. (Eds.), *Analytical Ultracentrifugation in Biochemistry and Polymer Science*, Royal Society of Chemistry, Cambridge, United Kingdom, 1992, pp. 90–125.
- [23] J. Wen, T. Arakawa, J.S. Philo, *Anal. Biochem.* 240 (1996) 155–166.
- [24] S.C. Onuoha, E.T. Couistock, J.G. Grossmann, S.E. Jackson, *J. Mol. Biol.* 379 (2008) 732–744.
- [25] C. Garnier, D. Lafitte, P.O. Tsvetkov, P. Barbier, J. Leclerc-Devin, J.M. Millot, C. Briand, A.A. Makarov, M.G. Catelli, V. Peyrot, *J. Biol. Chem.* 277 (2002) 12208–12214.
- [26] L. Whitesell, S.L. Lindquist, *Nat. Rev. Cancer* 5 (2005) 761–772.
- [27] L.M. Gava, C.H.I. Ramos, *Curr. Chem. Biol.* 3 (2009) 10–21.
- [28] A.O. Tiroli-Cepeda, C.H.I. Ramos, *Protein Pept. Lett.* 18 (2011) 101–109.
- [29] S. Koyasu, E. Nishida, T. Kadowaki, F. Matsuzaki, K. Iida, F. Harada, M. Kasuga, H. Sakai, I. Yahara, *Proc. Natl. Acad. Sci. USA* 83 (1986) 8054–8058.
- [30] Y. Minami, H. Kawasaki, Y. Miyata, K. Suzuki, I. Yahara, *J. Biol. Chem.* 266 (1991) 10099–10103.
- [31] T. Nemoto, Y. Oharanemoto, M. Ota, T. Takagi, K. Yokoyama, *Eur. J. Biochem.* 233 (1995) 1–8.
- [32] D.H.A. Corrêa, C.H.I. Ramos, *Afr. J. Biochem. Res.* 3 (2009) 164–173.
- [33] J.D. Morriset, J.S.K. David, H.J. Pownall, A.M. Gotto, *Biochemistry* 12 (1973) 1290–1299.
- [34] N. Greenfield, G.D. Fasman, *Biochemistry* 8 (1969) 4108–4116.
- [35] M.M.U. Ali, S.M. Roe, C.K. Vaughan, P. Meyer, B. Panaretou, P.W. Piper, C. Prodromou, L.H. Pearl, *Nature* 440 (2006) 1013–1017.
- [36] M.R. Eftink, *Biophys. J.* 66 (1994) 482–501.
- [37] D.C. Goncalves, L.M. Gava, C.H.I. Ramos, *Protein Pept. Lett.* 17 (2010) 492–498.
- [38] F. Yi, I. Doudevski, L. Regan, *Protein Sci.* 19 (2010) 19–25.
- [39] J.C. Borges, C.H.I. Ramos, *BMB Rep.* 42 (2009) 166–171.
- [40] K.P. da Silva, J.C. Borges, *Protein Pept. Lett.* 18 (2011) 132–142.

CAPÍTULO 5

5. Discussão geral

5.1 Hop

A Hop é uma co-chaperona que está envolvida em importantes processos celulares, como por exemplo, o recrutamento da chaperona Hsp90 para atuação no complexo Hsp70/receptor esteróide pré-existente, promovendo assim a associação e maturação funcional do receptor (Chen & Smith, 1998; Smith, 2004). A Hop recombinante humana – D456G (nomeada apenas Hop nessa seção), produto de uma mutação pontual de um resíduo de aspartato para um resíduo de glicina, foi produzida pura (figura 2 - capítulo II) e enovelada, constituída, predominantemente, por hélices- α (~64% tabela 1 – capítulo II e figura 3A – capítulo II). A análise do espectro de emissão de fluorescência do único resíduo de Trp da Hop apresentou um máximo de intensidade em 339 ± 1 nm e um centro de massa espectral de 345 ± 1 nm (figura 3B – capítulo II), sugerindo que o resíduo de Trp está protegido no interior da estrutura da proteína. Os ensaios de desenovelamento térmico monitorados por CD indicaram uma T_m de 53 ± 1 °C (tabela 1 – capítulo II), valor que está dentro da margem de erro reportada para a proteína selvagem (Carrigan et al., 2006). De modo geral, esses resultados indicam que a Hop estudada apresenta estrutura secundária e estabilidade térmica similar à proteína selvagem.

A análise conjunta dos experimentos de SE (sedimentação em equilíbrio) e BNPAGE indica que a Hop pode ser encontrada como uma mistura de espécies monoméricas e diméricas. Nos experimentos de SE a proteína foi encontrada como uma única espécie de massa molecular (MM) estimada em 66 ± 2 kDa (figura 4A e tabela 2 – capítulo II), que está de acordo como a MM teórica predita

de 66,4 kDa para o monômero da proteína. No experimento de BNPAGE (figura 5 – capítulo II) a Hop migrou majoritariamente como monômero, mas a amostra de proteína também apresentou outras espécies oligoméricas, provavelmente diméricas e espécies maiores.

As análises hidrodinâmicas da Hop foram feitas no intuito de se obter uma visão geral sobre sua forma global. Os experimentos de gel filtração analítica, usados para estimar o raio de Stokes (R_s) da proteína, mostraram que a Hop foi eluída como uma espécie homogênea (figura 6 *inset* – capítulo II) com um R_s de 44 ± 2 Å. O valor de R_s foi utilizado para calcular o fator de Perrin, que é informativo sobre a forma das moléculas. O fator de Perrin é a razão do coeficiente friccional medido (f) pelo coeficiente friccional para uma esfera hipotética (f_0), cujo raio hipotético é calculado a partir da MM. Nesse sentido, o fator de Perrin (f/f_0) fornece informação sobre a forma da molécula, quanto mais próximo de 1, mais esférica ou globular é a molécula. O f/f_0 calculado para a Hop foi de 1,6, sugerindo que se trata de uma proteína assimétrica.

Adicionalmente, os experimentos de espalhamento dinâmico de luz (DLS) foram utilizados para estimar o coeficiente de difusão (D) da Hop em várias concentrações de proteínas. Em seguida, o coeficiente de difusão padrão ($D_{20,w}$) para cada concentração de proteína foi calculada e adicionada no gráfico da figura 7 (capítulo II). No intuito de estimar, por extrapolação, o $D_{20,w}$ na concentração de 0 mg/mL foi estimado o valor de $D_{20,w}^0$ para a Hop de $6,2 \times 10^{-7}$ cm²/s (figura 7 e tabela 2 – capítulo II). Por fim, uma esfera rígida com a MM idêntica ao monômero da Hop, teoricamente, teria um R_s de 27 Å, um $D_{20,w}^0$ de $8,0 \times 10^{-7}$ cm²/s e portanto um fator de Perrin de 1,3. Essa divergência entre os valores do fator de Perrin pode ser explicada pelo efeito de hidratação, que pode

aumentar o volume efetivo de proteínas e, portanto aumentar o R_s afetando os resultados. De qualquer forma, os resultados demonstram que a Hop é monomérica que parece ser alongada e bastante hidratada.

Enfim, a presença de ambas as espécies (monômero e dímero) da Hop pode estar associada à especificidade a uma proteína cliente ou outro fator relacionado, variando de acordo com a estequiometria da interação ou regulação do ciclo de interação. Recentemente, Southworth & Agard, publicaram resultados que corroboram a existência da Hop como uma espécie monomérica e que pode oligomerizar em altas concentrações (Southworth & Agard, 2011).

A caracterização estrutural dessa proteína torna possível delinear novos alvos de investigação dentro da maquinaria Hsp90-Hsp70, essencialmente do complexo Hop-Hsp90, relacionado à manutenção de várias associações com proteínas clientes.

5.2 Tom70

O receptor de importação mitocondrial Tom70 (translocase da membrana mitocondrial externa) interage com complexos (chaperona/proteína precursora) por meio de dois domínios estruturais: um domínio liga a chaperona molecular Hsp70/Hsp90 e um segundo liga as proteínas precursoras. A definição do estado oligomérico da Tom70 tem sido controversa, com evidência para ambas as formas: monomérica (Mills et al., 2009; Li et al., 2009) e homodimérica (Wu & Sha, 2006). Nesse trabalho, a Tom70 é apresentada como um monômero funcional, com implicações na sua atividade de importação de proteínas para a mitocôndria.

Baseado nos experimentos de UCA em conjunto com os experimentos de cross-linking e SEC-MALS (esses últimos realizados por colaboradores) foi

possível aferir que o fragmento citosólico da Tom70 existe em equilíbrio entre monômero e dímero, sendo funcionalmente monomérica com oligômeros formados de maneira transiente ou em condições particulares, como alta concentração de proteína. Na verdade, os dados de VS (velocidade de sedimentação) e SE (figuras 1B e 1C – capítulo III) e SEC-MALS (figura 2B – capítulo III), mostram que embora a espécie monomérica da Tom70 seja a maioria da população, os dímeros são claramente evidentes.

O encaminhamento e interação de proteínas precursoras com a Tom70 foram mais eficientes com a forma monomérica da proteína, sem interferir na interação com as chaperonas, assim os dados obtidos sugerem que a Tom70 recebe e interage com as proteínas precursoras no estado monomérico.

Estudos estruturais recentes da Tom70 (Mills et al., 2009) e da Tom71 (Li et al., 2009) de levedura apóiam nosso modelo monomérico da Tom70 e ilustram um mecanismo que pode ser conservado. Todavia, dado que a Tom70 humana recombinante pode formar homodímeros, não podemos descartar a possibilidade da Tom70 estar presente na membrana mitocondrial externa como um homodímero.

5.3 C-Hsp90

A Hsp90 é uma das chaperonas moleculares mais importantes, é essencial para a vida em eucariotos, suas proteínas clientes são normalmente associadas com ciclo e sinalização celular e sua associação faz dessa chaperona molecular um alvo potencial para drogas (Whitesell & Lindquist, 2005; Gava & Ramos, 2009). A Hsp90 é um dímero alongado, com o sítio de dimerização localizado no domínio C-terminal (Minami et al., 1994; Nemoto et al., 1995). O C-terminal

apresenta o motivo MEEVD que está envolvido na ligação de proteínas que apresentam domínios TPR. No caso da Hsp90 α humana esse motivo está localizado nos resíduos 729-732 e é essencial para a ligação da Hsp90 com co-chaperonas da classe TPR.

No intuito de obter mais informações sobre o mecanismo de interação da Hsp90 com a Tom70, o fragmento C-terminal da Hsp90 humana (C-Hsp90) foi caracterizado e disponibilizado, posteriormente, para ensaios de interação com a co-chaperona. C-Hsp90 foi produzida pura e solúvel, os espectros de CD mostraram uma proteína enovelada com mínimo de sinal em 209 nm ($-10.840 \text{ deg.cm}^2.\text{dmol}^{-1}$) e 222 nm ($-10.670 \text{ deg.cm}^2.\text{dmol}^{-1}$) como apresentado na figura 1A (capítulo IV). Aplicando métodos simples de predição de estrutura secundária, como os propostos por Morrisset e colaboradores (Morrisset et al., 1973) e Greenfield e Fasman (Greenfield & Fasman, 1969), a porcentagem de hélices- α e folhas- β foi estimada em aproximadamente 26% e 37%, respectivamente. Essas porcentagens estão em concordância com a estrutura cristalográfica do C-terminal da Hsp90 ortóloga de *Saccharomyces cerevisiae* (nº de acesso ao PDB: 2CG9), na qual o C-terminal compreende três folhas- β posicionadas abaixo de uma hélice- α curvada que está de frente para um feixe de três hélices (Ali et al., 2006).

O método de espectroscopia de emissão de fluorescência do Trp é plausível para acessar informação acerca do ambiente onde esse resíduo está situado em uma proteína, assim o Trp é uma sonda local do estado enovelado de uma proteína (Eftink, 1994). C-Hsp90 tem apenas um resíduo de Trp, a análise do espectro de emissão de fluorescência desse resíduo apresentou um máximo de intensidade em $343 \pm 1 \text{ nm}$ e um centro de massa espectral de $341 \pm 1 \text{ nm}$ (figura

1B – capítulo IV), indicando que o resíduo de Trp está protegido no interior da estrutura da proteína.

Os experimentos de SE foram usados para determinar a MM e, portanto o estado oligomérico da C-Hsp90. Os resultados obtidos a partir de três concentrações de proteína em cinco velocidades distintas foram analisados globalmente com o uso do programa SEDPHAT (ver seção de material e métodos do capítulo IV). Foi determinada para a C-Hsp90 a MM de 43 ± 1 kDa, valor consistente com um dímero em solução, dado que a MM predita a partir da estrutura primária do monômero é de 21.850,75 Da. Tomando os dados em conjunto, os resultados obtidos indicam que a C-Hsp90 foi produzida enovelada e é um dímero em solução.

5.4 Interação entre C-Hsp90 e Tom70

Após a obtenção de ambas as proteínas C-Hsp90 e Tom70 solúveis, enoveladas e como uma espécie única em solução, foram realizados experimentos de interação entre elas. A interação foi inicialmente estudada utilizando ensaios de *pull-down*. Para tal, a Tom70 teve a cauda de poli-histidina mantida e foi utilizada como isca, enquanto a proteína C-Hsp90 (teve sua cauda de poli-histidina clivada pela protease TEV) foi utilizada como presa. O experimento mostrou (figura 3 – capítulo IV) que a Tom70 usada como controle permaneceu ligada à resina, enquanto a C-Hsp90 não se ligou. Mas, quando a mistura da Tom70 com a C-Hsp90 foi incubada na resina, a mistura ou complexo permaneceu ligada, sendo liberado apenas após a eluição com imidazol. Portanto, o ensaio de *pull-down* demonstrou que a C-Hsp90 de fato, interage com

a Tom70. O próximo passo foi determinar o estado oligomérico das proteínas no complexo medindo sua MM por SEC-MALS.

A técnica de SEC-MALS fornece uma determinação precisa de MM independente da forma da molécula ou de parâmetros hidrodinâmicos. Na figura 4A (capítulo IV) estão apresentadas as medidas de SEC-MALS para as proteínas isoladas e para o complexo, as figuras 4B e 4C (capítulo IV) confirmam a presença das proteínas nas amostras analisadas. Como esperado, a C-Hsp90 livre teve sua MM determinada no valor de ~43 kDa (figuras 4A e B – capítulo IV), que está de acordo com a MM teórica de 43,7 kDa calculada para o dímero, e corrobora os resultados de SE. Para a Tom70 livre a MM determinada foi de ~62 kDa (figuras 4A e B – capítulo IV), consistente com a MM teórica de 59,7 kDa calculada para um monômero da Tom70, que é apoiada por dados prévios de análises do estado oligomérico da Tom70 em solução (Fan et al., 2010). A mistura de Tom70 com C-Hsp90 foi eluída em um único pico e teve sua MM determinada no valor de ~110 kDa (figuras 4A e C – capítulo IV), sugerindo que a estequiometria do complexo é de um monômero da Tom70 para um dímero da C-Hsp90.

A estequiometria encontrada nos experimentos de SEC-MALS foi confirmada pelos experimentos de ITC (figura 5 – capítulo IV). A estequiometria de ligação (n) determinada pelo ITC foi de $1,2 \pm 0,1$ indicando que um monômero da Tom70 liga um dímero da C-Hsp90. A constante de dissociação K_D encontrada foi de 360 ± 30 nM, sugerindo que o complexo tem alta afinidade. A ΔH_{app} da interação foi de $-2,6 \pm 0,1$ kcal/mol, e a entropia da interação foi de 21 ± 1 cal/mol.K, indicando que a interação é guiada por ambas, entalpia e entropia. Interessantemente, a Hop e Cyp40, outras co-chaperonas TPR de humanos ligam

o C-terminal da Hsp90 humana com um K_D aproximadamente dez vezes maior que aquele para a Tom70, numa interação que é dirigida pela entalpia, embora a interação com a Cyp40 seja dirigida pela entropia (Scheufler et al., 2000; Onuoha et al., 2008).

As estruturas cristalográficas do MEEVD da Hsp90 em complexo com o domínio TPR da Hop humana (Scheufler et al., 2000) e da Tom71 de levedura (Li et al., 2009) estão disponíveis. Visto que os resíduos da Tom71 que interagem com o MEEVD são conservados na Tom70 humana, a estrutura da ortóloga de levedura pode ser utilizada como um modelo de interação da Tom70 com a Hsp90. A interação do MEEVD com os domínios TPR da Hop e Tom71 envolve principalmente o dicarboxilato do resíduo de aspartato do C-terminal do MEEVD e duas lisinas dos domínios TPR (figura 6 – capítulo IV), numa interação de natureza eletrostática. O motivo MEEVD parece estar mais internamente envolvido pelo domínio TPR da Hop do que da Tom71, sugerindo que a interação entre o MEEVD e Hop é mais organizada e, portanto tem um maior custo entrópico.

Esses resultados sugerem que a interação de proteína TPR com chaperonas moleculares é mais complexa e diversa do que esperado. Além disso, é possível nesse caso, que a interação com apenas um monômero da C-Hsp90 permita outras interações adicionais com outras co-chaperonas TPR ou proteínas clientes, abrindo a possibilidade de uma modulação funcional por meio dessas interações. Contudo, mais evidências experimentais são necessárias para amparar essa hipótese.

As informações produzidas são bastante relevantes, pois complexos TPR-chaperonas têm sido alvos para várias investigações acerca de seu potencial como alvo para drogas. Dado que a Hsp90 está envolvida na estabilização do fenótipo tumoral, a interferência na interação do EEVD com motivos TPR pode inibir a entrega de proteínas clientes para a Hsp90.

CAPÍTULO 6

6. Conclusões

As proteínas C-Hsp90, Hop e Tom70 humanas recombinantes foram produzidas por expressão heteróloga em *E. coli* com bom rendimento; foram purificadas solúveis e enoveladas como mostrado pelos experimentos de dicroísmo circular e espectroscopia de emissão de fluorescência do triptofano.

A proteína C-Hsp90 teve seu estado oligomérico determinado como um dímero em solução, com massa molecular estimada em 43 ± 1 kDa por ultracentrifugação analítica, pelo método de sedimentação em equilíbrio; e com massa molecular de 43 kDa por gel filtração analítica acoplada a espalhamento de luz em multi-ângulos.

A proteína Hop teve seu estado oligomérico determinado por várias técnicas analisadas em conjunto. Foi determinado como, majoritariamente, monômero com a presença de oligômeros em situações particulares. Por ultracentrifugação analítica, aplicando o método de sedimentação em equilíbrio a massa molecular foi determinada em 66 ± 2 kDa. A análise dos dados hidrodinâmicos experimentais e teóricos indicaram que a Hop é monomérica que parece ser alongada e bastante hidratada, com um fator de Perrin de 1,6. Os ensaios de BNPAGE indicaram a presença de oligômeros, possivelmente dímeros e oligômeros maiores, numa condição de alta concentração proteica.

A proteína Tom70 foi caracterizada como monômero funcional em solução, podendo ser encontradas espécies diméricas. Por ultracentrifugação

analítica, o método de velocidade de sedimentação apresentou coeficientes de sedimentação de 3,8 S e 6,2 S consistentes com massas moleculares aproximadas de 60 e 120 kDa, respectivamente. O método de sedimentação em equilíbrio indicou que a proteína é encontrada num equilíbrio monômero-dímero com uma constante de dissociação da ordem de 10^{-5} M. Por SEC-MALS foi possível obter uma massa molecular de aproximadamente 62 kDa para a Tom70.

A interação da C-Hsp90 e Tom70, foi detectada com sucesso por experimentos de *pull-down*. A massa molecular do complexo foi determinada em aproximadamente 110 kDa por SEC-MALS, indicando uma estequiometria de 1 monômero da Tom70 para 1 dímero da C-Hsp90. Essa estequiometria foi confirmada pelo dado de $n = 1,2 \pm 0,1$ obtido por calorimetria de titulação isotérmica. A técnica de ITC também produziu a constante de dissociação (K_D) no valor de 360 ± 30 nM, sugerindo que o complexo tem alta afinidade. A ΔH_{app} da interação foi de $-2,6 \pm 0,1$ kcal/mol, e a entropia da interação foi de 21 ± 1 cal/mol.K, sugerindo que a interação é guiada por ambas, entalpia e entropia.

CAPÍTULO 7

7. Referências bibliográficas

1. Abe, Y., T. Shodai, T. Muto, K. Mihara, H. Torii, S. Nishikawa, T. Endo, and D. Kohda. 2000. Structural basis of presequence recognition by the mitochondrial protein import receptor Tom20. *Cell* 100:551-560.
2. Ali, M. M. U., S. M. Roe, C. K. Vaughan, P. Meyer, B. Panaretou, P. W. Piper, C. Prodromou, and L. H. Pearl. 2006. Crystal structure of an Hsp90-nucleotide-p23/Sba1 closed chaperone complex. *Nature* 440:1013-1017.
3. Anfinsen, C. B. 1973. Principles That Govern Folding of Protein Chains. *Science* 181:223-230.
4. Anfinsen, C. B., E. Haber, M. Sela, and F. H. White. 1961. Kinetics of Formation of Native Ribonuclease During Oxidation of Reduced Polypeptide Chain. *Proceedings of the National Academy of Sciences of the United States of America* 47:1309-&.
5. Ansar, S., J. A. Burlison, M. K. Hadden, X. M. Yu, K. E. Desino, J. Bean, L. Neckers, K. L. Audus, M. L. Michaelis, and B. S. J. Blagg. 2007. A non-toxic Hsp90 inhibitor protects neurons from A beta-induced toxicity. *Bioorganic & Medicinal Chemistry Letters* 17:1984-1990.
6. Bardwell, J. C. A. and E. A. Craig. 1987. Eukaryotic Mr 83,000 Heat-Shock Protein Has A Homolog in Escherichia-Coli. *Proceedings of the National Academy of Sciences of the United States of America* 84:5177-5181.
7. Barraclough, R. and R. J. Ellis. 1980. Protein-Synthesis in Chloroplasts .9. Assembly of Newly-Synthesized Large Subunits Into Ribulose Bisphosphate Carboxylase in Isolated Intact Pea-Chloroplasts. *Biochimica et Biophysica Acta* 608:19-31.
8. Beddoe, T. and T. Lithgow. 2002. Delivery of nascent polypeptides to the mitochondrial surface. *Biochimica et Biophysica Acta-Molecular Cell Research* 1592:35-39.
9. Bhangoo, M. K., S. Tzankov, A. C. Y. Fan, K. Dejgaard, D. Y. Thomas, and J. C. Young. 2007. Multiple 40-kDa heat-shock protein chaperones function in Tom70-dependent mitochondrial import. *Molecular Biology of the Cell* 18:3414-3428.
10. Blatch, G. L. and M. Lassel. 1999. The tetratricopeptide repeat: a structural motif mediating protein-protein interactions. *Bioessays* 21:932-939.
11. Borges, J. C. and C. H. I. Ramos. 2005. Protein folding assisted by chaperones. *Protein and Peptide Letters* 12:257-261.
12. Borkovich, K. A., F. W. Farrelly, D. B. Finkelstein, J. Taulien, and S. Lindquist. 1989. Hsp82 Is An Essential Protein That Is Required in Higher Concentrations for Growth of Cells at Higher Temperatures. *Molecular and Cellular Biology* 9:3919-3930.
13. Brix, J., K. Dietmeier, and N. Pfanner. 1997. Differential recognition of preproteins by the purified cytosolic domains of the mitochondrial import receptors Tom20, Tom22, and Tom70. *Journal of Biological Chemistry* 272:20730-20735.
14. Caplan, A. J. 2003. What is a co-chaperone? *Cell Stress & Chaperones* 8:105-107.
15. Carrigan, P. E., L. A. Sikkink, D. F. Smith, and M. Ramirez-Alvarado. 2006. Domain : domain interactions within Hop, the Hsp70/Hsp90 organizing protein, are required for protein stability and structure. *Protein Science* 15:522-532.

16. Chacinska, A., C. M. Koehler, D. Milenkovic, T. Lithgow, and N. Pfanner. 2009. Importing Mitochondrial Proteins: Machineries and Mechanisms. *Cell* 138:628-644.
17. Chen, S. Y. and D. F. Smith. 1998. Hop as an adaptor in the heat shock protein 70 (Hsp70) and Hsp90 chaperone machinery. *Journal of Biological Chemistry* 273:35194-35200.
18. Csermely, P., T. Schnaider, C. Soti, Z. Prohaszka, and G. Nardai. 1998. The 90-kDa molecular chaperone family: Structure, function, and clinical applications. A comprehensive review. *Pharmacology & Therapeutics* 79:129-168.
19. Cunningham, C. N., K. A. Krukenberg, and D. A. Agard. 2008. Intra- and intermonomer interactions are required to synergistically facilitate ATP hydrolysis in Hsp90. *Journal of Biological Chemistry* 283:21170-21178.
20. DeLano, W. L. 2004. The PyMOL Molecular Graphics System. DeLano Scientific, San Carlos, CA, USA.
21. DeZwaan, D. C. and B. C. Freeman. 2008. HSP90 - The Rosetta stone for cellular protein dynamics? *Cell Cycle* 7:1006-1012.
22. Dyson, H. J. and P. E. Wright. 2005. Intrinsically unstructured proteins and their functions. *Nature Reviews Molecular Cell Biology* 6:197-208.
23. Eftink, M. R. 1994. The Use of Fluorescence Methods to Monitor Unfolding Transitions in Proteins. *Biophysical Journal* 66:482-501.
24. Ellis, J. 1987. Proteins As Molecular Chaperones. *Nature* 328:378-379.
25. Ellis, R. J. 2001. Macromolecular crowding: an important but neglected aspect of the intracellular environment. *Current Opinion in Structural Biology* 11:114-119.
26. Endo, T., H. Yamamoto, and M. Esaki. 2003. Functional cooperation and separation of translocators in protein import into mitochondria, the double-membrane bounded organelles. *Journal of Cell Science* 116:3259-3267.
27. Fan, A. C. Y., M. K. Bhangoo, and J. C. Young. 2006. Hsp90 functions in the targeting and outer membrane translocation steps of Tom70-mediated mitochondrial import. *Journal of Biological Chemistry* 281:33313-33324.
28. Fan, A. C. Y., L. M. Gava, C. H. I. Ramos, and J. C. Young. 2010. Human mitochondrial import receptor Tom70 functions as a monomer. *Biochemical Journal* 429:553-563.
29. Fan, A. C. Y. and J. C. Young. 2011. Function of Cytosolic Chaperones in Tom70-Mediated Mitochondrial Import. *Protein and Peptide Letters* 18:122-131.
30. Felts, S. J., L. M. Karnitz, and D. O. Toft. 2007. Functioning of the Hsp90 machine in chaperoning checkpoint kinase 1 (Chk1) and the progesterone receptor (PR). *Cell Stress & Chaperones* 12:353-363.
31. Fink, A. L. 1999. Chaperone-mediated protein folding. *Physiological Reviews* 79:425-449.
32. Forafonov, F., O. A. Toogun, I. Grad, E. Suslova, B. C. Freeman, and D. Picard. 2008. p23/Sba1p protects against Hsp90 inhibitors independently of its intrinsic chaperone activity. *Molecular and Cellular Biology* 28:3446-3456.
33. Gaestel, M. 2006. Molecular Chaperones in Signal Transduction. In *Molecular Chaperones in Health and Disease*. S. Rallison, editor. Springer-Verlag, Berlin-Heidelberg. 93-110.

34. Garcia-Cardena, G., R. Fan, V. Shah, R. Sorrentino, G. Cirino, A. Papapetropoulos, and W. C. Sessa. 1998. Dynamic activation of endothelial nitric oxide synthase by Hsp90. *Nature* 392:821-824.
35. Garnier, C., D. Lafitte, P. O. Tsvetkov, P. Barbier, J. Leclerc-Devin, J. M. Millot, C. Briand, A. A. Makarov, M. G. Catelli, and V. Peyrot. 2002. Binding of ATP to heat shock protein 90 - Evidence for an ATP-binding site in the C-terminal domain. *Journal of Biological Chemistry* 277:12208-12214.
36. Gava, L. M. and C. H. I. Ramos. 2009. Human 90 kDa heat shock protein Hsp90 as a target for cancer therapeutics. *Current Chemical Biology* 3:10-21.
37. Gava, L. M., D. C. Gontalves, J. I. C. Borges, and C. H. I. Ramos. 2011. Stoichiometry and thermodynamics of the interaction between the C-terminus of human 90 kDa heat shock protein Hsp90 and the mitochondrial translocase of outer membrane Tom70. *Archives of Biochemistry and Biophysics* In Press, Uncorrected Proof.
38. Goncalves, D. C., L. M. Gava, and C. H. I. Ramos. 2010. Human Hsp70/Hsp90 Organizing Protein (Hop) D456G Is a Mixture of Monomeric and Dimeric Species. *Protein and Peptide Letters* 17:492-498.
39. Gray, P. J., M. A. Stevenson, and S. K. Calderwood. 2007. Targeting Cdc37 inhibits multiple signaling pathways and induces growth arrest in prostate cancer cells. *Cancer Research* 67:11942-11950.
40. Greenfield, N. and G. D. Fasman. 1969. Computed Circular Dichroism Spectra for Evaluation of Protein Conformation. *Biochemistry* 8:4108-8.
41. Hainzl, O., M. C. Lapina, J. Buchner, and K. Richter. 2009. The Charged Linker Region Is an Important Regulator of Hsp90 Function. *Journal of Biological Chemistry* 284:22559-22567.
42. Hendrick, J. P. and F. U. Hartl. 1993. Molecular Chaperone Functions of Heat-Shock Proteins. *Annual Review of Biochemistry* 62:349-384.
43. Hernandez, M. P., W. P. Sullivan, and D. O. Toft. 2002. The assembly and intermolecular properties of the hsp70-Hop-hsp90 molecular chaperone complex. *Journal of Biological Chemistry* 277:38294-38304.
44. Holmes, J. L., S. Y. Sharp, S. Hobbs, and P. Workman. 2008. Silencing of HSP90 cochaperone AHA1 expression decreases client protein activation and increases cellular sensitivity to the HSP90 inhibitor 17-allylamino-17-demethoxygeldanamycin. *Cancer Research* 68:1187-1196.
45. Holt, S. E., D. L. Aisner, J. Baur, V. M. Tesmer, M. Dy, M. Ouellette, J. B. Trager, G. B. Morin, D. O. Toft, J. W. Shay, W. E. Wright, and M. A. White. 1999. Functional requirement of p23 and Hsp90 in telomerase complexes. *Genes & Development* 13:817-826.
46. Johnson, J. L. and C. Brown. 2009. Plasticity of the Hsp90 chaperone machine in divergent eukaryotic organisms. *Cell Stress & Chaperones* 14:83-94.
47. Kelley, P. M. and M. J. Schlesinger. 1978. Effect of Amino-Acid Analogs and Heat Shock on Gene-Expression in Chicken-Embryo Fibroblasts. *Cell* 15:1277-1286.
48. Keppler, B. R., A. T. Grady, and M. B. Jarstfer. 2006. The biochemical role of the heat shock protein 90 chaperone complex in establishing human telomerase activity. *Journal of Biological Chemistry* 281:19840-19848.

49. Kimmins, S. and T. H. Macrae. 2000. Maturation of steroid receptors: an example of functional cooperation among molecular chaperones and their associated proteins. *Cell Stress & Chaperones* 5:76-86.
50. Krukenberg, K. A., T. O. Street, L. A. Lavery, and D. A. Agard. 2011. Conformational dynamics of the molecular chaperone Hsp90. *Quarterly Reviews of Biophysics* 44:229-255.
51. Kubota, H., S. Yamamoto, E. Itoh, Y. Abe, A. Nakamura, Y. Izumi, H. Okada, M. Iida, H. Nanjo, H. Itoh, and Y. Yamamoto. 2010. Increased expression of co-chaperone HOP with HSP90 and HSC70 and complex formation in human colonic carcinoma. *Cell Stress & Chaperones* 15:1003-1011.
52. Laskey, R. A., B. M. Honda, A. D. Mills, and J. T. Finch. 1978. Nucleosomes Are Assembled by An Acidic Protein Which Binds Histones and Transfers Them to Dna. *Nature* 275:416-420.
53. Lemaux, P. G., S. L. Herendeen, P. L. Bloch, and F. C. Neidhardt. 1978. Transient Rates of Synthesis of Individual Polypeptides in Escherichia-Coli Following Temperature Shifts. *Cell* 13:427-434.
54. Levinthal, C. 1969. How to fold graciously. J. T. P. DeBrunner and E. Munck, editors. University of Illinois Press, Monticello, Illinois. 22-24.
55. Li, J., K. Richter, and J. Buchner. 2011. Mixed Hsp90-cochaperone complexes are important for the progression of the reaction cycle. *Nature Structural & Molecular Biology* 18:61-+.
56. Li, J. X., X. G. Qian, J. B. Hu, and B. D. Sha. 2009. Molecular Chaperone Hsp70/Hsp90 Prepares the Mitochondrial Outer Membrane Translocon Receptor Tom71 for Preprotein Loading. *Journal of Biological Chemistry* 284:23852-23859.
57. Lu, Y. M., S. Ansar, M. L. Michaelis, and B. S. J. Blagg. 2009. Neuroprotective activity and evaluation of Hsp90 inhibitors in an immortalized neuronal cell line. *Bioorganic & Medicinal Chemistry* 17:1709-1715.
58. Lund, P. A. and R. J. Ellis. 2008. The chaperone function: meanings and myths. In *THE BIOLOGY OF EXTRACELLULAR MOLECULAR CHAPERONES*. D. J. Chadwick and J. Goode, editors. London. 23-44.
59. Marcu, M. G., A. Chadli, I. Bouhouche, M. Catelli, and L. M. Neckers. 2000. The heat shock protein 90 antagonist novobiocin interacts with a previously unrecognized ATP-binding domain in the carboxyl terminus of the chaperone. *Journal of Biological Chemistry* 275:37181-37186.
60. Mayer, M. P. and B. Bukau. 1999. Molecular chaperones: The busy life of Hsp90. *Current Biology* 9:R322-R325.
61. McAlister, L. and D. B. Finkelstein. 1980. Heat-Shock Proteins and Thermal-Resistance in Yeast. *Biochemical and Biophysical Research Communications* 93:819-824.
62. McClellan, A. J., Y. Xia, A. M. Deutschbauer, R. W. Davis, M. Gerstein, and J. Frydman. 2007. Diverse cellular functions of the Hsp90 molecular chaperone uncovered using systems approaches. *Cell* 131:121-135.
63. McDowell, C. L., R. B. Sutton, and W. M. J. Obermann. 2009. Expression of Hsp90 chaperone proteins in human tumor tissue. *International Journal of Biological Macromolecules* 45:310-314.

64. Mickler, M., M. Hessling, C. Ratzke, J. Buchner, and T. Hugel. 2009. The large conformational changes of Hsp90 are only weakly coupled to ATP hydrolysis. *Nature Structural & Molecular Biology* 16:281-286.
65. Mills, R. D., J. Trehwella, T. W. Qiu, T. Welte, T. M. Ryan, T. Hanley, R. B. Knott, T. Lithgow, and T. D. Mulhern. 2009. Domain Organization of the Monomeric Form of the Tom70 Mitochondrial Import Receptor. *Journal of Molecular Biology* 388:1043-1058.
66. Minami, Y., Y. Kimura, H. Kawasaki, K. Suzuki, and I. Yahara. 1994. The Carboxy-Terminal Region of Mammalian Hsp90 Is Required for Its Dimerization and Function In-Vivo. *Molecular and Cellular Biology* 14:1459-1464.
67. Morriset, J. D., J. S. K. David, H. J. Pownall, and A. M. Gotto. 1973. Interaction of An Apolipoprotein (Apolp-Alanine) with Phosphatidylcholine. *Biochemistry* 12:1290-1299.
68. Nemoto, T., Y. Oharanemoto, M. Ota, T. Takagi, and K. Yokoyama. 1995. Mechanism of Dimer Formation of the 90-Kda Heat-Shock Protein. *European Journal of Biochemistry* 233:1-8.
69. Nicolet, C. M. and E. A. Craig. 1989. Isolation and Characterization of Sti1, A Stress-Inducible Gene from *Saccharomyces-Cerevisiae*. *Molecular and Cellular Biology* 9:3638-3646.
70. Onuoha, S. C., E. T. Couistock, J. G. Grossmann, and S. E. Jackson. 2008. Structural studies on the co-chaperone hop and its complexes with Hsp90. *Journal of Molecular Biology* 379:732-744.
71. Ostermann, J., A. L. Horwich, W. Neupert, and F. U. Hartl. 1989. Protein Folding in Mitochondria Requires Complex-Formation with Hsp60 and Atp Hydrolysis. *Nature* 341:125-130.
72. Panaretou, B., G. Siligardi, P. Meyer, A. Maloney, J. K. Sullivan, S. Singh, S. H. Millson, P. A. Clarke, S. Naaby-Hansen, R. Stein, R. Cramer, M. Mollapour, P. Workman, P. W. Piper, L. H. Pearl, and C. Prodromou. 2002. Activation of the ATPase activity of Hsp90 by the stress-regulated cochaperone Aha1. *Molecular Cell* 10:1307-1318.
73. Park, S. J., S. Suetsugu, and T. Takenawa. 2005. Interaction of HSP90 to N-WASP leads to activation and protection from proteasome-dependent degradation. *Embo Journal* 24:1557-1570.
74. Pearl, L. H. 2005. Hsp90 and Cdc37 - a chaperone cancer conspiracy. *Current Opinion in Genetics & Development* 15:55-61.
75. Pearl, L. H. and C. Prodromou. 2006. Structure and mechanism of the Hsp90 molecular chaperone machinery. *Annual Review of Biochemistry* 75:271-294.
76. Peterson, L. B. and B. S. J. Blagg. 2009. To fold or not to fold: modulation and consequences of Hsp90 inhibition. *Future Medicinal Chemistry* 1:267-283.
77. Pfanner, N., N. Wiedemann, C. Meisinger, and T. Lithgow. 2004. Assembling the mitochondrial outer membrane. *Nature Structural & Molecular Biology* 11:1044-1048.
78. Pratt, W. B., Y. Morishima, and Y. Osawa. 2008. The Hsp90 chaperone machinery regulates signaling by modulating ligand binding clefts. *Journal of Biological Chemistry* 283:22885-22889.
79. Pratt, W. B. and D. O. Toft. 2003. Regulation of signaling protein function and trafficking by the hsp90/hsp70-based chaperone machinery. *Experimental Biology and Medicine* 228:111-133.

80. Prodromou, C., G. Siligardi, R. O'Brien, D. N. Woolfson, L. Regan, B. Panaretou, J. E. Ladbury, P. W. Piper, and L. H. Pearl. 1999. Regulation of Hsp90 ATPase activity by tetratricopeptide repeat (TPR)-domain co-chaperones. *Embo Journal* 18:754-762.
81. Ramos, C. H. I. and S. T. Ferreira. 2005. Protein folding, misfolding and aggregation: Evolving concepts and conformational diseases. *Protein and Peptide Letters* 12:213-222.
82. Rehling, P., Brandner, K. and Pfanner, N. 2004. Mitochondrial import and the twin-pore translocase. *Nature Reviews Molecular Cell Biology* 5(7): 519-530.
83. Ritossa, F. 1962. New Puffing Pattern Induced by Temperature Shock and Dnp in *Drosophila*. *Experientia* 18:571-&.
84. Ritossa, F. 1996. Discovery of the heat shock response. *Cell Stress & Chaperones* 1:97-98.
85. Ryan, M. T., H. Muller, and N. Pfanner. 1999. Functional staging of ADP ATP carrier translocation across the outer mitochondrial membrane. *Journal of Biological Chemistry* 274:20619-20627.
86. Ryan, M. T., D. J. Naylor, P. B. Hoj, M. S. Clark, and N. J. Hoogenraad. 1997. The role of molecular chaperones in mitochondrial protein import and folding. ACADEMIC PRESS INC, SAN DIEGO.
87. Scheibel, T., H. I. Siegmund, R. Jaenicke, P. Ganz, H. Lilie, and J. Buchner. 1999. The charged region of Hsp90 modulates the function of the N-terminal domain. *Proceedings of the National Academy of Sciences of the United States of America* 96:1297-1302.
88. Scheufler, C., A. Brinker, G. Bourenkov, S. Pegoraro, L. Moroder, H. Bartunik, F. U. Hartl, and I. Moarefi. 2000. Structure of TPR domain-peptide complexes: Critical elements in the assembly of the Hsp70-Hsp90 multichaperone machine. *Cell* 101:199-210.
89. Scroggins, B. T. and L. Neckers. 2007. Post-translational modification of heat-shock protein 90: impact on chaperone function. *Expert Opinion on Drug Discovery* 2:1403-1414.
90. Smith, D. F. 2004. Tetratricopeptide repeat cochaperones in steroid receptor complexes. *Cell Stress & Chaperones* 9:109-121.
91. Smith, J. R. and P. Workman. 2009. Targeting CDC37 An alternative, kinase-directed strategy for disruption of oncogenic chaperoning. *Cell Cycle* 8:362-372.
92. Song, H. Y., J. D. Dunbar, Y. X. Zhang, D. Q. Guo, and D. B. Donner. 1995. Identification of A Protein with Homology to Hsp90 That Binds the Type-1 Tumor-Necrosis-Factor Receptor. *Journal of Biological Chemistry* 270:3574-3581.
93. Soti, C., C. Pal, B. Papp, and P. Csermely. 2005. Molecular chaperones as regulatory elements of cellular networks. *Current Opinion in Cell Biology* 17:210-215.
94. Soti, C., A. Racz, and P. Csermely. 2002. A nucleotide-dependent molecular switch controls ATP binding at the C-terminal domain of Hsp90 - N-terminal nucleotide binding unmask a C-terminal binding pocket. *Journal of Biological Chemistry* 277:7066-7075.
95. Soti, C., A. Vermes, T. A. J. Haystead, and P. Csermely. 2003. Comparative analysis of the ATP-binding sites of Hsp90 by nucleotide affinity cleavage: a distinct nucleotide specificity of the C-terminal ATP-binding site. *European Journal of Biochemistry* 270:2421-2428.
96. Southworth, D. R. and D. A. Agard. 2011. Client-Loading Conformation of the Hsp90 Molecular Chaperone Revealed in the Cryo-EM Structure of the Human Hsp90:Hop Complex. *Molecular Cell* 42:771-781.

97. Stebbins, C. E., A. A. Russo, C. Schneider, N. Rosen, F. U. Hartl, and N. P. Pavletich. 1997. Crystal structure of an Hsp90-geldanamycin complex: Targeting of a protein chaperone by an antitumor agent. *Cell* 89:239-250.
98. Stuart, R. A., D. M. Cyr, E. A. Craig, and W. Neupert. 1994. Mitochondrial Molecular Chaperones - Their Role in Protein Translocation. *Trends in Biochemical Sciences* 19:87-92.
99. Sun, W., B. C. Xing, Y. Sun, X. J. Du, M. Lu, C. Y. Hao, Z. A. Lu, W. Mi, S. F. Wu, H. D. Wei, X. Gao, Y. P. Zhu, Y. Jiang, X. H. Qian, and F. C. He. 2007. Proteome analysis of hepatocellular carcinoma by two-dimensional difference gel electrophoresis. *Molecular & Cellular Proteomics* 6:1798-1808.
100. Taipale, M., D. F. Jarosz, and S. Lindquist. 2010. HSP90 at the hub of protein homeostasis: emerging mechanistic insights. *Nature Reviews Molecular Cell Biology* 11:515-528.
101. Tirolì-Cepeda, A. O. and C. H. I. Ramos. 2011. An Overview of the Role of Molecular Chaperones in Protein Homeostasis. *Protein and Peptide Letters* 18:101-109.
102. Tissiere, A., H. K. Mitchell, and U. M. Tracy. 1974. Protein-Synthesis in Salivary-Glands of *Drosophila-Melanogaster* - Relation to Chromosome Puffs. *Journal of Molecular Biology* 84:389-&.
103. Tompa, P. 2002. Intrinsically unstructured proteins. *Trends in Biochemical Sciences* 27:527-533.
104. Tompa, P. 2005. The interplay between structure and function in intrinsically unstructured proteins. *Febs Letters* 579:3346-3354.
105. Trepel, J., M. Mollapour, G. Giaccone, and L. Neckers. 2010. Targeting the dynamic HSP90 complex in cancer. *Nature Reviews Cancer* 10:537-549.
106. Vabulas, R. M., S. Raychaudhuri, M. Hayer-Hartl, and F. U. Hartl. 2010. Protein Folding in the Cytoplasm and the Heat Shock Response. *Cold Spring Harbor Perspectives in Biology* 2.
107. van der Laan, M., D. P. Hutu, and P. Rehling. 2010. On the mechanism of preprotein import by the mitochondrial presequence translocase. *Biochimica et Biophysica Acta-Molecular Cell Research* 1803:732-739.
108. Vaughan, C. K., M. Mollapour, J. R. Smith, A. Truman, B. Hu, V. M. Good, B. Panaretou, L. Neckers, P. A. Clarke, P. Workman, P. W. Piper, C. Prodromou, and L. H. Pearl. 2008. Hsp90-dependent activation of protein kinases is regulated by chaperone-targeted dephosphorylation of Cdc37. *Molecular Cell* 31:886-895.
109. Versteeg, S., A. Mogk, and W. Schumann. 1999. The *Bacillus subtilis* htpG gene is not involved in thermal stress management. *Molecular and General Genetics* 261:582-588.
110. Voos, W. and K. Rottgers. 2002. Molecular chaperones as essential mediators of mitochondrial biogenesis. *Biochimica et Biophysica Acta-Molecular Cell Research* 1592:51-62.
111. Walsh, N., A. Larkin, N. Swan, K. Conlon, P. Dowling, R. McDermott, and M. Clynes. 2011. RNAi knockdown of Hop (Hsp70/Hsp90 organising protein) decreases invasion via MMP-2 down regulation. 180-189.
112. Wandinger, S. K., K. Richter, and J. Buchner. 2008. The Hsp90 chaperone machinery. *Journal of Biological Chemistry* 283:18473-18477.

113. Wegele, H., L. Muller, and J. Buchner. 2004. Hsp70 and Hsp90 - a relay team for protein folding. SPRINGER-VERLAG BERLIN, BERLIN.
114. Welch, W. J. and C. R. Brown. 1996. Influence of molecular and chemical chaperones on protein folding. *Cell Stress & Chaperones* 1:109-115.
115. Welch, W. J. and J. R. Feramisco. 1982. Purification of the Major Mammalian Heat-Shock Proteins. *Journal of Biological Chemistry* 257:4949-4959.
116. Whitesell, L. and S. L. Lindquist. 2005. HSP90 and the chaperoning of cancer. *Nature Reviews Cancer* 5:761-772.
117. Wolfe, K. J. and D. M. Cyr. 2011. Amyloid in neurodegenerative diseases: Friend or foe?
118. Wu, Y. K. and B. D. Sha. 2006. Crystal structure of yeast mitochondrial outer membrane translocon member Tom70p. *Nature Structural & Molecular Biology* 13:589-593.
119. Young, J. C., N. J. Hoogenraad, and F. U. Hartl. 2003. Molecular chaperones Hsp90 and Hsp70 deliver preproteins to the mitochondrial import receptor Tom70. *Cell* 112:41-50.
120. Young, J. C., I. Moarefi, and F. U. Hartl. 2001. Hsp90: a specialized but essential protein-folding tool. *Journal of Cell Biology* 154:267-273.
121. Zanata, S. M., M. H. Lopes, A. F. Mercadante, G. N. M. Hajj, L. B. Chiarini, R. Nomizo, A. R. O. Freitas, A. L. B. Cabral, K. S. Lee, M. A. Juliano, E. de Oliveira, S. G. Jachieri, A. Burlingame, L. Huang, R. Linden, R. R. Brentani, and V. R. Martins. 2002. Stress-inducible protein 1 is a cell surface ligand for cellular prion that triggers neuroprotection. *Embo Journal* 21:3307-3316.